T-PM-Sym-1 TARGETTING ALTERED DNA CONFORMATIONS WITH CHIRAL METAL COMPLEXES.
Jacqueline K. Barton, Department of Chemistry, Columbia University, New York, NY 10027.

Chiral metal complexes serve as uniquely sensitive probes to examine the local variations in DNA conformation along the helical strand. Complexes have been designed which distinguish left and right-handed conformations. A new surface bound probe selectively recognizes helices adopting the A-conformation. Time resolved emission spectroscopy using ruthenium complexes permits the identification of binding modes and dynamics. For complexes of cobalt and rhodium, photoactivation results in oxidative strand cleavage. Hence coupling conformation-specific binding to photoreactions yields conformation-specific DNA cleavers. These DNA cleavers have been used to map distinct conformations along native DNA substrates. Remarkably high site specificity is observed. Examples will be described where distinct secondary structures are found at sites important to biological function.

T-PM-Sym-2 INTRINSIC-INDUCED DNA BINDING. Donald Crothers, Yale University, New Haven, CT.

T-PM-Sym-3 THE CRUCIFORM EXTRUSION REACTION - MECHANISMS AND LONG-RANGE EFFECTS.

David M J Lilley, Biochemistry Department, The University, Dundee DD1 4HN, U K.

Inverted repeat sequences in negatively supercoiled DNA molecules may undergo an extrusion reaction, whereby a cruciform structure becomes formed. Kinetic studies of cruciform extrusion by different sequences have revealed two classes, which we term C- and S-type. C-type cruciforms extrude at low salt and relatively low temperatures, but with very large Arrhenius activation energies (Ea). In contrast, S-type cruciforms require salt to facilitate extrusion,which occurs with a much smaller Ea. We believe that the different kinetic properties reflect alternative mechanistic pathways for the extrusion reaction. The C-type reaction probably proceeds *via* a transition state in which the entire inverted repeat is unpaired, whilst the S-type transition state probably possesses significant four-way junction character. The S-type mechanism is supported by detailed studies of the kinetic effects of a range of cations, and of sequence changes within the inverted repeat. Recently we have observed that C-type character is conferred by A+T rich sequences flanking the inverted repeat - indeed the sequence of the inverted repeat itself is of relatively minor kinetic importance. C-type inducing sequences operate in *cis*, are independent of polarity and may function over significant distances along DNA molecules. When an inverted repeat is flanked by one C-type and one S-type sequence, then the resulting mechanism is determined by the ionic strength, which appears to determine which sequence is dominant. Possible mechanisms for C-type induction will be discussed, and experimental evidence for these presented

T-PM-Sym-4 STRUCTURE OF THE LAMBDA REPRESSOR - OPERATOR COMPLEX. Carl Pabo, Johns Hopkins University, Baltimore, MD 21218.

T-PM-Sym-5 NMR STUDIES OF COVALENT CARCINOGENIC LESIONS IN DNA: O-ALKYLATION. Dinshaw J. Patel*, Matthew Kalnik*, Benjamin F. Lee+ and Peter F. Swann+. Department of Biochemistry and Molecular Biophysics, Columbia University, New York, NY, 10032 and +Courtauld Institute of Biochemistry, Middlesex Hospital Medical School, London, England.

The most important DNA modification in nitrosamine carcinogenesis results from O^6 alkylation of guanosine and O^4 alkylation of thymidine. We have undertaken high resolution proton and phosphorus NMR studies on a series of self-complementary dodecanucleotides with the general sequence d(CGCXAGCTYGCG). The first dodecanucleotide series compares the properties of X.Y equal to G.C and O^6alkG.C where alkyl stands for methyl, ethyl and isopropyl groups. The second series compares the properties of G.T, O^6alkG.T and G.O^4alkT while the third series compares the properties of A.T, A.C and A.O^4alkT. Our two dimensional NMR studies are aimed at gaining insight into the base pairing properties of these alkylated bases and at estimating the perturbations in the conformation and dynamics at and adjacent to the modification site in solution.

T-PM-A1 IONIC STRENGTH DEPENDENCE OF CA-ACTIVATED FORCE IN TnC-EXTRACTED FIBERS SUPPORTS THE HYPOTHESIS OF DUAL REGULATION MECHANISM.

J. Gulati and A. Babu, Albert Einstein College, Bronx, NY 10461

The force generating step in the cross-bridge mechanism appears to be associated with the transition of a weakly attached cross-bridge state into a strong state (AF Huxley: Proc R Soc 183, 83, 1973; Eisenberg & Hill: Science 299, 999, 1985; HE Huxley & Kress: J Mus Res & Cell Mot 6, 153, 1985). The present study was made with TnC extracted fibers (psoas m of hamsters at various ionic strengths (I.S) to further characterize this transition step. Extraction was in 10mM imidazole, 5 EDTA, pH 7.2, at 30°C for 5 to 30 min and stopped when force in pCa4 was zero (range: 0 to 0.15 Po; Po, tension in pCa 4, 200mM I.S). By SDS PAGE (silver stained) the residual TnC content was 26%. The extracted fiber still showed Ca sensitivity in 20 to 40 mM ionic strength (LIS) with tension 0.5 to 1.0 Po (4mM free Mg). Also, the fiber stiffness in LIS was unaffected by TnC extraction (Babu: FEBS, 203, 20, 1986). The data suggested that activation occurs in two steps (dual regulation mechanism): One step controls the formation of weak bridges and the second is rate limiting for the weak to strong transition. The Ca-tension in TnC extracted fibers decreases with ionic strength (20 to 200mM), paralleling the intensity change (1, 1/1, 0) by x-ray diffraction on fibers in Ca-free solutions (Podolsky: Biophys J 46,299, 1984). The results suggest that the first step controlling the formation of weak bridges requires Ca in physiological ionic strength but not in LIS. Further, the control of the second step (weak→strong) by Ca (in all ionic strengths) may be mediated by the residual TnC or a myosin moiety or both. (Supported by NSF-8303045 and NIH-AM 33736 & HL 18824).

T-PM-A2 pCa-TENSION RELATIONSHIPS FOR HUMAN MUSCLE FIBERS

by R.L. Ruff, Depart. of Neurology, Cleveland VAMC and Case Western Reserve University, Cleveland, OH 44106

Muscle biopsies were obtained from the lateral gastrocnemius muscles of 5 normal adults. Fibers were chemically skinned according to the technique of Wood et al. (Science 187:1075,1975) with previously described modifications (Laszewski & Ruff, Am J Physiol 248: 363,1985). Each skinned fiber was divided in two: one piece used for histochemical fiber type determination and the other piece used for calcium sensitivity and tension measurements. The figure shows the average calcium sensitivity relationships for 15 fast and 11 slow twitch fibers. The smooth curves are least squares fits of the data to the Hill equation with half-maximal tension at pCa = 5.61 for fast and pCa = 5.88 for slow twitch fibers studied in solutions with [Mg] = 1 mM. The Hill coefficients were 2.27 for fast and 1.64 for slow twitch fibers. The maximum normalized tensions were (kg/cm^2) 2.24 ± 0.16 for fast and 2.19 ± 0.09 for slow twitch fibers.

Therefore, human muscle fibers are similar to other mammalian muscle fibers in that the fast twitch fibers have a lower calcium sensitivity and a steeper pCa-tension curve.

Supported by the Veterans Administration.

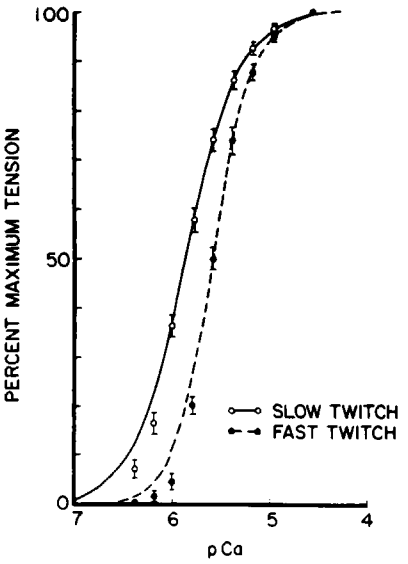

T-PM-A3 EFFECTS ON SHORTENING VELOCITY DUE TO OSMOTIC COMPRESSION OF SKINNED SKELETAL MUSCLE FIBERS AT MAXIMAL AND SUBMAXIMAL LEVELS OF THIN-FILAMENT ACTIVATION.

J.M. Metzger and R.L. Moss. Dept of Physiology, Univ of Wisconsin, Madison, WI 53706.

This study examined the effects on maximum shortening velocity (Vmax) due to osmotic compression induced by dextran (2.5, 5 and 10 g/100 ml) in rat slow soleus (SOL) and fast superficial vastus lateralis (SVL) single skinned fibers. At maximal activation (pCa 4.5), Vmax progressively declined in all fibers as dextran concentration was increased. At 10% dextran, which yielded a 33-38% reduction in cell width, Vmax was 28.4±2.9 and 26.1±1.6 % of the value in 0% dextran for SVL and SOL fibers, respectively. The effect of osmotic compression was reversible since Vmax returned to control values when the fibers were again placed in 0% dextran. Vmax was also examined at various levels of thin-filament activation with and without 5% dextran. In the absence of dextran biphasic shortening records (Moss, J Physiol 377:487,1986) were elicited at pCa 5.7 and greater. In contrast, compressed fibers did not exhibit biphasic shortening until pCa was increased to 6.0. Biphasic shortening was induced under both conditions when peak Ca-activated force was reduced to ~85% of the maximum value in 0% dextran. Two separate mechanisms are proposed to explain these results. 1) Reduced Vmax with dextran may be related to physical constraints on cross-bridge movement due to reduced lattice separation. 2) Biphasic shortening may involve a subpopulation of cross-bridges with a reduced rate of detachment thus providing resistance to further shortening (Moss, 1986). It is hypothesized that the apparent cooperativity of thin-filament activation by cycling cross-bridges is enhanced with dextran leading to increased activation at a given pCa, thereby decreasing the Ca^{2+} threshold for biphasic shortening. Supported by NIH.

T-PM-A4 THE VELOCITY OF UNLOADED SHORTENING OF SKELETAL MUSCLE AT LONG SARCOMERE LENGTHS.

Dennis R. Claflin, David L. Morgan* and Fred J. Julian, Dept. Anesthesia Research, Brigham and Women's Hospital, Boston, MA 02115; *Monash Univ., Clayton, Victoria, Australia.

According to current models of skeletal muscle contraction, the rate at which myosin crossbridges interact with actin is independent of both the degree of overlap and the lateral spacing of the myosin and actin filaments. The velocity of unloaded shortening (Vu) is thought to reflect the maximum rate of crossbridge turnover. We tested the hypothesis that Vu is independent of sarcomere length at lengths above those optimum for force generation. Single, intact fibers were isolated from tibialis anterior muscles of frogs (R. temporaria) and maintained at 4.5°C during the experiments. Vu was determined by the "slack test" at each of five sarcomere lengths. For a given test, all step length releases were initiated from the same sarcomere length. Release amplitudes were, in order of application (% fiber length): 8,10,12,14,16; 16,14,12,10, & 8. Implementation of the slack test at long sarcomere lengths required two procedural precautions due to significant levels of resting tension: 1) the smallest release amplitude (8%) was chosen sufficiently large to absorb contributions to velocity from passive recoil and 2) all releases within a test were initiated from the same resting tension to equalize the passive contribution among steps. The Vu values (fiber lengths/s) and sarcomere lengths corresponding to the 12% releases (μm) were, in order of determination: 2.53 ± 0.10, 2.1; 2.49 ± 0.06, 2.5; 2.55 ± 0.06, 2.9; 2.50 ± 0.06, 3.1; and 2.40 ± 0.06, 2.1 (means ± SEM, n=5). We conclude that careful application of the slack test under conditions of high resting tension yields constant values for Vu, supporting the view that the rate of crossbridge cycling is independent of both the degree of filament overlap and lateral filament spacing. Supported by NIH grant HL35032 (FJJ).

T-PM-A5 **ARCHITECTURE OF SARCOMERE MATRIX IN SKELETAL MUSCLE -- NEBULIN FILAMENT AS A THIN FILAMENT SCAFFOLD.**

Kuan Wang & John Wright. Clayton Foundation Biochemical Institute & Department of Chemistry, The University of Texas at Austin, Austin, TX 78712

Nebulin, a giant myofibrillar protein (0.6 x 10^6 Mr subunit) abundant in skeletal muscles, has been proposed as a component of a set of cytoskeletal filaments which coexist with thick and thin filaments within the sarcomere. We have utilized a monospecific antiserum to localize nebulin in mechanically-skinned single fiber from rabbit psoas muscle at electron microscopic resolution. These labeled fibers exhibited six to seven pairs of transverse bands of various intensities within the I band and the A band of each sarcomere. Studies of their axial distribution at different sarcomere lengths indicated that nebulin epitopes maintained a fixed distance to the closest Z line, suggesting a rigid structural linkage to the Z line. In other words, nebulin does not exhibit the types of elastic stretch found in the I band domain of titin filaments. This observation suggests that nebulin constitutes a distinct filament in parallel with titin filaments. The possibility is also raised that the nebulin filament may act as a scaffold for thin filaments in skeletal muscle sarcomeres. (Supported in part by NIH AM20270 and an American Heart Association Established Investigatorship.)

T-PM-A6 THICK FILAMENT MOVEMENT AND THE EFFECT OF TITIN FILAMENTS IN ACTIVATED SKELETAL MUSCLE

Robert Horowits and Richard J. Podolsky, NIAMS, NIH, Bethesda, MD 20892

Electron microscopy was used to study the positional stability of thick filaments in isometrically contracting skinned rabbit psoas muscle at 7 °C as a function of sarcomere length. Following calcium activation at a sarcomere length of 2.6 μm, where resting stiffness is low, sarcomeres become nonuniform in length. The dispersion in sarcomere length is complete by the time maximum tension is reached. A-bands generally move as a unit from their central position, and continue moving after tension has plateaued at its maximum level. The extent of A-band movement depends on the final length of the individual sarcomere. After 7.5 minutes of activation, all sarcomeres between 1.9 and 2.5 μm long exhibit A-bands that are adjacent to a Z-disc, with no intervening I-band. Sarcomeres 2.6 or 2.7 μm long exhibit a partial movement of A-bands. At longer sarcomere lengths, where the resting stiffness exceeds the slope of the active tension-length relation, the A-bands remain perfectly centered during contraction. When fibers are stretched to sarcomere lengths greater than 2.8 μm and then activated, the sarcomeres remain more uniform in length and the A-bands tend to remain centered within the sarcomere. Sarcomere symmetry and length uniformity are restored upon relaxation. These results indicate that the central position of the thick filaments in the resting sarcomere becomes unstable upon activation, as predicted by the crossbridge theory. The elimination of A-band movement as passive stiffness increases is evidence that titin filaments, which join thick filaments to Z-discs, produce almost all of the resting tension in skinned rabbit psoas fibers and act to resist the movement of thick filaments away from the center of the sarcomere during contraction. The strained titin filaments may also help maintain the constant level of tension that is observed during and after the completion of A-band movement.

T-PM-A7 E.M. STRUCTURE OF THICK AND THIN FILAMENTS IN WATERBUG FLIGHT MUSCLE FIBERS STRETCHED TO NON-OVERLAP. M.C. Reedy, A.D. Magid, and M.K. Reedy. Department of Anatomy, Duke University Medical Center, Durham, N.C. 27710.
In demembranated, relaxed Lethocerus flight fibers stretched immediately after dissection from living muscles, new features are demonstrated by myofilaments in non-overlap regions. In the I band, diagonal stripes every 38.7nm are formed by staggered register of elongated beads on adjacent thin filaments, unlike the transverse stripes formed by troponin in the vertebrate I band. Thick filaments in fully non-overlap sarcomeres, in addition to a 14.5-nm axial period, exhibit a 39nm helical period, which cannot arise from interaction with actin, and is clearly different from the 43nm helical repeat of other thick filaments. In optical diffraction patterns, the radial maxima on the 1/39nm layer line are at 1/15.2nm (closest to J=4), compatible with models requiring 4-stranded symmetry of the thick filament. In these non-overlap sarcomeres, the relaxed periodicities (14.5, 39nm) persist undiminished for >45 minutes after ATP washout. With partial overlap, upon ATP washout, a rigor crossbridge lattice sets up rapidly (<2 min) as tension develops. Rigor crossbridges show good lateral register in spite of the disturbance of register between thick filaments produced by stretch. This emphasizes the importance of actin targets in establishing the rigor lattice. In partial-overlap sarcomeres of relaxed muscle, thick filaments are richly periodic, in contrast to the H-zone of rigor sarcomeres, which shows only a very weak 14.5 nm repeat. This suggests cooperative changes within thick filament structure caused by crossbridge attachment. The diameter of relaxed thick filaments is uniform but, in rigor, abruptly increases 23% between the overlap zone and the H band, a manifestation of detached crossbridges.

T-PM-A8 CAN RIGOR BE ENTERED BY A SINGLE SYNCHRONIZED ATP TURNOVER OF CROSSBRIDGES? M. K. Reedy and W. Longley. Department of Anatomy, Duke University Med. Center, Durham NC 27710.
We are exploring mechanics and EM structure of crossbridges in 1-2 fiber bundles of glycerinated insect (Lethocerus) flight muscle when rigor induction begins from the minimum ATP concentration that can keep fibers relaxed. We hope to restrict each crossbridge to a single power stroke while rigor develops during rapid ATP washout. At 24° C, 20-40 uM MgATP prevents any rise in stiffness or tension; cooling lowers MgATP requirement to <10 uM. Myosin heads are ~200 uM, averaged over whole fiber volume. Fibers are rigorized (in 2-8 sec) by flushing with rigor solution containing 1 mM $CaCl_2$. >80% of heads must therefore enter rigor in one cycle; <20% can bind ATP for a second cycle, because myosin heads outnumber available MgATP within the fibers by 5:1 to 10:1. We measured unloaded shortening with a computer-controlled transducer system, sampling tension every 1 ms and slackening length whenever tension was ≥1 uN. Length fell to a plateau, after shortening of about 2% (60 um for 3 mm fiber length) (range 1.5-2.5%; typically 1.8-2.2%). This represents 28 nm shortening (range 20-35 nm) in typical half-sarcomeres of 1.4 um length. Before claiming 25-30 nm as the length of one synchronized power stroke, we must minimize chances for multiple powerstrokes early in shortening (by further lowering ATP, and using Ca^{++} jump activation) and for slippage after crossbridge attachment (by lowering ionic strength). Meanwhile, EMs of fibers fixed 30 sec after completing isotonic rigorization show typical rigor crossbridges forming some 30 double chevrons, one every 38.7 nm, along every thin filament in each half-sarcomere. There is no lattice disorder to suggest slippage or asynchronous final power-strokes. Ca^{++}-activated strokes halt in the same final crossbridge form found after other modes of rigor induction. Support: NIH, AR 14317.

T-PM-A9 FORCE GENERATION BY MUSCLE FIBERS IN RIGOR: A LASER TEMPERATURE-JUMP STUDY. Julien S. Davis and William F. Harrington. Department of Biology, The Johns Hopkins University, Baltimore, MD 21218.
A clear prediction of the helix-coil model for force generation in muscle is that force should be produced when the equilibrium (helix-coil) of a rigor (or activated) fiber is perturbed by a T-jump near the melting temperature of the LMM/HMM hinge. An infrared, iodine-photodissociation laser was used to heat the fibers by ~5°C in under 1 μsec. Under ionic conditions where rigor bridges are predominantly associated with the thick filament backbone, an abrupt drop in tension typical of normal thermoelastic expansion was seen (see Goldman, McCray and Ranatunga (1985) J. Physiol. 369, 73p). A similar response was observed below 41°C for thick filament-released rigor bridges. Above this temperature, a rubber-like thermoelastic response was obtained typical of a helix-coil transition. At temperatures near 50°C, the amount of force generated by a rigor fiber was large and comparable to that seen for an activated fiber at 5°C. The relaxation spectra of force generation obtained for both systems (rigor and activated) show a step change followed by a bi-exponential kinetic process. The reciprocal relaxation times and amplitudes for these individual processes in activated and rigor fibers differ only by factors of 2 to 4. Force generation in the rigor muscle appears to arise from melting in the S-2 hinge region of the myosin molecule since binding of S-2 to the thick filament backbone inhibits force production. No significant force generation was observed following T-jumps of relaxed fibers.

T-PM-A10 THEORY OF OPTICAL ELLIPSOMETRIC SPECTROSCOPY FROM MUSCLE DIFFRACTION STUDIES. Y. Yeh and R. J. Baskin, Depts. of Applied Science and Zoology, University of California, Davis, California, 95616.

Interpretation of optical ellipsometric data from muscle fibers requires the unambiguous separation of the two basic components in such spectra: intrinsic and form contributions. Diffraction ellipsometry allows for such a separation because both the total birefringence, Δn_T, and the total depolarization ratio, r_T, are independently obtained. For the simplest model of the fiber consisting of myofibrillar elements with both isotropic and anisotropic molecules, the intrinsic depolarization ratio, r_I, is enhanced on the diffraction order over that of the form depolarization ratio, r_F, by a factor of $\Delta\varepsilon$ / $\Delta\varepsilon_{AI}$, where $\Delta\varepsilon$ is the refractive index differential between fiber material and the solution medium, and $\Delta\varepsilon_{AI}$ is the differential A-I refractive indices. The origin of this scaling factor is the fact that r_T is normalized to the sum of the amplitudes of collected light. On the diffracted order, this sum is proportional to the $\Delta\varepsilon_{AI}$ index differential. Total birefringence has no normalizing factor, and consequently, there is no partial signal enhancement. Thus it is possible for a fiber system with a dominant form birefringence to simultaneously exhibit strong intrinsic depolarization ratio. Since form effects are closely related to the measured lattice spacing of the filaments, we show that the spectral difference between relaxed intact fiber and relaxed skinned fiber can be explained using lattice spacing as a variable parameter influencing the form contribution. In addition, the decrease in total depolarization ratio and the simultaneous small decrease in total birefringence upon the relax-to-rigor transition or upon activation can be explained using this theory. Work supported by NIH through grant AM-26817.

T-PM-A11 ALPHA ADRENERGIC CONTROL OF V_3 MYOSIN IN RAT HEART, Saul Winegrad, Andrea Weisberg and S. Kristina Wahlstrom, Department of Physiology, University of Pennsylvania, Philadelphia, PA 19104-6085

Beta adrenergic stimulation of rat ventricular myocardium increases Ca and actin activated ATPase of myosin in proportion to the amount of the V_1 isozyme that is present (Winegrad et al, Circul. Res. 58: 83, 1986). The effect of alpha adrenergic stimulation has been studied by the same method, which uses microphotometry to measure the amount of inorganic phosphate liberated by cryostatic sections of quickly frozen hearts. Hearts from young and middle aged euthyroid rats and from hypothyroid rats were used since they contain respectively, high, intermediate and low concentrations of V_1. Alpha stimulation was produced by 0.3 uM phenylephrine and by 1 um norepinephrine in the presence of 5 uM phentolamine. Propranolol was used to block the beta stimulation. In hearts from young rats with almost entirely V_1, alpha adrenergic stimulation had little or no effect. In older rats and hypothyroid rats, alpha stimulation by phenylephrine or norepinephrine plus propranolol increased total myosin ATPase activity by 21±3%. The increase was entirely inhibited by phentolamine. In serial sections of hearts that responded to alpha adrenergic stimulation, alpha stimulation had no effect when V_3 had been inhibited by a brief exposure to alkalinity although norepinephrine still produced a significant increase in ATPase activity that was completely inhibited by propranolol. These results indicate that alpha adrenergic stimulation specifically increases the ATPase activity of V_3 in rat ventricle. (supported by grants HL15835 and HL33924 from N.I.H.)

T-PM-A12 SPEED OF SHORTENING OF RED MUSCLE FIBERS DURING SWIMMING IN CARP LC ROME, RMcN ALEXANDER, R FUNKE, G LUTZ, MA FREADMAN. ZOOLOGY, U TENN, KNOXVILLE TN; U LEEDS, UK; MBL, WOODS HOLE

Although much is known about the contractile properties of different muscle fiber types, little is known about how they function during locomotion. It is generally assumed that slow twitch fiber types are more efficient than fast ones at slow speeds of locomotion, but they cannot shorten fast enough to enable the animal to locomote at high speeds. Fish provide an excellent model to test this hypothesis because of the discrete recruitment of the different muscle fiber types (Rome et al,1985)

We used two different methods to determine the velocity (**V**) at which the red (slow) muscle fibers shorten during swimming. Both methods involved analyzing high speed motion pictures (200 frames/s) of carp at 15°C. In the first, fish were sacrificed and fixed in the body positions observed in the film. The sarcomere length of red fibers were measured by light microscopy. In the second, the fiber length was calculated from the curvature of the fish's body by mathematical model.

Preliminary analysis suggests that during normal swimming, sarcomere length undergoes excursions of +/- 0.15 um around a central value of 1.90 um. This would suggest that fibers are operating on the ascending limb of the force-sarcomere length curve. At 50 cm/s, a swimming speed at which the white (fast) muscle is recruited in addition to the red, the **V** of the red muscle was calculated to be 2.5 muscle lengths/s. During the escape response (elicited by a 100ms, 150hz sound pulse) the **V** was about 3-fold greater. These values exceed that measured for the maximum speed of shortening (**Vmax**) of red fibers (Johnston et al.,JEB 1985). This would suggest that the fast fibers force the slow fibers to shorten at speeds greater than their **Vmax**, and thus the slow fibers cannot contribute to force generation at high swim speeds and during rapid escapes.

Supported by MBL Summer Fellowship, UTFDA and UTRIA to LCR, and NSF # OCE-8416257 to MAF.

T-PM-A13 TENSION/pCa CHARACTERISTICS AND REGULATORY PROTEINS OF SINGLE FIBERS FROM CHICKEN NEONATAL AND ADULT FAST AND SLOW SKELETAL MUSCLES. P.J. Reiser†, M.L. Greaser* and R.L. Moss†, †Dept. of Physiol. & *Muscle Biology Laboratory, Univ. of Wis., Madison, WI 53706.

The objective of this study was to determine if differences in the regulatory proteins, especially the subunits of troponin (Tn), of mature and neonatal skeletal muscles are correlated with differences in the Ca-sensitivity of tension (T) generation of skinned single fibers. Fibers were dissected from the fast pectoralis major (PM) and slow anterior and fast posterior latissimus dorsi (ALD and PLD) muscles of 2 wk post-hatch and adult chickens. T developed during submaximal activation ($7.4 \leq pCa \leq 4.8$) was normalized to the tension at maximal activation (pCa 4.5). The Ca^{2+} sensitivity of T generation among the adult fibers was greatest for the PM (pCa yielding 50% P_o=6.2), lower for the ALD (pCa_{50}=6.0) and lowest for the PLD (pCa_{50}=5.9). SDS-PAGE of these fibers revealed two isoforms of TnC: one form in PM and PLD fibers and another in ALD fibers. One isoform of TnI was observed in both PLD and PM fibers and a different one in ALD fibers. The fiber composition of TnT was more complex. The content of the 41 kDa (apparent m. wt.) TnT isoform relative to the smaller TnT forms was higher in adult PM than in adult PLD fibers which correlated with the greater Ca-sensitivity of the PM fibers. A shift in the T/pCa curves of 2 wk post-hatch versus adult PM and PLD fibers was also observed and this too appeared to be related to the proportion of the 41 kDa TnT isoform present. The T/pCa data obtained from the neonatal ALD fibers virtually superimposed on the curve for the adult ALD fibers. No differences were observed in the TnC, TnI or TnT compositions of the neonatal compared to the adult ALD fibers. It is concluded that differences in both TnC and TnT isoforms affect the calcium requirements for T generation in adult and developing chicken muscle fibers. Supported by NIH.

T-PM-A14 CONTRACTILE PROPERTIES OF SKELETAL MUSCLES FROM YOUNG, ADULT, AND AGED MICE. Susan V. Brooks and John A. Faulkner. Department of Physiology and Bioengineering Program, University of Michigan, Ann Arbor, Michigan, 48109.

Hypotheses were tested that compared with skeletal muscles from young and adult mice, the skeletal muscles from aged mice would have: 1. a decrease in the generation of maximum tetanic tension, 2. a decrease in shortening velocities at any given after load, and 3. a decrease in peak instantaneous power output. Tension generation and velocity of shortening of extensor digitorum longus (EDL) and soleus muscles from young (2-3 month), adult (9-10 month), and aged (26-27 month) C57BL/6 mice were measured in vitro at 25°C with a Cambridge 300-H ergometer. Power output was calculated from force and velocity. Compared to data on young and adult mice, muscles from aged mice showed a significant decrease in maximum tetanic tension from 413±16 to 304±6 mN for EDL muscles and from 249±13 to 201±11 mN for the soleus muscles. Part of the decrease in the generation of tension resulted from the decreased mass of the muscle, but significant decreases of 27% and 17% were observed for the maximum specific tension (N/cm^2) of the EDL and soleus muscles, respectively. The decrease in specific tension of muscles from aged mice suggests a decrease in the concentration of contractile protein per unit mass of muscle. No differences were observed in the maximum velocity of shortening of the EDL or the soleus muscle. The peak power outputs of the EDL and soleus muscles of aged mice were significantly less than those of young and adult mice. The power outputs at 35°C for young, adult, and aged mice, respectively were 418±18, 425±13, 301±29 w/kg for the EDL muscles and 166±8, 168±9, and 150±6 w/kg for the soleus muscles. We conclude that maximum tension and peak power of fast and slow muscles of aged mice decrease, but shortening velocities are not different. Supported by NIH grant AG 06157.

T-PM-B1 SELECTIVE CALCIUM CHANNEL EXPRESSION IN PYRAMIDAL AND NONPYRAMIDAL CELLS OF THE RAT NEOCORTEX. O.P. Hamill*, J.R. Huguenard and D.A. Prince. Dept. Neurology, Stanford University, California 94305.

The expression of Ca^{++} currents in pyramidal and nonpyramidal cells of the rat neocortex have been compared. Whole cell current recordings were made from acutely isolated neurons under ionic conditions (symmetrical concentrations of 145mM choline Cl) that block Na^{+} and K^{+} currents. A puffer pipette in which 20mM choline Cl was replaced by 15mM $CaCl_2$ was used to selectively perfuse neurons. Both cell types express equally, a high threshold, persistent Ca^{++} current that shows little inactivation when the holding potential was reduced from -100mV to -40mV (Fig). In pyramidal cells, an additional, low threshold, transient (T) Ca^{++} current that was completely inactivated when V_H was reduced to -60mV was evident (Fig). This low threshold current was typically smaller than the high threshold Ca^{++} current recorded in the same pyramidal cell (Fig) but was absent or barely detectable in nonpyramidal cells. The selective expression of a T Ca^{++} current may underlie the tendency of certain pyramidal cells to initiate transient high frequency bursts of action potentials in response to depolarization. Supported by NIH grants NS06477 and NS12151.

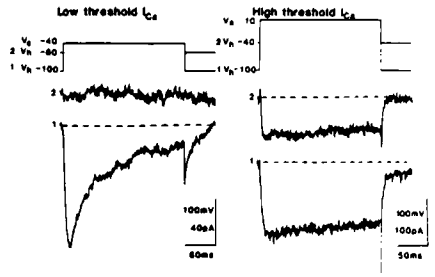

*Permanent address: Neurobiology and Behavior, Cornell Univ., Ithaca, NY 14853.

T-PM-B2 CALCIUM CHANNELS MODULATED BY BAY K 8644 APPEAR LESS SUSCEPTIBLE TO DEPHOSPHORYLATION. D.Armstrong, C.Erxleben & D.Kalman, Dept.Biology, UCLA, Los Angeles, California (Intr. by A.S. Hobbs)

Recent experiments on a mammalian cell line (GH3) with the patch clamp technique have demonstrated that a prominent class of voltage-activated Ca channels stop responding to depolarization in cell-free patches unless both ATP and the catalytic subunit of cyclic AMP-dependent protein kinase are present at the cytoplasmic side of the membrane (Armstrong & Eckert, 1985, J.Gen. Physiol.86,25a). We have studied the modulation of those channels by BAY K 8644, a dihydropyridine agonist that dramatically increases the mean open time of the channels in intact cells (Schramm et al., 1983, Nature 303,535; Hess et al., 1984, Nature 311,538). We have observed that BAY K 8644 also increases the mean open time of Ca channels in cell-free patches when it is applied in the presence of protein kinase and ATP. However, BAY K 8644 alone (0.1-10 uM) was unable to restore Ca channel activity once it had run down in patches exposed to a minimal solution lacking ATP. In contrast, if intact cells were exposed to BAY K 8644 (1 uM) before the patches were excised, BAY K 8644 not only modified Ca channel gating, it substantially delayed the loss of activity in the minimal solution. Evidence in other systems suggests that dephosphorylation by an endogenous Ca-dependent phosphatase is responsible for both run down and Ca-dependent inactivation of these channels (Chad & Eckert, 1986, J.Physiol. in press). BAY K 8644 (1 uM) also inhibits the Ca-dependent inactivation of Ca currents in GH3 cells. These results suggest that Ca channels modulated by BAY K 8644 are less susceptible to dephosphorylation, and that may underlie the effect of BAY K 8644 on gating. Supported by USPHS NS-8364 to Roger Eckert.

T-PM-B3 CA^{++} CHANNELS IN FRESHLY-DISSOCIATED RAT CEREBELLAR PURKINJE CELLS. L.J. Regan, Dept. of Neurobiology, Harvard Medical School, Boston, MA 02115. (Intro. by Stuart Lipton).

The whole-cell patch-clamp technique was used to record Ca^{++} currents from acutely dispersed rat cerebellar neurons tentatively identified as Purkinje cells by morphological criteria (the presence of a large diameter soma, a single stump of apical dendrite, and a short segment of axon). The dissociation procedure ($1\frac{1}{2}$ hrs. in 200 units of papain at 34-37°C) was performed on sections of cerebellar cortex from 3 week-postnatal rats, when the Purkinje cells had attained their adult structure and synaptic organization (Altman 1972, J. Comp. Neurol., vol. 145). Patch pipettes contained (in mM) 140 Cs-glutamate, 10 EGTA, 5 $MgCl_2$, 3 Mg-ATP, 0.8 GTP, 12 phosphocreatine, 42 units/ml creatine phosphokinase, and 10 HEPES, pH 7.4. The external solution contained 10 Ba^{++} or Ca^{++}, 154 TEA-Cl, 2 $MgCl_2$, 10 glucose, and 10 HEPES, pH 7.4, 22°C.

Two components of calcium current were identified. One component was transient (T_h = 29 ms at -30 mV), required holding potentials of -70 mV or below, had an apparent activation level of -50 mV, and peaked at -30 mV. The second component was long-lasting, could be activated from holding potentials of -30 mV, had an apparent activation level of -30 to -20 mV, and was maximal at -20 to -10 mV. Both current components were somewhat labile under the whole-cell recording conditions. Further work is needed to determine whether these currents correspond directly to the "T" (transient) and "L" (long-lasting) currents which have been described in peripheral neurons (Nowycky, Fox, and Tsien 1985, Science, vol. 316). Preliminary results indicate that, as in peripheral sensory neurons (Dunlap and Fischbach 1981, J. Physiol., vol. 317), the long-lasting current is decreased by norepinephrine.

T-PM-B4 Ca^{2+} CHANNELS IN OSTEOSARCOMA CELLS. S.E. Guggino. Gerontology Research Center, National Institute on Aging, Baltimore, Maryland 21224.

The patch-clamp technique was used to characterize the channels present in the osteoblast-like clonal rat osteosarcoma cell line ROS 17/2.8. The most frequently occurring channel in cell-attached patches with Na^+ Ringer free of divalent cations in the pipette was an inward channel with a single channel conductance (γ) of 27 pS. The γ decreased to 12 pS when Na Ringer containing 1 mM Ca^{2+} and Mg^{2+} was present in the pipette. In cell-excised patches with 10^{-7} M Ca^{2+}, 1 mM Mg^{2+} K^+ Ringer in the pipette and Na^+ Ringer free of divalent cations in the bath, the γ was 14 pS with a reversal potential of -23 mV with respect to pipette ground. Upon addition of 10^{-7} M Ca^{2+} and 1 mM Mg^{2+} to the bath the γ decreased to 3 pS and the reversal potential shifted to -87 mV close to the Nernst potential for Na^+. When bath Ca^{2+} was raised to 1 mM the γ was further reduced and the reversal potential shifted towards the Nernst potential for Ca^{2+}. In cell-excised patches with K^+ Ringer in the pipette and Na^+ Ringer containing no divalent ions in the bath, the probability of channel opening was decreased 60% by 25 μM verapamil an effect accounted for in part by a 50% decrease in mean open time. Desmethoxyverapamil 1 μM also caused a decrease in probability of opening. The results of ion substitution and inhibitor block suggest that this channel has characteristics associated with Ca^{2+} channels found in excitable tissues.

T-PM-B5 TWO POPULATIONS OF Ca CHANNELS IN BOVINE ADRENAL GLOMERULOSA CELLS. C.J. COHEN#, R.T. McCARTHY, P.Q. BARRETT* & H. Rasmussen*. Miles Inst. Preclin. Pharmacol. & *Dept. of Medicine, Yale Univ., New Haven, CT. (#Present address: Merck Sharp & Dohme, Rahway, NJ 07065).

Ca channel currents were studied in freshly dispersed bovine adrenal glomerulosa cells using the whole cell variation of the patch electrode voltage clamp technique. All cells contained a population of Ca channels that deactivate slowly ($\tau \cong 17$ ms at -45 mV). These channels are similar to the transient Ca channels that are found in GH, A10 and A7r5 cells. The curves describing steady state activation and inactivation overlap, so that there is a steady state current through these channels. The steady state current increases with potential from -70 to -40 mV, and then decreases with further depolarization. Ca dependent aldosterone secretion has a similar dependence on voltage when stimulated by increasing bath K. Nitrendipine block of the transient Ca channels is voltage dependent, and can be accounted for by the modulated receptor theory, with $K_d \cong 170$ nM for the inactivated state and >1 μM for the rested state. Nitrendipine block of aldosterone secretion in normal and high K is quantitatively consistent with the block of transient Ca channels. 10 nM angiotensin II increases the transient Ca channel currents by $\approx 50\%$ and slows the rate of deactivation by 30-100%. $\approx 20\%$ of the cells also had a second component of Ca channel current that deactivates rapidly ($\tau \cong 1.2$ ms at -35 mV) and activated and inactivated at more positive potentials than the transient Ca channels. (-) BAY k 8644 slowed the rate of deactivation of these channels, but not of the transient Ca channels. Hence, these channels probably account for the high affinity binding sites for ^{3}H-nitrendipine reported in adrenal glomerulosa cells. Our studies show that the transient Ca channels are the physiologically more important Ca channel for mediating Ca dependent aldosterone secretion.

T-PM-B6 HIGH AFFINITY NIMODIPINE BLOCK OF Ca CHANNELS IN CLONAL VASCULAR SMOOTH MUSCLE CELLS. R.T. McCarthy and C.J. Cohen*. Miles Inst. for Preclin. Pharmacol., New Haven, CT 06509

Ca channel currents were studied in A10 and A7r5 clonal rat thoracic aorta muscle cells. The whole cell variation of the patch electrode voltage clamp technique was used. Two types of Ca channels were found in each cell line that have different activation, inactivation and deactivation kinetics and different susceptibilities to block by nimodipine. The 2 types of Ca channels are termed "slowly inactivating" and "transient". Nimodipine block of the slowly inactivating Ca channels is time and voltage dependent. As in our studies with GH_4C_1 cells, the kinetics of nimodipine block are accounted for by a model that postulates 1:1 drug binding to open Ca channels; the apparent dissociation constant (K_O) in A7r5 and A10 cells is 16-45 pM. In A7r5 cells, the rate of onset of nimodipine block increases >100-fold as the potential is increased from -40 to +30 mV, as predicted by the model. The apparent association rate (f) is 1.4×10^9 $M^{-1}s^{-1}$; the dissociation rate (b) is 0.024 s^{-1}. In GH_4C_1 cells, K_O is 30X larger; b is only twice as fast, but f is 15 times slower. The much larger f in A7r5 cells can be accounted for by differing lipid composition in the plasmalemmas of the 2 cell lines, so that nimodipine diffuses much faster or has a larger partition coefficient into the plasmalemma of A7r5 cells than for GH_4C_1 cells. If the lipid composition of the plasmalemma determines the relative potency of nimodipine block, then channels common to A7r5 and GH cells should be more potently blocked by nimodipine in A7r5 cells. Consistent with this prediction, we found that nimodipine block of the transient Ca channels is voltage dependent and can be accounted for by preferential binding to inactivated channels with $K_I \cong 140$ nM in A7r5 cells; in GH_3 cells, $K_I \cong 400$ nM.

*(Present address: Merck Sharp & Dohme, Rahway, NJ 07065)

T-PM-B7 MONOCLONAL ANTIBODIES AGAINST THE DIHYRDOPYRIDINE RECEPTOR FROM RABBIT SKELETAL MUSCLE. Albert T. Leung, Toshiaki Imagawa and Kevin P. Campbell. Dept. of Physiology and Biophysics, University of Iowa, Iowa City, IA 52242.

Monoclonal antibodies capable of immunoprecipitating [^{3}H]PN200-110 labeled dihydropyridine receptor of rabbit skeletal muscle have been produced. BALB/C mice were immunized with skeletal muscle membrane vesicles enriched in the dihydropyridine receptor and boosted with partially purified dihydropyridine receptor. Hybridoma supernatants were screened for the production of anti-dihydropyridine receptor antibodies with an immunodot assay. Antibodies from hybridoma colonies that reacted positively against the partially purified dihydropyridine receptor were screened with an immunoprecipitation assay for anti-dihydropyridine receptor activity. Goat-anti-mouse IgG Sepharose beads preincubated with culture media or ascites fluid from these cell lines were used to immunoprecipitate [^{3}H]PN200-110 binding activity from digitonin solubilized membranes. The amount of [^{3}H]PN200-110 binding activity in the immunoprecipitate was determined by counting the beads directly and the amount in the void was determined by a polyethylene glycol precipitation assay. The dihydropyridine binding activity in the void of the beads was found to correlate inversely with that in the immunoprecipitate. Four monoclonal antibodies were found to immunoprecipitate [^{3}H]PN200-110 binding activity from solubilized membranes and all of them stained a protein with a relative molecular mass of 170,000 Da on immunoblots. We propose that this 170,000 Da protein is tightly associated with the dihydropyridine binding subunit of the receptor and is possibly a subunit of the calcium channel. (Supported by NIH-HL-37187.)

T-PM-B8 IDENTIFICATION AND PURIFICATION OF COMPONENTS OF THE 1,4-DIHYDROPYRIDINE RECEPTOR. Alan H. Sharp, Toshiaki Imagawa, Albert T. Leung, Alyson K. Fletcher and Kevin P. Campbell. Dept. of Physiology and Biophysics, University of Iowa, Iowa City, IA 52242.

Photoaffinity labeling with [^{3}H]azidopine has been used to identify, characterize and monitor purification of the molecular components of the 1,4-dihydropyridine receptor in skeletal and cardiac muscle. Photoaffinity labeling of isolated T-tubular membranes from rabbit skeletal muscle resulted in the covalent incorporation of [^{3}H]azidopine into proteins of approximately 170,000 and 30,000 Da. These proteins were not labeled in the presence of excess unlabeled nitrendipine. The light sarcoplasmic reticulum membrane fraction of skeletal muscle, which has little [^{3}H]PN200-110 binding activity, was not specifically labeled by [^{3}H]azidopine. The 1,4-dihydropyridine receptor of skeletal muscle, labeled to high specific activity with [^{3}H]azidopine, was solubilized with digitonin and adsorbed to WGA-Sepharose. Proteins were eluted with N-acetylglucosamine, subjected to SDS-PAGE and transferred to nitrocellulose membranes. Bound azidopine was visualized on immunoblots after reaction with anti-dihydropyridine antibodies, revealing specific labeling of a single band of approximately 170,000 Da. Blots were also probed with monoclonal antibodies capable of immunoprecipitating [^{3}H]PN200-110 labeled dihydropyridine receptor. These methods have been used to clarify the identity of the skeletal muscle dihydropyridine receptor and to monitor its further purification. These techniques are also being used to identify and characterize components of the canine cardiac dihydropyridine receptor. In isolated canine cardiac sarcolemmal membranes [^{3}H]azidopine specifically photoaffinity labeled proteins of approximately 185,000 and 60,000 Da. (Supported by NIH HL-37187).

T-PM-B9 VOLTAGE CLAMP PULSES IN SQUID AXONS AFFECT $[Ca]_i$. J. Requena, J. Whittembury and L. J. Mullins. Centro de Biociencias, IDEA, Apartado 17606, Caracas 1015A, Venezuela; Dept. of Physiology, Case Western Reserve University, Cleveland, Ohio and Dept. of Biophysics, University of Maryland, 660 W. Redwood Street, Baltimore, MD. 21201.

Squid giant axons were injected with aequorin and tetraethylammonium and had pH sensitive electrodes and current and voltage electrodes inserted. The axons were bathed in a solution containing 150 mM Na, K, Tris and either normal [Ca] or zero Ca. Voltage clamp pulses were delivered repetitively to the extent necessary to produce a change in the aequorin light signal or the membrane potential was held at values that represented deviations from the normal resting membrane potential in 150 mM K ($\sim$-15 mV). Axons were subjected to voltage clamp pulses while in Ca-free seawater in order to examine the extent to which such pulsing might affect intracellular Ca release by the production of changes in pH_i. The results indicated that depolarizing pulses of several seconds duration and an amplitude of about 20 mV caused significant changes in pH_i and in $[Ca]_i$ even though Ca_o was zero. Pulses of a duration of 10 msec or less and with amplitudes of 120 mV at repetition rates of 20/s were without effect on $[Ca]_i$ under similar circumstances.

Using pulses of a duration such that internal pH was not significantly affected, we show that the magnitude of the increase in Ca entry from either 1 or 3 mM Ca seawater varied with $[Na]_i$ and that half activation of such signals occurred at Na_i = 26 mM, a value identical to that obtained both for steady depolarization with KCl or with Na-free solutions. Hyperpolarization with similar pulse protocols decreased the aequorin light signal. These findings clearly show that Ca entry during depolarizing pulses is principally via Na/Ca exchange.

T-PM-B10 CALCIUM CHANNEL CURRENTS IN CULTURED RETZIUS CELLS OF THE LEECH.
Richard J. Bookman and Yuan Liu. Dept. of Pharmacology, Biocenter, University of Basel, CH-4056, Switzerland.

Single Retzius cells (70-100μm) can form a serotonergic synapse with a pressure sensory (P) neuron in culture (J.Physiol.,323,195-210). We have studied the voltage-dependent calcium conductance of the 'pre-synaptic' Retzius cell. Macroscopic currents were recorded with a two-electrode voltage clamp technique using a ~0.5 MΩ gigasealed patch pipette as the current electrode. In response to voltage step commands, membrane potential settled in 30-120μs. Calcium channel currents were isolated from other currents by bathing the cells in 75mM $BaCl_2$, 50mM TEA-Cl, 20mM HEPES, pH 7.4 and with a pipette solution containing 100mM CsCl, 50mM TEA-Cl, 2mM EGTA, 20mM HEPES, pH7.4. Currents during depolarizing pulses from a holding potential of -60mV activated with sigmoidal kinetics (t 1/2: 6ms at -10mV, 2.5ms at +30mV), peaked at ~+15mV, and deactivated with bi-exponential kinetics (τ_1~200us; τ_2~2.2ms). Peak current amplitude depended on the permeant divalent ion in the order Sr>Ba>Ca. Inactivation during 300ms pulses was minimal and slow in Ba, but larger and faster (though still incomplete) in Ca or Sr. Cadmium blocked the Ca channel current and revealed a small transient outward current with no reversal potential that may be due to charge movement in the membrane.

Supported in part by a grant from the Swiss National Fund to J.G.Nicholls.

T-PM-B11 CALCIUM CHANNELS IN MOUSE 3T3 AND HUMAN FIBROBLASTS. Chinfei Chen and Peter Hess, Depts. of Physiology and Neurobiology, Harvard Med. School, Boston MA 02115.

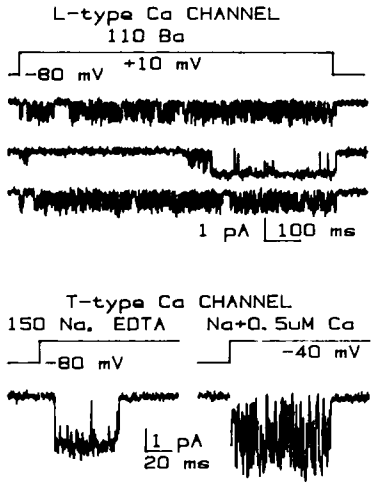

Ca entry has recently been implicated in the control of cell growth and gene expression. We have found two kinds of voltage dependent Ca channels in mouse 3T3 fibroblasts. Whole cell currents contain a slowly inactivating, dihydropyridine (DHP) sensitive component activated at positive potentials (L-type channel) and a low-voltage activated, DHP resistant, transient current (T-type channel). Human foreskin fibroblasts contain L- but not T-type Ca channels. L-type activity (25 pS with 110 mM Ba, top Fig.) is characterized by the typical bursts of brief events, occasional periods of long lasting openings, and frequent failures to open after depolarization. The conductance of T-type channels is 8 pS with 110 mM Ba or Ca and 50 pS with 150 mM Na in the absence of divalent ions. Submicromolar Ca blocks the Na movement (bottom Fig.) suggesting that, like L-type channels, T-type channels select for Ca by high affinity binding.

We have found that activators of C-kinase (TPA and OAG) can increase L-type currents (range 10-100%). Thus, an important role of Ca channels in fibroblasts may be to mediate effects of growth factors known to act through the C-kinase pathway.

T-PM-B12 SELECTIVITY OF THE CALCIUM BINDING SITES OF A Ca^{2+}-ACTIVATED K^+ CHANNEL.

A. Oberhauser, O. Alvarez, and R. Latorre. Centro de Estudios Científicos de Santiago, P.O. Box 16443, Santiago 9, Chile and Department of Biology, Faculty of Sciences, Santiago, Chile.

We have studied the selectivity to divalent cations of the Ca^{2+} binding sites of a large unitary conductance Ca^{2+}-activated K^+ channel incorporated into planar bilayers. We studied the efectiveness of the several divalent cation in activating the channel by measuring the fraction of time that channel remains open at different voltages and divalent cations concentrations.

We found that Ca^{2+} is the most effective cation followed by Cd^{2+}, Sr^{2}, Fe^{2+} and Co^{2+} with relative efficacies of 1.0, 10^{-2}, 5.5×10^{-3}, 1.3×10^{-3}, 9×10^{-4} respectively, Mg^{2+}, Ni^{2+}, Cu^{2+}, Zn^{2+}, Hg^{2+}, Pb^{2+}, and Ba^{2+} are ineffective. In the presence of these divalent cations the voltage dependence of channel activation is the same as that found with Ca^{2+}. Hill plots of the open-closed equilibrium suggest that the minimum number of divalent cations bound to the channel for complete activation vary from one (Fe^{2+}) to four (Cd^{2+}). It is concluded that effectiveness of a divalent cation in activating the Ca^{2+}-activated K^+ channel is related to its ionic radius, and that the site of activation can accomodate ions of radii between 0.072nm (Co^{2+}) and 0.113 nm (Sr^{2+}). In the presence of contaminant amounts of Ca^{2+} (3 to 10 uM), 4mM Mg^{2+} and 500 uM Ni^{2+} increase the Hill number for Ca^{2+} to four. These results suggest the presence of an allosteric site which is able to reveal new binding sites for Ca^{2+} upon binding of Mg^{+2} or Ni^{+2}.

Supported by NIH grant GM35981-01 and the Tinker Foundation.

T-PM-B13 CALCIUM-PERMEABLE CHANNELS ACTIVATED BY EXTRACELLULAR ATP IN SINGLE ARTERIAL SMOOTH MUSCLE CELLS. C.D. Benham and R.W. Tsien. Department of Physiol. Yale Univ. New Haven, CT 06510.

"Receptor-operated Ca channels" have long been postulated as a pathway for Ca entry into smooth muscle but there has been little direct evidence for their existence. We have obtained whole cell and single channel recordings of ATP-activated Ca currents in single smooth muscle cells dissociated from rabbit ear artery. Puffer applications of ATP (0.1-10 μM) evoked clear inward currents with isotonic $CaCl_2$ (110 mM) in the external solution. Unlike voltage-gated Ca channels, the ligand-gated Ca current can be seen even at very negative potentials (-140 mV), is not blocked by 5 μM nifedipine or 0.5 mM Cd and is less selective for Ca over Na. With 2 mM Ca plus 130 mM N-methylglucosamine outside and 130 mM Na inside, reversal potential determinations gave an average value of -30.6±1.6 mV (s.e.m., n=5), corresponding to a 12:1 selectivity for Ca over Na ions as calculated from the Fatt-Ginsborg version of the Goldman equation. In outside-out patches at -140 mV (Figure), unitary currents had amplitudes of ~0.6 pA with 110 mM external Ca or 110 mM Ba, and ~1.8 pA with 130 mM Na plus 1 mM EGTA.

The ATP receptor was activated by the non-hydrolyzable ATP analogs ATP-γ-S and AMP-CPP. The receptor seems closely coupled to the channel: reversible activation by external ATP was observed in outside-out patches regardless of whether the cytoplasmic solution lacked GTP or contained GTP-γ-S, arguing against involvement of a GTP-binding protein; channels in cell-attached patches were not activated by applying ATP to to the rest of the cell, arguing against mediation by a readily diffusible second messenger.

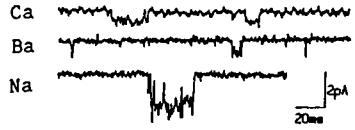

T-PM-B14 CA CHANNELS IN CELL BODIES, GROWTH CONES AND AXONS OF FROG SYMPATHETIC NEURONS STUDIED WITH CA IMAGING AND SINGLE CHANNEL RECORDING. D. Lipscombe, M. Poenie*, H. Reuter, R. Y. Tsien* & R. W. Tsien, Dept. of Physiology, Yale Univ. Sch. of Med., New Haven CT 06510 and *Dept. Physiology-Anatomy, U.C. Berkeley CA 94720. (Intro. by H. Affolter).

We have used a combination of Ca imaging and whole cell and single channel recordings to study Ca channels in neurons enzymatically dissociated from frog sympathetic ganglia. Recordings were obtained from neurons up to 5 days following dissociation. Imaging of free cytoplasmic Ca was carried out with the fluorescent Ca indicator fura-2. Experiments demonstrated resting values of free cytoplasmic Ca concentration (Ca_i) of the order of 0.1-0.2 μM and no clear evidence for standing gradients between cell body, axon and growth cones. Brief exposure to 30 mM K or repetitive focal extracellular stimulation of the cell body produced rises in Ca_i of up to 1 μM in cell body, axons and terminals that decayed over seconds. During stimulation, Ca_i was seen to spread inward from the surface of the cell body toward the center.

To establish which Ca channels contribute to Ca influx in various parts of the neuron, we carried out cell-attached patch clamp recordings with ~100 mM Ba as the charge carrier. We found L-type Ca channels (characterized by a slope conductance of 25 pS, availability even at depolarized holding potentials, and sensitivity to dihydropyridines) and N-type Ca channels (characterized by a smaller unitary amplitude and inactivation with steady depolarization to -40 mV). Both channel types were observed in cell-attached patch recordings from cell bodies, growth cones and axons. Ca channel activity was observed in 20 out of 22 cell-attached patch recordings from growth cones and in 3 out of 3 recordings from axons. Many patches showed simultaneous openings of several channels.

T-PM-C1 STRUCTURAL INVESTIGATION OF CYTOCHROME c MONOLAYERS ELECTROSTATICALLY BOUND TO ULTRATHIN LIPID MULTILAYERS. **J.M. Pachence, P.L. Dutton, and J.K. Blasie. Dept. of Chemistry, University of Pennsylvania, Philadelphia, PA 19104**

X-ray diffraction and spectroscopic techniques were used to characterize ultrathin fatty acid multilayers having a bound surface layer of cytochrome c. Three or five monolayers of arachidic acid were deposited onto an alkylated glass surface, using the Langmuir-Blodgett method. These fatty acid films were stored either in a 1 mM $NaHCO_3$ pH 7.5 solution or a buffered 10 μM cytochrome c solution, pH 7.5. After washing extensively with buffer, the films were assayed for bound cytochrome c by optical spectroscropy. It was found that the number of bound cytochrome c molecules was 1.1 x $10^{13}/cm^2$, which is 10% less than the theoretical value for a close-packed cytochrome c monolayer. Optical linear dichroism was also used to show that the orientation of cytochrome c was restricted with respect to the multilayer surface. The protein was released from the film when treated with > 100 mM KCl solution. Meridional x-ray diffraction data were collected from the arachidic acid films with and without a bound cytochrome c layer. A box refinement technique, previously shown to be effective in deriving the profile structures of non-periodic ultrathin films, was used to determine the multilayer electron density profiles. The electron density profiles and their autocorrelation functions showed that bound cytochrome c resulted in an additional electron dense feature on the multilayer surface, consistent with a bound cytochrome c monolayer. The position of the bound protein relative to the multilayer surface was independent of the number of fatty acid monolayers in the multilayer. Future studies will utilize these methods to investigate the structures of membrane protein complexes bound directly to the surface of multilayer films.

T-PM-C2 STRUCTURAL STUDY OF MOUSE STRATUM CORNEUM AND EXTRACTED LIPIDS. Stephen H. White[1], Glen I. King[1], and Dorla Mirejovsky[2]. Dept. of Physiology and Biophysics[1], Univ. of Calif., Irvine, CA 92717 and Allergan Pharmaceuticals[2], Irvine, CA 92715.

The stratum corneum (s.c.) is the principal barrier to the permeation of the skin by water and drugs. It consists of many layers of keratin-filled corneocytes whose interstitial spaces contain a complex mixture of lipids which appear to form multilamellar structures by electron microscopy (Grayson and Elias, J. Invest. Derm. 78:128[1982]). Further, the interstitial lipids show endothermic phase transitions at about 40° and 60°C both in situ and in vitro (Rehfeld and Elias, loc cit, 79:1[1982]). We have performed a small-angle x-ray diffraction study of intact s.c. of nude mice (100% RH) and of s.c. lipid extracts (excess water). The intact s.c. at 25°C shows a strong lamellar powder pattern with a Bragg spacing of ~135Å, a faint line at ~9.8Å attributed to keratin, and two strong sharp high-angle lines at 4.15Å and 3.75Å attributed to the interchain lipid spacings. These latter two lines, but not the 9.8Å line, are also observed in lipid extracts. The small-angle pattern of the extracts has a much more complex pattern. The largest Bragg spacing observed is ~62Å and preliminary indexing suggests two coexistent lamellar phases. The presence of a protein component amongst the lamellae of the lipid is a possible explanation for the different low angle patterns in vitro and in situ. Research supported by Allergan and the NIH.

T-PM-C3 Small Angle Neutron Scattering Study of Brij-58 Micelles

J. Schefer,* R. V. McDaniel** and B. P. Schoenborn *,**
*Department of Biology, Brookhaven National Laboratory, Upton, NY 11973
**Department of Biochemistry, Columbia University, NY, NY 10032

Brij-58 is a nonioic polyoxethylene detergent (Molecular weight 1123) used to solubilize membrane proteins such as Na/K ATPase [1,2,3]. Small angle neutron scattering measurements were performed on .2 and .4 weight % Brij-58 solutions in order to determine molecular weight and shape of the micelles. 3.2 vol % glycerol have been added in order to simulate the storage buffer used in membrane experiments. Our data is consistant with a cylindrical model of 250,000 $Å^3$ volume containing 60 Brij-58 monomers. The linear behavior of the Stuhrmann plot (Radius of gyration Rg^2 vs inverse contrast) indicats a two shell model, built by a central hydrocarbon core and an outer shell of the head groups intermixed with bulk water. This model explains both, volume and Rg of the Guinier plots. The radius of gyration at indefinite contrast has been observed to be 31.5 Å.

[2] Esman M., Skou J.C. and Christiansen C., Biochim. Acta 567:410 (1979).
[1] Pachence J.M., Edelman I.S. and Schoenborn B.P., J. Biol. Chem. in press (1986).
[3] Craig W., Biochemistry 21:2667 (1982)

Work has been supported by NIH Grant AM31089-05.

T-PM-C4 THE TWO-STAGE MODEL OF GLOBULAR MEMBRANE PROTEIN FOLDING. Donald M. Engelman and Jean-Luc Popot*, Dept. of Molecular Biophysics and Biochemistry, Yale University, *College de France and Institut de Biologie Physico-Chimique, F-75005 Paris.

It is suggested that two stages are involved in the folding of many globular membrane proteins. In the first stage, independently stable helices are formed across the hydrophobic region of the membrane lipid bilayer. In the second stage the helices interact with one another to give a functional, globular membrane protein. The folding argument is derived from both theoretical and experimental perspectives, many of which concern work on bacteriorhodopsin.

It is striking that the known transbilayer structural elements in helical membrane proteins are well predicted by polarity analyses that do not consider helix-helix interactions in the folded structure; helices are treated independently. Additional interactions, such as those provided by polar effects, packing interactions with the lipid bilayer, interactions with prosthetic groups, or the constraints of polypeptide links between helical segments must be involved to some extent in producing a final, folded structure from the helical segments. Experimental evidence concerning the two stage hypothesis will be discussed.

T-PM-C5 INTERDIGITATED LIPID PHASES FRACTURE WITHIN THE HYDROPHOBIC REGION. M.J. Costello, T.J. McIntosh, S.A. Simon, A.D. Magid and E.K. Williamson. Departments of Anatomy, Anesthesiology and Physiology, Duke University Medical Center, Durham, NC 27710

Gel phase dipalmitoylphosphatidylcholine (DPPC) bilayers can be induced to form interdigitated phases by addition of small molecules such as chlorpromazine and glycerol. X-ray diffraction has shown that the acyl chains from one monolayer penetrate to the first or second CH_2 of the apposing monolayer. Because the interpenetration of apposing acyl chains could be expected to influence the fracture properties of the lipid, interdigitated phases were examined with the freeze-fracture/etch technique. Samples shown by x-ray diffraction to be in an interdigitated phase were ultra-rapidly frozen in thin layers sandwiched between copper sheets. Fractured samples were replicated with platinum/carbon. DPPC in 100% glycerol produced one smooth fracture surface per lipid layer. Steps were observed from these surfaces to the surrounding fluid phase which was smooth but clearly different in texture from the lipid fracture surface. Similar patterns were obtained for DPPC-chlorpromazine (mole ratio 2:1) interdigitated phases. For some of the chlorpromazine samples TMV was included to help identify the aqueous layer. The TMV rods were visible as deformations in surrounding bilayers and as hollow tubes in oblique fractures through the aqueous layer. In etched samples the rods were more clearly seen since surrounding water was partially removed. Etching did not alter the fracture faces but exposed new surfaces which blended in with the aqueous layers containing the TMV molecules. Thus the fracture patterns of interdigitated phases are similar to those of normal lipid bilayers indicating that fracturing pulls apart the interdigitated monolayers producing hydrophobic fracture surfaces.

T-PM-C6 SEPARATION AND QUANTIFICATION OF THE HYDRATION AND STERIC FORCES BETWEEN LECITHIN BILAYERS. T.J. McIntosh, S.A. Simon, and A.D. Magid, Departments of Anatomy and Physiology, Duke University Medical Center, Durham, NC 27710.

Egg lecithin bilayers, subjected to vapor and osmotic pressures, P, in the range of $4x10^5$ to $2x10^9$ dynes/cm^2 have been analyzed by x-ray diffraction methods. The lamellar repeat period, d, decreases linearly with lnP until there is a break in the plot at d≈51Å. Fourier synthesis analysis provides the bilayer thickness, d_b, and the fluid thickness, d_f, for each P. A plot of lnP versus d_f has two distinct, linear regions: region I from d_f≈13Å to d_f≈5Å with a decay length of λ≈1.7Å, and region II from d_f≈5Å to d_f≈1.5Å, with λ≈0.8Å. The number of waters per lipid molecule (n) has been obtained from our x-ray phase diagrams and from adsorption isotherms of Jendrasiak and Hasty (BBA 337, 79). Over this entire pressure range we obtain a linear plot for lnP versus n. This shows that the hydration pressure, P_h, is an exponential function of water content, from n=23 to n=2. This indicates that the break in the plot of lnP versus d_f is not due to a discontinuity in P_h, but is due to the onset of steric hindrance between apposing lipid headgroups. Therefore, region I corresponds solely to P_h, whereas region II corresponds to the sum of P_h and a steric pressure, P_s. These data provide an estimate for both the range and magnitude of P_s between lecithin bilayers. The d_f where the onset of P_s is observed is consistent with the NMR data of Hauser (BBA 646, 203), which indicate that the PC head group rotates so that the trimethylammonium extends 2 to 3Å farther into the fluid space than when it is coplanar with the phosphate moiety. The measured magnitude of P_s is in general agreement with models of steric interactions between polymer chains.

T-PM-C7 DISORDER IN MEMBRANE-PAIR ASSEMBLIES.

C.R. Worthington, Depts. of Biological Sciences and Physics,
Carnegie-Mellon University, Pittsburgh, PA 15213

Multi-layered membrane-pair assemblies may contain lattice disorder and positional disorder. We treat the case of positional disorder. Positional disorder is due to a variation in the separation of the two membranes comprising the membrane pair and it gives rise to diffuse scattering which is superimposed on the X-ray data. In previous work (Biophys. J. 49:98, 1986) a solution to the diffuse scattering problem using an iterative procedure has been described. The starting point of the analysis is the set of integrated intensities which includes the unwanted diffuse scattering and a particular set of phases. The end result is a set of undistorted intensities together with an estimate of the positional c-parameter. Our procedure has been verified using model X-ray data. Only a few iteration steps are needed to obtain the correct c-value. Note that in the model analysis we started with the correct phases. We have also obtained a set of the positional c-parameters for nerve myelin, swollen nerve and photoreceptor membranes (Biophys. J. 49:98, 1986). At this time, we treat the dependence of the derived c-parameters on the starting phase choices. We find the diffuse scattering component to be fairly insensitive to the phases. Interestingly, the choice of phases for the three membrane systems so far studied is of no consequence because these three systems have little or no positional disorder.

T-PM-C8 **NEUTRON SCATTERING STUDIES OF ISOLATED SUBUNITS FROM NA/K ATPASE.**

R. V. McDaniel (1,2), J. Schefer (2), D. Elstein (1), B. P. Schoenborn (1,2), and I. S. Edelman (1). 1-Dept. of Biochemistry, Columbia University, NY, NY, and 2-Dept. of Biology, Brookhaven National Laboratory, Upton, NY.

Alpha and beta subunits were isolated from guinea pig renal Na/K ATPase by electroelution from SDS-PAGE gels. Protein was solubilized in buffers of 100, 200, and 350 mM monovalent salt concentration, containing 0.02% SDS. Small angle neutron scattering indicated that the molecular weight of the protein-SDS complexes depended upon salt concentration. The molecular weight data are consistent with a monomeric alpha subunit plus 120 SDS molecules in 350 mM NaCl, and a monomeric beta subunit plus 210 SDS molecules in 100 mM NaCl. The low matchpoints (~25% D2O) and the small radii of gyration also indicate that SDS is associated with the protein. Increasing the salt concentration favors dimers of the beta subunit and monomers of the alpha subunit, as expected from the relative hydrophobicity of the two subunits.

Supported by NIH grant AM31089-05.

T-PM-C9 DIFFERENCES IN ELECTRON MICROSCOPIC IMAGES OF THE MITOCHONDRIAL CHANNEL, VDAC, CAUSED BY ITS EFFECTORS.

C.A. Mannella and J. Frank, Wadsworth Center for Laboratories and Research, New York State Department of Health, Albany, NY 12201.

The channels in outer membranes isolated from Neurospora mitochondria can occur in crystalline 2-D arrays. We have examined the effects of three effectors of the channel (VDAC) on electron microscopic images of negatively stained arrays. (1) Succinic anhydride abolishes the V-dependence of VDAC and reverses its normal anion selectivity, suggesting that lysines are involved in both mechanisms (Doring and Colombini, J. Memb. Biol. 83:81). Pretreatment of VDAC arrays with succinic anhydride dramatically changes images of arrays stained with phosphotungstate (PTA) but not uranyl acetate (UA). Since PTA and not UA selectively stains basic amino acids, such changes may arise from succinylation of exposed lysines. Comparison of correlation-averaged images of PTA-stained VDAC arrays +/- succinic anhydride suggests the presence of a lysine-rich region at the opening of each channel. (2) A synthetic polyanion inhibits VDAC conductance (Yeung et al., Biophys. J. 49: 206a). Pretreatment of VDAC arrays with 5 μM polyanion causes rapid loss of long-range order. This may be the result of a large-scale conformational change in the channel (e.g. closure) or disruption of electrostatic interactions between the array components. Correlation-averaging has been successfully applied to partially disordered fields of UA-stained VDAC arrays pretreated briefly with the polyanion. Increasing lattice disorder appears to be associated with increased stain accumulation in the vicinity of the channel openings. (3) DCCD apparently inhibits the hexokinase-binding activity of VDAC in rat liver mitochondria (Nakashima et al., Biochemistry 25:1015). DCCD has no obvious effect on projection images of the fungal VDAC array. (Supported by NSF grants PCM 83-15666 and PCM 83-13045.)

T-PM-C10 COMPARISON OF THE MOLECULAR INTERACTION OF A CALCIUM CHANNEL ANTAGONIST (NIMODIPINE) AN AGONIST (BAY K 8644) WITH MEMBRANE BILAYERS. L. Herbette and G. Gonye, Univ. of Conn. Health Center, Biomolecular Structure Analysis Center, Farmington, CT 06032.

Nimodipine, a 1,4-dihydropyridine calcium channel antagonist, and Bay K 8644, a 1,4-dihydropyridine calcium channel agonist, bind to receptors in cardiac sarcolemmal membranes. This study sought to provide a structural comparison for the interaction of these drug substances with a membrane bilayer. Previous studies with the 1,4-dihydropyridine calcium channel antagonists indicated that these agents locate their membrane receptors by first partitioning into the membrane and then diffusing in a plane in the membrane to a receptor site within the membrane bilayer. Membrane partition coefficients of $5x10^3$ (nimodipine) and 10^4 (Bay K 8644), were determined for these agents in skeletal muscle sarcoplasmic reticulum membranes devoid of specific receptors for these agents. The apparent on-rate for binding of nimodipine to sarcolemmal receptor was measured as a function of the viscosity of the aqueous medium in order to support or refute a direct aqueous pathway for the binding of nimodipine to its receptor. For nimodipine, the apparent binding rate was nearly independent of the viscosity of the aqueous medium, thus refuting an aqueous pathway. Kinetic measurements and structural studies are being carried out with Bay K 8644 to ascertain if the nonspecific interaction of the agonist is similar to the antagonist. Previous neutron scattering studies indicated that nimodipine was located near the hydrocarbon core/water interface of the membrane bilayer in skeletal muscle sarcoplasmic reticulum membranes. These data support the contention that the antagonists and the agonists use a lipid bilayer pathway for locating their membrane receptor. Supported by HL-33026, Whitaker Foundation and the Patterson Trust Foundation. Dr. Herbette acknowledges his affiliation as an Established Investigator of the AHA.

T-PM-D1 PROTEIN FOLDING AS A MARKOV PROCESS. Zhenqin Li and Harold A. Scheraga, Baker Laboratory of Chemistry, Cornell University, Ithaca, New York 14853-1301.

We assume (1) that protein folding is a Markov process, with Boltzmann transition probabilities, as a scheme used in Nature to overcome the multiple-minima problem. We further assume (2) that, as a consequence of natural selection, a native protein exists as a unique structure (undergoing small fluctuations), and therefore that the Markov process converges to this unique structure. A Minimization-Metropolis Monte Carlo (MMMC) procedure is used to implement the first hypothesis; validity of the second assumption would guarantee the convergence of the MMMC procedure to the native structure from any starting conformation. Preliminary tests of the MMMC procedure on Met-enkephalin, using the ECEPP algorithm (in the absence of water), led to a fluctuating β-bend structure with an energy lower than that of any previously computed one. Inclusion of water (by means of a hydration shell model) led to a markedly different (essentially extended) structure with large fluctuations. We are now extending the computations to larger polypeptides to examine the upper limit of size that can be treated by this procedure with presently available computing systems.

T-PM-D2 METHOD FOR QUICKLY GENERATING RANDOM CONFORMATIONS OF RING-LIKE STRUCTURES FOR SUBSEQUENT ENERGY MINIMIZATION OR MOLECULAR DYNAMICS: APPLICATION TO ANTIBODY HYPERVARIABLE LOOPS. P.S. Shenkin, D.L. Yarmush, R.M. Fine and C. Levinthal, Dept. of Biological Sciences, Columbia University, New York, NY 10027.

To have a reasonable chance of finding the conformation of minimum energy for a molecule containing more than a few atoms, it is necessary to perform minimization (coupled or not to more exhaustive search procedures such as dynamics or Monte Carlo calculations) from many starting conformations. Where there are constraints on the conformations -- as in a ring molecule, or a loop starting and ending in conserved regions in one of a class of homologous proteins -- generating many such starting conformations, all satisfying the constraints, quickly has been a problem in the past. We have devised an algorithm, which we call random tweak, which performs this task in the context of a torsional description of a molecule, and have applied it to predicting the conformations of the complementarity determining regions (CDRs) of antibodies. The method involves setting each dihedral angle of the molecule to a random value, then using a linearized LaGrange multiplier method to enforce the constraints. For the CDRs of mcpc603, one structure is produced every ~2 CPU-seconds on a VAX 11/780. The implementation and performance of this algorithm will be presented, together with a discussion of how it is used and how many structures are necessary to fill conformational space.

T-PM-D3 ENERGETICS OF MODEL REARRANGEMENTS IN PROTEINS. Lyndon S. Hibbard, Departments of Radiology and Anesthesia, The M.S. Hershey Medical Center, The Pennsylvania State University, Hershey, Pennsylvania 17033.

The conformational potential energy of a protein includes contributions from steric factors, dispersion and electrostatic forces, hydrogen bonding, and solvent entropy (hydrophobic effect). Each of these components may undergo significant changes during folding, complexation, or the structural fluctuations associated with chemical function, and the gradients of these components may be considered as forces which impel or resist these changes. Following earlier precedents (Honig, et al., PNAS 73, 1974 (1976); Richmond and Richards, J. Mol. Biol. 119, 537 (1978)), the author has examined unhindered "model rearrangements" in proteins with the goal of obtaining at least qualitative answers to several questions. First, what is the relative importance of the components for a particular rearrangement, or type of rearrangement? For structures translated together from some distance, the hydrophobic free energy related to solvent accessible surface area undergoes large decreases beyond the range at which the van der Waals or electrostatic components change significantly. For rearrangements by bond rotations, the opposite result is often seen, probably because parts of the structures are close together throughout the transition. Second, can potential well shapes reveal something new about interaction complementarity or mechanisms? Plots of potential energy versus dihedral angle or translation distance range from linear to sigmoidal, to more complex forms, hinting at cooperativity and presenting a picture of interaction specificity which has not been explored for larger peptides or proteins. Third, how is the order of serial rearrangements related to total system free energy? Studies of these questions are underway using interactive molecular graphics and programmed experiments.

T-PM-D4 ARTIFICIAL INTELLIGENCE TOOLS FOR THE STUDY OF PROTEIN STRUCTURE, Arthur L. Williams, Jr.(1) and Michael N. Liebman (1,2), Departments of Physiology and Biophysics (1,2) and of Pharmacology (2), Mount Sinai School of Medicine, New York, NY 10029.

We are developing an artificial intelligence system to analyze and predict protein structure. The system integrates molecular modeling with expert system design, pattern recognition, interactive molecular graphics and data base management. In this paper we describe some of the computational tools that we have developed to perform representation, analysis, and prediction of the three-dimensional structure of proteins. We have developed a dynamic-programming (DP) algorithm that matches a three-dimensional structure transform termed linear distance plot (LDP). The LDP is a profile of the local folding of a polypeptide chain. Application of the DP algorithm permits comparison of partial or entire protein structures by comparison of the LDPs of the proteins or protein fragments. The algorithm thus permits for direct comparison of proteins or protein segments and is being utilized to develop a library of structural features of varying residue length. Sequence-dependent properties can also be represented by an analogous mapping procedure. These properties include hydropathy, chain flexibility, bulk hydrophobicity, conformational preference, hydration potential, bulk size, polarity, free energy of transfer to water, as well as others. A learning program is being developed to evaluate the correlation of properties intrinsic to the amino acid sequence with regions that are structurally equivalent. We envision that the ability to correlate properties that are intrinsic to the amino acid sequence with the structurally homologous regions of know protein structures will enable our development of rules with predictive capabilities.
This research was funded by a generous grant from ImClone Systems, Inc.

T-PM-D5 THE WATER STRUCTURE AROUND PROTEINS: CRAMBIN AS A MODEL. Martha M. Teeter, Dept. of Chem., Boston College, Chestnut Hill, MA 02167.

Crystals of the hydrophobic protein crambin (5000 MW) diffract to better than 1.0 Å resolution and have more than 80% of the solvent in the crystal ordered. This protein provides an excellent opportunity to study the distribution of water molecules at a protein surface in atomic detail that is not generally available for other protein crystal structures. Water is important not only in stabilizing a protein in its folded conformation but also can contribute to an enzyme's activity through binding at its active site. The function of the plant protein crambin is not yet known, however it is homologous to the membrane-active plant toxins purothionin (from wheat germ) and viscotoxin (from mistletoe), which have been shown to bind calmodulin and appear to bind lipids.

Crambin's X-ray diffraction data to 0.945 Å at 300 K and to 0.83 Å at 140 K have been collected and the model of the structure has been refined. Two types of water networks are formed: chains at the hydrophilic protein surface and rings, primarily pentagons, at the hydrophobic protein surface. Insight into role of water in stabilizing the protein is gained which applies to stablization of proteins in general and to modelling the effect of changes on protein conformation on this water structure. The resulting atomic picture of the role of water at a protein surface permits more realistic predictions of hydration at a protein surface to be made.

T-PM-D6 CURRENT PROGRESS ON THE STRUCTURE OF ALPHA$_1$-PUROTHIONIN. Marc Whitlow and Martha M. Teeter, Department of Chemistry, Boston College, Chestnut Hill, MA 02167. (Introduced by Dr. Donald Plocke, S.J.).

The current progress on the X-ray structure determination of the protein alpha$_1$-purothionin will be described. Alpha$_1$-purothionin crystallizes in the tetragonal space group I422, a = b = 53.48 Å, c = 69.56 Å, V = 198,950 Å^3, Z = 16. Data set has been collected both crystallographic area detector at MIT and Nicolet P2$_1$ diffractometer. We have attempted to solve the structure in two ways: i) We have predicted the structure of alpha$_1$-purothionin from its homology with crambin using molecular graphics, potential energy minimization and "quenching dynamics". Molecular replacement of these models have been examined. ii) From the anomalous scattering of the four disulfide groups. We will report the solution of disulfide positions and the figure of merit Fp map based on this solution.

T-PM-D7 **ROLE OF ELECTROSTATIC INTERACTIONS IN ASSEMBLY OF E.COLI ASPARTATE TRANSCARBAMYLASE.** M. Glackin and N. Allewell, Wesleyan University, Middletown, CT 06457; J. Matthew, Dupont Experimental Station, Wilmington, DE 19898.

Aspartate transcarbamylase has five unique interchain interfaces: c_1c_3, c_1c_4, r_1r_6, c_1r_1, and c_1r_4. The Matthew-Gurd discrete charge static solvent accessibility model (cf **Biochemistry 18,** 1919 (1979)) has been used to assess the electrostatic component of the free energy of forming these interfaces (ΔG_{el}) and to identify ionizable residues whose pK values are perturbed. Crystallographic coordinates (Ke et al., **Proc. Natl. Acad. Sci. USA, 81,** 4037 (1984)) were taken from the Brookhaven PDB. At pH 7 and I=0.02M, ΔG_{el} is greatest for c_1c_4 (-4.9 kcal) and smallest for r_1r_6 (-0.4 kcal). Corresponding values for c_1c_3, c_1r_1, and c_1r_4 are -4.2, -4.0 and -2.4 kcal, respectively. Virtually all ionizable groups undergo at least minor changes in pK values. Some perturbations extend to regions far removed from interfaces. Residues perturbed most strongly by formation of the c_1c_4 interface are located in the equatorial domain or near the polar-equatorial interface. pK values of Lys 164 and Tyr 165 on both chains shift by 2.1 and 1.0 pH units, respectively. When c_1 and c_3 dock, pK values of seven residues shift by more than 0.5 pH units; those of Tyr 98 and Asp 100 of c_1 shift by -2.0 and -1.8 pH units, respectively. Assembly of c_1r_1 strongly perturbs the "Zn finger" including Arg 130, whose pK value increases by 1.6 pH units. Docking of c_1r_4 perturbs the 240s loop through Asp 271 of c_1 and the Zn domain of r_4. Significant changes in pK values occur in residues of the allosteric domain. The pattern of residues affected by formation of these interfaces suggests that there are electrostatic channels of communication between binding sites. Supported by NIH grant AM-17335.

T-PM-D8 CALCULATION OF ELECTROSTATIC ENERGIES IN PROTEINS BY A FINITE DIFFERENCE METHOD. M.K. Gilson[1], K. Sharp[1], B. Honig[1], R. Fine[2], & R. Hagstrom[3].
[1]Dept. of Biochem & Molecular Biophysics, Columbia Univ., N.Y., N.Y. 10032. [2]Dept. of Biological Sciences, Columbia Univ., N.Y., N.Y. 10027 & Dept. of Structural Biology, Brookhaven National Lab., Upton, N.Y. 11973. [3]High Energy Physics Div., Argonne National Laboratories, Argonne IL 60439.

We present a method for calculating electrostatic energies in macromolecular systems of arbitrary shape. The linearized Poisson-Boltzmann equation is solved by finite differences on a STAR array processor to yield a potential field which is a function of the charge distribution, the molecule's internal dielectric constant, the dielectric constant of the solvent, the shape of the molecule, and the ionic strength of the solvent. A focussing technique permits the simultaneous achievement of accurate boundary conditions and fine grid size.

The accuracy of the method has been assessed by comparison with the analytic results for an isolated charge, and for a charge system in a dielectric sphere surrounded by a Debye-Huckel electrolyte (Tanford-Kirkwood equations). The errors are low (within about 15%) for charges up to one grid unit from a charge or a dielectric boundary. A number of applications have been made, including the calculation of enzyme active site potentials, the influence and interactions of alpha-helix dipoles, and the energy balance of buried ionizable groups. Because the method can be used in the calculation of self-energies of individual charges it should have important applications relating to protein stability and specific binding.

T-PM-D9 CONFORMATIONAL PREFERENCES OF THE AMINO ACIDS VARY AS A FUNCTION OF THE AVERAGE HYDROPATHY OF NEIGHBORING RESIDUES. Robert W. Williams & Sheila Loughran, Department of Biochemistry, Uniformed Services University of the Health Sciences, Bethesda, MD 20814-4799.

Predictions of transmembrane protein secondary structure based on the secondary structure preferences of the amino acids in globular proteins have not been satisfactory, often indicating beta-strand where helix exists [Green & Flanagan (1976) Biochem. J. 153, 729.] We have derived preference functions from the globular proteins that appear to correctly predict transmembrane helices. Secondary structures have been assigned using the program by Kabsch and Sander [(1983) Biopolymers 22, 2577] for 212 proteins in the Brookhaven protein structure data base. The preference of amino acid i for secondary structure j in environment class k is estimated as $P_{ijk} = (N_{ijk}/N_{ik})/(N_j/N)$ where N_{ijk}/N_{ik} is the probability of finding amino acid i in structure j with environment class k, and N_j/N normalizes the probabilities so that neutral preference is approximately equal to 1. The environment E_n of residue n is defined as the average hydropathy of residues n-4 through n+4, excluding residue n. P_{ijk} is plotted as a function of environment and a linear regression line is calculated. The slope m_{ij} and y intercept b_{ij} of this regression line is used to calculate preferences for residue n in a protein with unknown structure, $P_{nj} = m_{ij}E_n + b_{ij}$. Residue n is assigned to structure j when P_{nj} is greater than decision constant d_j. Several different hydropathy scales have given similar predictions of structure applicable to globular proteins as well as to membrane proteins.

T-PM-D10 CONFORMATIONAL PREFERENCES OF THE AMINO ACIDS VARY AS A FUNCTION OF THE SOLVENT ACCESSIBLE SURFACE AREA OF NEIGHBORING SIDE CHAINS. Davor Juretic & Robert W. Williams, Department of Biochemistry, Uniformed Services University of the Health Sciences, Bethesda, MD 20814-4799.

Secondary structures have been assigned using the program by Kabsch and Sander [(1983) Biopolymers 22, 2577] for 212 proteins in the Brookhaven protein structure data base. The environment of residue n in a primary structure of a protein is defined to be the average of the solvent accessible surface areas from Chothia [(1984) Ann. Rev. Biochem. 53, 537] for residues n-4 through n+4, excluding residue n. Environments are grouped into nine classes of approximately equal size. The preference of each amino acid i for secondary structure j in each class k is calculated as $P_{ijk} = (N_{ijk}/N_{ik})/(N_j/N)$. N_{ijk}/N_{ik} is the estimated probability of finding amino acid i in secondary structure j with environment class k, and N_j/N normalizes the probability so that neutral preference is approximately equal to 1. The preference values of all amino acids for helix increases as the value for the environment increases. For example: the preference of isoleucine, a beta former, found in low and high environment classes is 0.49 and 1.49 for helix, 1.85 and 1.42 for beta-sheet, and 0.65 and 0.44 for turn respectively, whereas constant preference values [Levitt (1978) Biochemistry 17, 4277] for isoleucine in helix, beta-sheet and turn are 0.97, 1.45 and 0.51 respectively.

T-PM-D11 ANALYSIS OF COOPERATIVE BLOCK ORGANIZATION IN COILED-COIL PROTEINS: ESTIMATION OF THE CONFORMATIONAL FREE ENERGY ASSOCIATED WITH CORE POSITION OCCUPANCY. Fred Schachat. Department of Anatomy, Duke University Medical Center, Durham, NC 27710. (Intr. by J.J. Blum)

Differences in the stability of neighboring segments of coiled-coil proteins have been implicated in force generation in skeletal muscle contraction (Ueno and Harrington, J. Mol. Biol., 1986). As an expanded sequence database for coiled-coiled proteins is generated from nucleic acid studies, methods for predicting regions of differential stability in coiled-coil proteins will be useful in functional correlation and sequence comparision. An empirical approach based on the frequency with which different residues are found in the hydrophobic core positions of coiled-coils is used to estimate the conformational free energy gained from core positions occupancy. The derived scale quantifies many experimental observations on coiled-coil proteins and is informatively different from similar hydrophobicity scales for globular proteins. It implies that both the surface area of hydrophobic residues and geometric contraints of the core determine the contribution to the conformational free energy. In combination with Chou-Fasman secondary structure analysis the boundaries of the cooperative blocks of skeletal muscle tropomyosin (Potekhin and Privalov, J. Mol. Biol., 1982) are fit with simple rules that appear to have predictive value. Furthermore, the principles behind this fitting suggest additional explanations for the parallel in-register arrangement of subunits in coiled-coil molecules.

T-PM-D12 RANDOM FRACTIONAL DEUTERATION IN PROTEIN NMR RESONANCE ASSIGNMENT. David M. LeMaster and Frederic M. Richards, Yale University, New Haven, CT 06511.

In the five years since the essentially complete assignment of BPTI was reported, comparatively little success has been achieved in extending extensive 2D NMR analysis to significantly larger proteins. Although partial assignments have been obtained on larger proteins, 10 kilodaltons remains a practical upper boundary for thorough analysis. The major limitation is a result of the decreased resolution due to an increase in resonance linewidth as well as numbers of resonances for larger proteins. Both of these constraints can be effectively overcome by isotopic substitution. Here we wish to describe experiments in which E. coli thioredoxin (M.W. 11,675) has been uniformly labeled with deuterium to the level of 75% by growth on deuterated carbon source in a deuterated medium. Since ^1H-^1H dipolar interaction is the major source of protein relaxation, isotopic dilution of nearby protons results in longer relaxation times and hence narrower linewidths. Furthermore, resolution is improved by the virtual elimination of passive coupling, that is spin coupling to nuclei not directly involved in the 2D transfer process. The resultant narrower crosspeaks exhibit comparable sensitivity to the corresponding peaks of the natural abundance spectrum despite the fact that the crosspeaks arise from only a fraction of the total sample molecules. Virtually all of the amide to alpha COSY crosspeaks for E. coli thioredoxin can be resolved in a single 2D spectrum. When combined with residue specific isotopic enrichment to provide initial assignment information, this labeling system renders as feasible extensive analysis for proteins in excess of 10 kilodaltons. (Support from GM22778 and PCM 8305203)

T-PM-D13 ENERGY SURFACE MAPPING OF HBS DOUBLE STRANDS*

Stan J. Watowich[1], Ray Hagstrom[2] and Robert Josephs[1]

[1]Department of Molecular Genetics and Cell Biology, University of Chicago, Chicago, Illinois.
[2]High Energy Physics Division, Argonne National Laboratory, Argonne, Illinois.

Under physiological conditions sickle cell hemoglobin (HbS) molecules form long helical fibers which are responsible for the pathological consequences of sickle cell anemia. In vitro these fibers associate into a well characterized set of polymorphic intermediates, which then crystallize. Electron microscopic and x-ray crystallographic studies have shown that the crystals and the fiber intermediates are composed of double strands of hemoglobin molecules. The major differences between the fibers and the crystals is that in the fibers the double strands are twisted and axially shifted whereas in the crystal the double strands are linear and aligned. Thus a key element in the process of crystallisation involves untwisting and shifting the double strands. An understanding of this process requires determining the relative stabilization energies and the changes in the intermolecular contacts that accompany the transition from hemoglobin fiber to crystal.

Towards this end the interaction energies between HbS molecules at the axial and lateral contact sites within each double strand have been evaluated by energy contour mapping to determine the HbS molecular configurations of lowest energy. The potential function is based on empirically determined force constants. Atomic coordinates for the HbS molecules are taken from energy minimized crystal coordinates. Calculations of the intermolecular potential were performed on a STAR-100 and sampled a 5 point lattice in 6-D space about the crystalline contact sites. *Supported by HL22654(RJ).

T-PM-E1 ASYMMETRY, DYNAMICS, AND ENZYMATIC HYDROLYSIS OF SHORT-CHAIN LECITHIN/LONG-CHAIN PHOSPHOLIPID UNILAMELLAR VESICLES. Mary F. Roberts and N. Elise Gabriel, F. Bitter
National Magnet Laboratory and Department of Chemistry, M.I.T., Cambridge, MA 02139

Asymmetric unilamellar vesicles are produced when short-chain phospholipids (fatty acyl chain lengths 6-8 carbons) are mixed with long-chain phospholipids (fatty acyl chain lengths 14 carbons or longer) in ratios 1:4 short-chain/long-chain component. Short-chain lecithins are preferentially distributed on the outer monolayer, while a short-chain phosphatidylethanolamine derivative appears to localize on the inner monolayer of these spontaneously forming vesicles. Lanthanide NMR shift experiments clearly show a difference in headgroup/ion interactions between the short-chain and long-chain species. The pathway of energy transfer studied through two-dimensional NMR spectroscopy suggests that the short-chain lecithin partitioned in the vesicle bilayer is more mobile and isolated from (i.e., non-interacting with) the long-chain phospholipid. These differences in the physical behavior of the two phospholipid components are critical to understanding why water-soluble phospholipases preferentially hydrolyze the short-chain species in these vesicles. (Supported by NIH Grant GM-26762.)

T-PM-E2 LYSOPHOSPHATIDYLCHOLINE MODULATES PHOSPHOLIPASE A_2 HYDROLYSIS OF PHOSPHATIDYLCHOLINE IN SMALL UNILAMELLAR VESICLES. V. V. Kumar and Wolfgang J. Baumann, The Hormel Institute, University of Minnesota, Austin, Minnesota 55912

Phosphorus-31 NMR (32.2 MHz) can be used to distinguish and quantify phosphatidylcholine (PC) and lysophosphatidylcholine (lysoPC) in the outer and in the inner leaflet of small unilamellar PC/lysoPC vesicles. We found that the respective signals are well resolved even in the absence of paramagnetic ions. 1-Palmitoyl-2-oleoyl-sn-glycero-3-phosphocholine (POPC) vesicles containing small proportions (5 mol %) of 1-palmitoyl-sn-glycero-3-phosphocholine (lysoPC) were shown to be drastically asymmetric with respect to lysoPC. They accommodate essentially all of the lysophospholipid in the outer vesicle shell (outside-to-inside ratio, $R_{o/i}$ 15). With increasing lysoPC content (10-30 mol %), $R_{o/i}$ for lysoPC rapidly approached a value of 5.0.

Phospholipase A_2 hydrolysis of POPC in POPC/lysoPC vesicles (250-300Å) was very much dependent upon the lysoPC concentration. Vesicles containing 2.5 mol % lysoPC became leaky after one hour of hydrolysis, whereas vesicles containing 20-30 mol % of lysoPC maintained an intact ion barrier beyond four days. Onset of leakage was characterized by rapid lysoPC flip-flop from the outer to the inner bilayer leaflet. POPC hyrolysis was shown to be stimulated in vesicles containing up to 12.5 mol % of lysoPC. At higher lysoPC levels, the rate of POPC hydrolysis was lower than that for pure POPC vesicles. In vesicles containing 20-30 mol % of lysoPC, POPC hydrolysis was completely inhibited. Complete inhibition occurred when the lysoPC-to-POPC ratio in the outer bilayer leaflet reached a value of 0.3. (Supported by NIH grants HL08214, NS14304 and by the Hormel Foundation.)

T-PM-E3 STRUCTURE AND THERMOTROPIC PROPERTIES OF HYDRATED ETHER-LINKED 1,2-DIHEXADECYL-sn-GLYCEROL-3-PHOSPHOCHOLINE (DHPC). J. T. Kim, J. Mattai and G.G. Shipley. Biophysics Institute, Boston University School of Medicine, Boston, Massachusetts 02118.

Thermotropic and structural properties of ether-linked DHPC at several hydrations were examined by means of differential scanning calorimetry (DSC) and X-ray diffraction. DSC of 4.8% hydrated DHPC exhibits a main endothermic transition, Tm, at 74.2°C (ΔH = 5.5 Kcal/mol). Increasing hydration progressively lowers Tm and increases ΔH until limiting values, T = 44.1°C, ΔH = 8.1 Kcal/mol, are observed. For hydration values $\geq$ 25%, DHPC exhibits a pretransition (Tp) at $\sim$ 36°C (ΔH = 1.1 Kcal/mol) while a subtranstion at $\sim$ 4°C (ΔH = 0.2 Kcal/mol) is observed at $\geq$ 30% hydration. X-ray diffraction patterns of 9.5% hydrated DHPC at 21°C show an untilted bilayer gel structure, d = 58.0Å which swells to a maximum between 25-30% water, d $\sim$ 64Å. At 32% water, two coexisting gel phases are observed, d = 64.0Å and 46.0Å respectively, while at higher hydration a single untilted gel phase is present which swells to a maximum at 35-40% water (d = 47.0Å). Two different gel phases of DHPC clearly exist at lower and higher hydration. Electron density profiles of the structure at lower hydration (9.5-30% H_2O) gave a bilayer thickness d_{p-p}, of 44Å while at higher hydration, d_{p-p} $\sim$ 30Å (see also Ruocco et al. (1985), Biochemistry 24, 2406). Thus, for DHPC a regular, two chain per head group bilayer gel phase is present at lower hydration while an interdigitated four chain per head group bilayer gel phase exists at higher hydration. In contrast to the gel phase, only a single liquid crystalline L_α phase exists at 65°C, with d increasing from 51.0 to 60.0Å over the hydration range 13-35% water (d_{p-p} = 39Å).

T-PM-E4 EMPIRICAL DETECTION OF THE INTERDIGITATED GEL PHASE IN DPPC. Elizabeth S. Rowe, Jeffrey A. Veiro, Parthasarathy Nambi, and Lourdes Herold. University of Kansas Medical School, Kansas City, KS. and VA Medical Center, Kansas City, MO

Dipalmitoylphosphatidylcholine (DPPC) exists in a fully interdigitated gel phase in the presence of certain amphipathic molecules including ethanol and glycerol [Simon, S.A., and McIntosh, T.J.(1984) Biochim. Biophys. Acta 773, 169-172]. We have been investigating the thermotropic properties of PC's in the presence of n-alcohols by spectrophotometry. We have previously shown that alcohols have a biphasic effect on the main transition temperature [Rowe, E.S.(1983) Biochemistry 22, 3299-3305], and that above the threshold alcohol concentration of the biphasic effect there is a marked hysteresis in the main transition [Rowe, E.S. (1985) Biochim. Biophys. Acta 813, 321-330]. In the current study we have investigated the effects of n-alcohols and glycerol on the pretransition of DPPC, and correlated these results with published x-ray diffraction data and the main transition effects. As a result of these investigations we have found that three simultaneous effects occur which are correlated with the induction of interdigitation in DPPC by alcohols: 1) Abrupt disappearance of the pretransition, 2) Inflection in the dependence of the main transition temperature on alcohol concentration, and 3) Onset of marked hysteresis in the main transition. These effects can be used as tentative criteria for determining whether a transition from the bilayer gel to the interdigitated gel has occured as a result of ligand interactions with DPPC. (Supported by the Veterans Administration and NIAAA).

T-PM-E5 CUBIC LIQUID CRYSTALS AND THE MEMBRANE OF *ACHOLEPLASMA LAIDLAWII*. Göran Lindblom*, Leif Rilfors*, Mats Sjölund* and Åke Wieslander†.*Department of Physical Chemistry and †Department of Biochemistry, University of Umeå S-901 87 Umeå, Sweden.

Phase diagrams of practically all the different lipids in the membrane of *A. laidlawii* have been determined and it is found that all the membrane lipids except one (monoglucosyldiglyceride, MGDG) form lamellar phases at all water concentrations in the growth temperature interval of the bacterium. MGDG, on the other hand, forms reversed cubic and hexagonal liquid crystalline phases, and it is found that the formation of non-lamellar phases by *A. laidlawii* lipids depends critically upon the MGDG concentration. The most important result is that for *in vivo* mixtures of membrane lipids, the transition temperature for the formation of a cubic or a hexagonal phase from a lamellar one is almost independent of the degree of unsaturation of the acyl chains but critically dependent on the MGDG content. *A. laidlawii* has also been grown in the presence of several foreign hydrophobic and amphiphilic compounds (*e.g.* dodecane, cyclohexane, alcohols and detergents). The membrane lipid composition is regulated in response to the incorporation of these molecules. It is found that *e.g.* dodecane can induce cubic and hexagonal phases at high water contents in a lipid bilayer system. The experimental observations and the lipid regulation in the *A. laidlawii* membrane are explained in terms of a simplified theory where the molecular shape of the lipids plays a dominant role. The structures of the various cubic phases have been investigated with different NMR techniques (*e.g.* diffusion, relaxation) and their possible biological relevance will also be discussed.

T-PM-E6 SOLVATION FORCES BETWEEN LECITHIN BILAYERS: DEPENDENCE ON SOLVENT SIZE AND INTERFACIAL DIPOLE POTENTIAL. A.D. Magid, T.J. McIntosh, and S.A. Simon. Departments of Anatomy and Physiology, Duke University Medical Center, Durham, NC 27710.

To better understand how the "hydration" pressure, P_h, depends upon the size of the solvent molecules and also upon the interfacial dipole potential, we are measuring the variation of osmotic pressure with distance between egg phosphatidylcholine (EPC) bilayers bathed in water and in the non-aqueous solvents, formamide (FOR) and 1,3-propanediol (PDO). These solvents have been chosen because: (1) EPC forms multilamellar bilayers in all three, (2) polyvinylpyrollidone (PVP-40) dissolves in all three and thus can be used to apply osmotic pressure, and (3) they provide a range of molecular sizes. Fluid thickness (d_f) and bilayer thickness (d_b) have been determined by x-ray diffraction techniques. Bilayer thickness depends on the solvent, possibly due to differences in interfacial surface pressure. For each solvent, however, d_b remains nearly constant over the range of pressures studied, as judged by sampling theorem and phase diagram criteria. Osmotic pressures have been measured for PVP in water and FOR, and are currently being measured in PDO. The dipole potential, ΔV_D, is measured to be 384mV, 246mV, and 170mV for EPC monolayers spread over water, FOR, and PDO, respectively. For both water and FOR, P_h obeys the relation $P_h = P_o \exp(-d_f/\lambda)$, where $\lambda \simeq 1.7$Å in water and 2.5Å in FOR, and $P_o \simeq 4\times10^8$ dynes/cm^2 in water and 8×10^7 dynes/cm^2 in FOR. Therefore, for these two solvents λ varies in proportion to $(MW)^{1/3}$, i.e., roughly in proportion to the solvent's radius, and P_o is proportional to $(\Delta V_D)^2$, in accord with the theoretical prediction of Cevc and Marsh (Biophys. J. 47:21). When osmometry with PDO is completed, we will be able to determine if these relations also hold for this larger molecule.

T-PM-E7 THE INFLUENCE OF A LIPID PERTURBER, BUTYLATEDHYDROXYTOLUENE, ON A MODEL MEMBRANE SYSTEM. K.R. Jeffrey, Biophysics Interdepartmental Group, University of Guelph, Guelph Ontario, CANADA.

The effects of butylatedhydroxytoluene. BHT, on a model membrane system consisting of mixtures of dipalmitoylphosphatidylcholine, DPPC, and water have been investigated using nuclear magnetic resonance, NMR, differential scanning calorimetry, DSC, and X-ray diffraction. ^{31}P NMR measurements of the anisotropic chemical shift of the phosphate group in DPPC clearly show that the phase transition from liquid-crystalline to gel is lowered in temperature and broadened with increasing BHT content. DSC results confirm this behavior while X-ray diffraction shows that up to 33 mol %, the liquid-crystalline phase remains lamellar.

^{2}H NMR spectra of selectively deuterated BHT incorporated into the model membrane system seems to indicate that the BHT molecule can be found in two environments. One is possibly deep within the acyl chain region where the molecule can orient freely leading to an isotopic peak in the deuterium spectrum. A second environment gives rise to quadrupolar split deuterium spectra suggesting that the molecule is located near the more ordered lipid/water interface.

T-PM-E8 INTERACTION OF N-ALKYLANTHRACYCLINES WITH LIPID BILAYERS USING HIGH SENSITIVITY DIFFERENTIAL SCANNING CALORIMETRY. P. P. Constantinides,[1] L. Ghosaini,[2] N. Inquchi,[1] S. Kitamura,[2] R. Seshadri,[3] M. Israel,[3] A. C. Sartorelli,[1] and J. M. Sturtevant.[2] [1]Dept. Pharmacol. and Comp. Cancer Ctr., Yale Univ. Sch. Med., New Haven, CT 06510, [2]Dept. Chem., Yale Univ., New Haven, CT 06520 and [3]Dept. Pharmacol., Univ. Tennessee Coll. Med., Memphis, TN 38163.

Thermotropic behavior of dipalmitoylphosphatidylcholine (DPPC) multilamellar vesicles or DPPC mixed with cardiolipin or cholesterol in the presence of various N-alkyl derivatives of both adriamycin (ADR) and ADR-14-valerate has been studied by high sensitivity differential scanning calorimetry. To establish structure/activity relationships, effects produced by these agents were compared to those caused by N-trifluoroacetyl-ADR-14-O-hemiadipate, in which the valerate group is replaced by the water-soluble hemiester, and by daunomycin, rubidazone, ADR octanoylhydrazone and cyanomorpholino ADR. Although the more lipophilic analogues (particularly the 14-valerate compounds) based on lipid/buffer, and to a lesser extent octanol/buffer partition coefficients, were more effective in depressing the t_m of employed lipids, correlations were not absolute. Other factors, such as distribution of drugs between gel and liquid-crystal bilayer phases, were also important. No major changes in transition enthalpy were observed with all drugs in the presence or absence of cardiolipin or cholesterol. With pure DPPC, curve fitting analysis based on ideal solution theory (Sturtevant, J.M., Proc. Natl. Acad. Sci. USA 81: 1398-1400, 1984), applied at drug concentrations where single-peak transitions were produced, adequately described the calorimetric behavior of corresponding drug-lipid mixtures. These results correlate with some biological effects of these N-alkylanthracyclines, most notably with DNA binding capacity.

T-PM-E9 BIOPHYSICAL STUDIES OF RETINOID-PHOSPHOLIPID INTERACTIONS. Carol A. Langsford*, Mark R. Albrecht*, Timothy M. Phelps†, William Stillwell* and Stephen R. Wassall†
Departments of Biology* and Physics†, Indiana University-Purdue University at Indianapolis, Indianapolis, IN 46223

The retinoids (vitamin A and derivatives) - retinol (vitamin A), retinal (vitamin A aldehyde) and retinoic acid (vitamin A acid) - form a group of amphiphilic molecules which vary in structure only at the polar end. They differ markedly in their essential support of biological function and become toxic at high doses. This toxicity may be due to membrane disruption and in the present study we investigate the interactions at the molecular level of retinoids with phospholipid model membranes.

We have employed ESR (electron spin resonance), osmotic swelling and fluorescence techniques to determine the effect that incorporation of each retinoid into PC (phosphatidylcholine) bilayers has on acyl chain motion and membrane permeability. ESR of nitroxide spin labelled stearic acids intercalated into the bilayer demonstrates that while all-trans retinol and retinal have negligible influence on molecular ordering in the upper portion of the acyl chain, all-trans retinoic acid disorders this region of the bilayer. This distinction of effect is confirmed by permeability measurements in which the rate of PC multilamellar liposome swelling in isotonic erythritol was monitored by optical absorbance. They show that retinoic acid greatly enhances permeability, whereas retinol and retinal affect permeability only slightly. Carboxyfluorescein and TEMPOcholine leakage through PC bilayers as measured by fluorescence and ESR, respectively, exhibit a similar trend.

T-PM-E10 POLARIZED FLUORESCENCE PHOTOBLEACHING RECOVERY FOR MEASURING FAST ROTATIONAL DIFFUSION. Marisela Velez and Daniel Axelrod, Biophysics Research Division, University of Michigan, Ann Arbor, MI 48109.

We have developed a variation of fluorescence photobleaching recovery techniques suitable for measuring the rate of fast rotational, rather than translational, molecular diffusion in solutions and membranes. In this technique, similar in principle to that presented by L. Smith et al (Biophys. J 36:73-91, 1981), a brief flash of polarized laser light preferentially bleaches those fluorophores with absorption dipoles parallel to the laser polarization. Subsequent rotational diffusion brings unbleached fluorophores into the polarization direction of the laser beam (attenuated for fluorescence excitation without further bleaching). However, our experiments, at time scales on the order of microseconds to milliseconds, present several problems not before encountered at longer time scales. (1) A fast reversible fluorescence recovery in rhodamine and fluorescein, presumably of photochemical origin and independent of molecular orientation or lateral motion, tends to obscure rotational effects. Switching bleaching polarizations with a Pockel cell along with an appropriate theoretical treatment overcomes this problem. (2) Fused silica substrates must be used to avoid long-decaying luminescence of ordinary glass. (3) Signal averaging, increased laser power, and automated sample translation must be employed to speed data gathering and improve statistical accuracy. Verification of this technique on model systems will be discussed. Polarized FPR, unlike techniques based on triplet states such as eosin phosphorescence anisotropy decay and ground state depletion decay, does not require sample deoxygenation (thereby making it more suitable for living cells) and works on any time scales from seconds to microseconds. Sptd. by NIH NS14565.

T-PM-E11 PRETRANSITIONAL CRITICAL BEHAVIOR AND P2/P4 CORRELATIONS FOR LIPID BILAYERS. Anthony J. Ruggiero and Bruce Hudson, Department of Chemistry, University of Oregon, Eugene, Oregon 97403.

Studies of the fluorescence decay and anisotropy behavior of parinaric acid in lipid bilayers formed by DPPC, DEPC and DEPC/cholesterol exhibit clear lifetime and dynamic heterogeneity in the temperature region 3-10° above the main thermal phase transition. This is demonstrated to be associated with density heterogeneity and is interpreted in terms of critical behavior. A critical exponent of 1.10 is obtained from the variation of the amplitude of the long lifetime component with reduced temperature. This is in good agreement with the value predicted by Mouritsen and Zuckermann from simulation studies [Eur. Biophys. J. 12, 75 (1985)]. In many cases the observed time dependence of the anisotropy exhibits upward curvature to an asymptotic limit at long times. This data has been analyzed in terms of two distinct environments, each having anisotropy decay behavior described by the general treatment of Szabo [J. Chem. Phys. 81, 150 (1984)] and van der Meer et al. [Biophys. J. 46, 515 (1984); Chem. Phys. 102, 37 (1986)]. This analysis leads to values of the perpendicular diffusion coefficient for the probe reorientation and the average values of the second- and fourth-rank orientational order parameters, $\langle P_2 \rangle$ and $\langle P_4 \rangle$. The resulting values are compared with specific models of the orientational distribution of acyl chains in bilayers and the distributions resulting from information theory are presented.

T-PM-E12 KINETICS OF CHARGE TRANSFER AT THE LIPID BILAYER-WATER INTERFACE ON THE NANOSECOND TIME SCALE. Martin Woodle, Jingwen Zhang and David Mauzerall, The Rockefeller University, 1230 York Avenue, New York, NY 10021.

Thru advances in fast electronics, we can now directly measure the forward reaction of charge transfer across the lipid bilayer-water interface with a response time of 3 ns. A 7 ns pulse of 560 nm light from a N_2 laser pumped dye laser excited MgOEP in a planar lipid bilayer, adjacent to an aqueous solution of an ionic acceptor on one side only. The rise of the photovoltage was the complement of an exponential to well over 90% of the range and the pseudo first order rate constant was linear in concentration of acceptor. The apparent second order rate constants for the reaction of excited MgOEP with methyl viologen, ferricyanide, and anthraquinone-2-sulfonate (2AQS) are 5×10^7, 1×10^9 and $4 \times 10^{10} M^{-1} s^{-1}$. Oxygen can mediate charge transfer, but has no effect on the apparent second order rate constant. The correlation between the rate constants and the saturation constants for the acceptors shows that the reaction is dynamic, not static, with a reactive state lifetime of 1 μs. The rate constants quantitatively demonstrate the effects inferred from previous amplitude measurements. The rate of reaction of methyl viologen di-cation is slowed by the electrostatic repulsion with the aqueous side positive dipolar self-polarization of the lecithin interface by the choline group. That of the tri-anion ferricyanide may in turn be enhanced. The value of the rate constant for 2AQS, larger than that calculated for an encounter limited reaction in free aqueous solution, is strongly indicative of binding at the interface. A general conclusion from the magnitude of these rate constants is that there exists very little if any barrier to free diffusion at the lipid bilayer-water interface. Any bound water and ions are mobile on the ns time scale. This research was supported by the PHS , grant GM-25693.

T-PM-F1 EXTENDED X-RAY ABSORPTION FINE STRUCTURE (EXAFS) MEASUREMENTS OF Cu_A-DEPLETED, p-(HYDROXYMERCURI)BENZOATE (pHMB) MODIFIED, AND NATIVE CYTOCHROME c OXIDASE

Peter Mark Li*, Jeff Gelles*, and Sunney I. Chan, *Noyes Laboratory of Chemical Physics 127-72, California Institute of Technology, Pasadena, CA 91125*
Richard Sullivan and Robert A. Scott, *Department of Chemistry, University of Illinois at Urbana-Champaign, Urbana, IL 61801*

Cytochrome c oxidase contains four redox-active metal centers, two heme irons (cytochromes a and a_3) and two copper ions (Cu_A and Cu_B). We herein report the specific depletion of Cu_A from the pHMB-modified cytochrome oxidase recently reported by Gelles and Chan (Biochemistry, 24, 3963-3972, 1985). Characterization of this enzyme shows that the remaining metal centers are essentially unperturbed by the Cu_A modification and depletion. EXAFS measurements on the Cu_A-depleted, pHMB-modified, and unmodified control enzymes have allowed for the deconvolution of the scattering into contributions from each of the copper centers in the protein. From these data, the ligand structures for Cu_A and Cu_B are derived.

This work is supported by grants GM 22432 (to SIC) from the National Institutes of General Medical Sciences, US Public Health Services, and DMB85-02707 (to RAS) from the National Science Foundation.

*Recipient of NSF Graduate Fellowship

T-PM-F2 CHEMICAL AND SPECTROSCOPIC EVIDENCE FOR THE FORMATION OF A FERRYL Fe_{a_3} INTERMEDIATE IN CYTOCHROME c OXIDASE: REOXIDATION WITH O_2 AND ACTIVATION BY H_2O_2. Stephan N. Witt and Sunney I. Chan. Noyes Laboratory of Chemical Physics, California Institute of Technology, Pasadena, CA 91125.

When partially reduced cytochrome c oxidase samples are reoxidized with dioxygen, a subpopulation of an EPR-silent intermediate, in which dioxygen is at the three-electron level of reduction, is trapped at the dioxygen reduction site. The intermediate has novel spectral features at 580 and 537 nm in the reoxidized-minus-resting difference spectrum. A homogeneous population of this trapped EPR-silent intermediate is produced after the addition of excess H_2O_2 to either "pulsed" or reduced cytochrome c oxidase, as judged by the intense symmetric bands at 580 and 537 nm in the difference spectrum. Combined optical and EPR results revealed that the trapped EPR-silent intermediate, as prepared by both methods, reacts rapidly with CO at 277-298 K causing abolition of the 580/537 nm features, the concomitant increase in intensity at 600-604 nm, and the appearance of a rhombic Cu_B EPR signal. An EPR-silent ferryl Fe_{a_3}/cupric Cu_B binuclear couple, or an intermediate at the same formal level of oxidation, is proposed to oxidize CO to CO_2 producing an EPR-detectable Cu_B adjacent to a ferrous Fe_{a_3}-O_2 (or CO) adduct. These results demonstrate that the same reactive trapped EPR-silent ferryl Fe_{a_3}/cupric Cu_B couple is produced whether (i) partially reduced samples are reoxidized with O_2 or (ii) H_2O_2 is used to activate cytochrome c oxidase. In the latter case, it is proposed that after reoxidation of the fully reduced enzyme with H_2O_2, an equivalent of H_2O_2 binds to the pulsed enzyme to produce a peroxidic adduct, namely, Compound C (Fe_{a_3}-O-O-Cu_B). The excess H_2O_2 can then act as a one-electron donor to Compound C to yield the trapped EPR-silent ferryl Fe_{a_3}/cupric Cu_B couple and superoxide.

T-PM-F3 CHEMICAL MODIFICATION OF THE Cu_A SITE IN CYTOCHROME c OXIDASE AFFECTS ITS PROTON PUMPING ACTIVITY.

Thomas Nilsson, Peter Mark Li, Jeff Gelles and Sunney I. Chan, Department of Chemistry, Noyes Lab, California Institute of Technology, Pasadena, CA 91125

Extensive modification of cytochrome c oxidase with the thiol reagent p-(hydroxymercuri) benzoate gives a derivative in which the Cu_A center is no longer redox active. The enzyme is, however, still electron transfer competent with an activity of ca 20% of that of the native enzyme (Gelles, J. and Chan, S. I. (1985) Biochemistry, 24, 3963-3972). We report here the reconstitution of this modified enzyme into phospholipid vesicles. These vesicles are weakly coupled and do not exhibit proton pumping activity in the potentiometric assay. Heat treatment of cytochrome oxidase has been reported to abolish proton pumping, while 80% of the electron transfer activity remains (Sone, N. and Nicholls, P. (1984) Biochemistry, 23, 6550-6554). We find that heat treatment leads to extensive changes in the EPR signal from the Cu_A site. Proton pumping measurements on reconstituted, heat-treated enzyme confirm the earlier report that it is not active in proton transport. The result that two different modifications of the Cu_A site abolish proton pumping strongly implicates the Cu_A site in the catalysis of this reaction. (This work is supported by Grant GM 22432 from the National Institute of General Medical Sciences, US Public Health Services. A post-doctoral fellowship from the Swedish Science Research Council to T. N. is acknowledged.)

T-PM-F4 THE MAGNETIC SUSCEPTIBILITIES OF RESTING, CYANIDE-BOUND, AND PEROXIDE-BOUND CYTOCHROME OXIDASE. Z. K. BARNES, G. T. Babcock, and J. L. Dye (Intr. by C. F. Yocum).

The temperature dependence of the magnetic susceptibility was measured for resting, cyanide-bound, and peroxide-bound cytochrome c oxidase. The effects of using different enzyme isolation techniques and different dispersing detergents were investigated; the susceptibility of the a_3 centers of the resting and cyanide-bound enzyme showed no significant dependence on either. The a_3 center of the resting enzyme was antiferromagnetically coupled. The cyanide-bound enzyme was magnetically heterogeneous with one component showing antiferromagnetic coupling between Cu_B and cytochrome a_3. The coupling of the a_3 center in the other component and in the peroxide-bound enzyme could not be determined, but the spin state of cytochrome a_3 in the latter was S = 3/2.

T-PM-F5 ELECTRON MICROSCOPY AND IMAGE PROCESSING OF STAINED TWO-DIMENSIONAL ARRAYS OBTAINED FROM E. COLI F_1 AND F_1F_0 PREPARATIONS. Uwe Lücken, Tracie Bork, Stephen J. Remington, R.A. Capaldi, Institute of Molecular Biology, University of Oregon, Eugene, OR 97403 (Intr. by Peter H. von Hippel)

An ultra-pure E. coli F_1 preparation with a low specific ATPase activity has been obtained. This preparation, activated twenty-fold by the detergent dodecylaminoxide, contains the five subunits α, β, γ, δ and ϵ in the stoichiometry 3:3:1:1:1. Two-dimensional arrays of the F_1 preparation have been obtained using a microdialysis procedure in the presence of lipids.

E. coli F_1F_0 has been isolated by cholate-deoxycholate extraction followed by sucrose gradient centrifugation in egg phosphatidylcholine. Further purification was achieved by reconstitution of F_1F_0 into liposomes. Two-dimensional crystalline arrays of this preparation have also been obtained by microdialysis using a protein to lipid ratio of 1.2:1.

The two-dimensional arrays of both EF_1 and EF_1F_0 are being studied by electron microscopy and image processing. Specimens have been stained with phosphotungstate and/or uranyl acetate and projection maps of both preparations have been obtained. These show an F_1 molecule with six electron-dense regions arranged as a hexagon with dimensions of about 90Å. Within the hexagon there is one region of high and another region of low density.

Studies in progress will provide a low resolution (25Å) three-dimensional reconstruction of both EF_1 and EF_1F_0.

T-PM-F6 SITE-DIRECTED MUTAGENESIS OF THE CATALYTIC SITE OF F_1-ATPASE. Derek Parsonage and Alan E. Senior Department of Biochemistry, University of Rochester Medical Center, Rochester, NY 14642.

Genes encoding β and ε subunits of Escherichia coli F_1-ATPase were included in a plasmid which allowed production of single-stranded plasmid DNA upon infection of transformed cells with helper phage. Single-stranded plasmid was then used for oligonucleotide-directed mutagenesis to substitute a Gln residue for Lys-155 of the β-subunit. Lys-155 is labelled by inhibitor NBD-Cl at high pH, it is highly conserved in a sequence which shows homology with several other nucleotide-binding proteins and it may interact with the α-phosphate of ATP bound at the catalytic site. The substitution affects the charge on residue 155 without gross change in side-chain size. Mutated plasmid was transformed into a Mu-induced $uncD^-C^-$ strain so that the effect of the mutation could be examined. The transformant strain (DP3) grew poorly on succinate medium and membranes prepared from it had substantially reduced ATPase and ATP-driven proton pumping activities. F_1-ATPase was purified from strain DP3 with a yield typical of that for a haploid unc^+ strain. The specific activity of the mutant F_1-ATPase was 12% of normal. The results show that Lys-155 is an essential residue in F_1-ATPase and should allow detailed study of the role of this residue in catalysis.

Supported by NIH grant GM25349.

T-PM-F7 DIRECT EVIDENCE FOR THE PRESENCE OF TYR-β311 NEAR THE γ-PHOSPHATE GROUP OF ATP BOUND AT THE HYDROLYTIC SITE OF F_1-ATPASE. Joe C. Wu, Hua Chuan and Jui H. Wang, Bioenergetics Laboratory, Acheson Hall, State Univ. of New York, Buffalo, NY 14214-3094.

The specific labeling of Tyr-β311 in mitochondrial F_1-ATPase (MF_1) by 7-chloro-4-nitro-2,1,3-benzoxadiazole (NBD-Cl) causes complete inactivation of the ATPase at a label to F_1 molar ratio of 1:1 [Ferguson, S.J., Lloyd, M.H., Lyons, M.H. & Radda, G.K. (1975), Eur. J. Biochem. 54, 117-126; Andrews, W.M., Hill, F.C. & Allison, W.S. (1984) J. Biol. Chem. 259, 8219-8225]. This inactivation could either be due to the direct participation of Tyr-β311 in catalytic hydrolysis or due to NBD-induced long range conformation change in the protein. If Tyr-β311 is indeed near the γ-phosphate group of the bound ATP [Ting, L.P. & Wang, J.H. (1980) Biochemistry 19, 5665-5670], it should be possible to design and synthesize an ATP analogue, with a mercaptoethyl group replacing the γ-phosphate of ATP, which could be bound very close to the NBD-label and react with the latter. We have succeeded in synthesizing P^1-(5'-adenosyl)-P^2-N-(2-mercaptoethyl)diphosphoramidate (AMEDA). In a solution containing 5 μM O-[^{14}C]NBD-F_1 and 5 μM AMEDA, the almost completely inhibited ATPase was reactivated rapidly. The observed rates of reactivation over a range of AMEDA concentration show that AMEDA is bound to the labeled enzyme with K_d = 14.5 μM. The reactivation was effectively retarded by low concentrations of ATP or ADP. After the reactivation of O-[^{14}C]NBD-F_1 was completed, the major low molecular weight product was isolated by HPLC and was shown to contain both adenine group and NBD-label in the same molecule. These results show that Tyr-β311 is indeed near the γ-phosphate group of ATP bound to the hydrolytic site of MF_1.

T-PM-F8 MOLECULAR CLONING OF THE BETA-SUBUNIT OF RAT LIVER F_1-ATPASE. D.N. Garboczi, S.L. Gerring, A.H. Fox and P.L. Pedersen (Department of Biological Chemistry, The Johns Hopkins School of Medicine) and P. Churchill and S. Churchill (Department of Molecular Biology, Vanderbilt University)

Using a polyclonal antiserum prepared in rabbits against the rat liver F_1-ATPase, we screened a rat liver cDNA library in lambda gt11 (constructed by P.C. and S.C.) The antiserum reacted on antibody blots to the α, β, and γ subunits. Of the eleven clones that were selected on the first round of antibody screening, three clones tested positive on additional screenings and were plaque-purified. Gel electrophoresis of the cDNA clones revealed inserts of 1200, 1100, and 800 base pairs, respectively. That these clones were of the β-subunit was confirmed by hybridization to a human β-subunit cDNA obtained from S. Ohta and Y. Kagawa (J.Biochem.(Tokyo) 99,135-141). Further screening with the human cDNA enabled the isolation of a 350 base pair clone which, together with the longest antibody-selected clone, codes for the mature β-subunit lacking only the N-terminal seven amino acids. The amino acid sequence of the rat liver β-subunit shows strong sequence homology to β-subunits of other F_0F_1 type ATPases. It also contains a short amino acid stretch exhibiting strong homology with the active site region of E_1E_2 type ATPases. A partial cDNA of the β-subunit has been overexpressed in E. coli. [Supported by Grant CA 10951 from the National Cancer Institute].

T-PM-F9 VOLTAGE SENSING OF MITOCHONDRIAL ATPase IN PULSED ELECTRIC FIELD INDUCED ATP SYNTHESIS. Francoise Chauvin*, R. Dean Astumian+ & Tian Yow Tsong*. *Biological Chemistry, Johns Hopkins Univ. School of Medicine, Baltimore, MD 21205 and +Biochemistry Laboratory, NHLBI, NIH, Bethesda, MD 20892

Our results show that under the conditions used by Knox and Tsong, ATP yield directly attributable to electric field induction is less than 1 ATP per F_oF_1 per 100 us pulse of 30 kV/cm. Most of the ATP formed was due to adenylate kinase activity stimulated by Joule heating. A similar conclusion has been reached by H. Rottenberg and R. Korenstein. However, we are now able to eliminate the adenylate kinase activity to less than 10% of total ATP forming activity, and ATP synthesis due to an applied electric field can be demonstrated with confidence. We have found that treatment of beef heart submitochondrial particles (SMP) with 5 mM dithiothreitol (DTT) enhances the rate of field induced synthesis nearly 10 fold (oligomycin sensitive). By a conservative estimate, the rate reaches 3-5 ATP per F_oF_1 complex per 100 us pulse of 20-30 kV/cm. The ATP yield in the presence of DTT suggests enzyme turnover during the 100 us pulse duration, with an unusually high rate. From thermodynamics, the rate of an electric field inducible reaction is dependent on the electric characteristics of the enzyme and the applied field strength. Enzyme turnover during a dc pulse may be achieved through local field modulation by charged groups. By measuring the dependence of rate on field intensity it is possible to obtain ΔM, i.e. change in the macroscopic polarization of the rate-limiting step. That sulfhydryl group(s) is involved in the voltage sensing is demonstrated by the treatment of SMP with iodoacetamide (IAA). IAA treatment abolishes the rate enhancement due to DTT. These results indicates that -SH group(s) confers upon the F_oF_1 its ability to respond to an electric field. (Supported by NIH Grant GM28795 to TYT)

T-PM-F10 ENERGY TRANSDUCTION FROM ELECTRIC NOISE BY MEMBRANE PROTEIN. R. Dean Astumian*, P. Boon Chock* and Tian Yow Tsong+. *Laboratory of Biochemistry, NHLBI, NIH, Bethesda, MD 20892 and +Department of Biological Chemistry, Johns Hopkins University School of Medicine, Baltimore, MD 21205.

Membrane proteins in the vicinity of a channel across which there exists an ion electrochemical gradient may be exposed to large, persistent non-equilibrium fluctuations in the local electric field strength. Such would be the case as well for an enzyme localized next to an electron transport protein. We have shown that these fluctuations (or regular oscillations) present a mechanism by which an enzyme can transduce energy from the driving source of the fluctuations. Previously, we proposed a four-state kinetic model to interpret the experimental observation that an applied ac field of appropriate frequency and amplitude can stimulate uphill transport of Rb in human erythrocytes mediated by (Na,K)-ATPase without apparent ATP hydrolysis. The essential feature of the model is that the transport protein is capable of absorbing and transmitting free energy from the ac field by "electroconformational coupling". When the electric and kinetic characteristics of the system match with the strength and frequency of the ac field, electric energy is transduced into chemical potential energy. Subsequently, we found that such an enzyme can also capture energy from randomly fluctuating electric fields. In the present paper we will discuss some general conclusions arising from these considerations. Of particular importance is the realization that the approximation used in the theory of fluctuations in homogeneous media may not be appropriate in the treatment of membrane localized systems.

T-PM-F11 FATTY ACIDS ENHANCE DISSIPATION OF PH GRADIENTS IN BRUSH BORDER MEMBRANE VESICLES. IMPLICATIONS FOR MECHANISMS OF CELL DEATH. Robert M. Lachowiez, Diana Leffel, Barbara Clayton, Maria Miller and James A. Dix, Department of Chemistry, State University of New York, Binghamton, NY 13901.

Proton gradients across brush border membranes isolated from the apical membrane of rat kidney proximal tubule dissipate more rapidly following treatment with calcium, mercury and mellitin, substances which activate phospholipase A_2. Dissipation rates are also enhanced by treatment with exogenous phospholipase A_2 or by direct addition of oleic acid. The treatments which affect proton conductance do not affect the water permeability of the membrane, implying that the membrane remains structurally intact. Cells killed by ischemia are unable to produce ATP, and also exhibit elevated levels of calcium as well as an increase in free fatty acid concentration of mitochondrial membranes. Our results imply that a key event in cell death is activation of phospholipase A_2 subsequent to a breakdown in cellular calcium homeostasis, followed by an increase in free fatty acids of mitochondrial membranes and uncoupling of oxidative phosphorylation. Supported in part by the American Heart Association, Broome County, New York State Chapter.

T-PM-F12 THE REGULATION OF THE MITOCHONDRIAL ATPase IN SLOW AND FAST HEART-RATE HEARTS. William Rouslin, Department of Pharmacology and Cell Biophysics, University of Cincinnati College of Medicine, Cincinnati, Ohio 45267-0575.

A survey of twelve species has revealed that the reversible ischemia-induced protonic inhibition of the cardiac muscle mitochondrial ATPase described by me earlier (Rouslin, W. (1983) J. Biol. Chem. 258, 9657-9661) occurs only in animals with heart rates lower than approximately 200 beats per min. It was thus fully demonstrable in rabbit, dog, sheep, human, pig and beef heart mitochondria. In contrast, the *in situ* ATPase inhibition was completely absent in six smaller species capable of heart rates of approximately 300 or more beats per min. These were chicken, pigeon, guinea pig, rat, hamster and mouse.

Analyses of the cardiac muscle mitochondria of nine of the twelve species studied showed them to contain normal levels of inhibitor; the three smallest species, rat, hamster and mouse, contained only very low levels of inhibitor. Thus, while chicken, pigeon and guinea pig heart mitochondria contained normal levels of ATPase inhibitor, they, like the rat, hamster and mouse, showed no *in situ* ischemia-induced ATPase inhibition. This and other observations suggest that the lack of *in situ* ATPase inhibition in hearts capable of 300 or more beats per min may be due to the presence of either an *in situ* nonfunctional ATPase inhibitor protein or to an *in situ* uninhibitable form of the mitochondrial ATPase in the faster paced hearts. A third possible explanation for the lack of *in situ* ATPase inhibition in the faster paced hearts is that the cardiac muscle mitochondria in these smaller species may be insulated somehow against the cytosolic acidosis which triggers the ATPase inhibition. In the faster paced hearts, ATP hydrolysis does not appear to be regulated by inhibitor binding to the ATPase under non-energizing conditions. (Supported by NIH grant HL-30926).

T-PM-F13 ^{23}NA AND ^{13}P STUDIES OF SALT STRESS IN THE CYANOBACTERIUM SYNECHOCOCCUS 6311

By: Lester Packer, Susan Spath, Jean M. Baptiste, Claude Robbie & Richard Bligny. Membrane Bioenergetics Group, Univ. of California, Berkeley, California, 94720, USA and Centre d'Etudes Nucleaires, Department de Recherche Fondamentale, 38041, Grenoble Cedex, France.

Exposure of a fresh water Cyanobacterium Synechococcus 6311 to a sudden NaCl shock of 0.5M inhibits photosynthesis and growth rate. Later, photosynthesis recovers and cells again become capable of log growth under saline conditions. NMR was used to study the initial changes that occur in the cells after a transfer to growth medium containing 0.5 NaCl. ^{23}Na-NMR showed that Na rapidly penetrates the cells, but after growth for several days in high salt medium the cells reestablish a low internal Na content and maintain a 200-fold concentration gradient. Sudden exposure to NaCl causes immediate changes in the ^{31}P metabolites; nucleotide triphosphate (NTP) peaks decrease and the inorganic phosphate (P_i) peak increases. Pyrophosphate added to cells is hydrolyzed to P_i extracellularly, allowing external and internal pools of P_i to be distinguished; this indicates Synechococcus 6311 produces extracellular phosphatase. A reaction compartment was made to exchange gases [N_2 and O_2] and illuminate cells with optical fibers. NTP levels fall almost as much when cells are incubated in darkness as under N_2, thus both respiration and photosynthesis maintain ATP levels. Salt-adapted cells revealed a similar ^{31}P pattern of metabolites as control cells, except that they contain a higher level and more peaks in the phosphate monoester (sugar phosphate region).

We are grateful to Dr. Roland Douce for valuable counsel and making facilities available. Research support by the Office of Biological Energy Research, Dept. of Energy, U.S.A. and Centre d'Etudes Nucleaires, CEA, France.

T-PM-F14 LOCALIZATION OF CREATINE KINASE ON HEART MITOCHONDRIA INCREASES THE RATE OF CREATINE PHOSPHATE SYNTHESIS FROM OXIDATIVE ATP. JS Ingwall, MK Dygert and SB Perry, HMS NMR Laboratory, Boston, MA

Localization of the mitochondrial creatine kinase isoenzyme (mito-CK) on the outer aspect of the inner mitochondrial membrane may create a microcompartment in which oxidative ATP drives the CK reaction in the direction of creatine phosphate (CrP). We have tested this postulate in two settings. 1) The rate of CrP synthesis was measured in mitochondrial suspensions prepared from neonatal and adult rabbit hearts and liver with constant amounts of citrate synthase (CS) (and hence mitochondrial mass) and total CK activities (i.e., the sum of bound mito-CK plus free CK in the bulk suspension), but for which the ratio of bound mito-CK activity to CS activity (R) ranged from 0 (liver) to 1.0 (adult heart). The rate of CrP synthesis (umoles min mg protein) increased monotonically as R increased: 8.2 $\pm$ 1.0 for R=0, 12 $\pm$ 0.7 for R=0.3, 18 $\pm$ 3.9 for R=0.7, and 39 $\pm$ 5.3 for R=1. Thus, as the fraction of bound CK increased, the rate of CrP synthesis increased. 2) The rate of CrP synthesis was also measured in the intact neonatal rabbit heart containing constant total CK activity but different amounts of mito-CK using magnetization transfer P-31 NMR. In these experiments, flux through the CK reaction was measured at three different levels of cardiac performance (and hence ATP synthesis rates). For a given rate of ATP synthesis, flux through the CK reaction increased 3-fold as %mito-CK increased from 0 to 12%. Fitting data to the Michaelis-Menten equation showed that 1) the rate of ATP synthesis at which flux through CK is half maximal decreased as mito-CK activity increased, and 2) maximal flux through CK increased as mito-CK activity increased. Results from these two experiments are consistent with functional coupling between mito-CK and the adenine nucleotide translocase.

T-Pos1 THE KINETIC ANALYSIS OF STATIONARY PATCH-CLAMP DATA USING AUTOCORRELATION TECHNIQUES. R. J. Bauer and J. L. Kenyon. Departments of Pharmacology and Internal Medicine, University of Texas Health Science Center, Dallas, TX 75235.

We have developed a general and systematic method for calculating rate constants for kinetic models from stationary patch-clamp data. The theory of Markov stochastic processes is used to derive the relationship between the autocorrelation function of channel gating and the rate constants of a specific kinetic model of n kinetic states and x conductance levels. This two-point correlation contains all of the kinetic information available in stationary patch-clamp data (Bauer and Bowman, this meeting). Then, estimates for the rate constants are obtained from the analysis of the point-by-point autocorrelation of the current levels recorded by the patch-clamp (not autocorrelations of dwell times as used by Labarca, et al. J. Neurosci. 4:502, 1984). Our method is particularly well suited for the analysis of data from patches containing more than one channel because it is able to use all of the data, regardless of the number of channels open at any time, in virtually the same amount of time it would take to analyze a similar amount of data containing a single channel. The autocorrelation method is also relatively insensitive to errors caused by the misidentification of short events due to limited bandwidth or a poor signal-to-noise ratio. In addition, we have developed the numerical methods for calculating the rate constants for any general kinetic model from autocorrelation functions. We have used this method for the kinetic analysis of the gating of inward rectifier channels of guinea pig ventricular cells using a C-C-O model and found that the rate constants compared well with those obtained using a standard dwell time histogram analysis. Supported by NIH HL26528.

T-Pos2 THE KINETIC INFORMATION CONTENT OF PATCH-CLAMP DATA. R. J. Bauer and B. F. Bowman (Intro. by D. M. Jameson). Departments of Pharmacology and Physiology. University of Texas Health Science Center, Dallas, TX 75235

We have developed a theoretical basis for the kinetic analysis of stationary and nonstationary patch-clamp data. We assume that channel gating is a Markov process that can be described by models of n kinetic states, x conductance levels, and n(n-1) rate constants describing the transitions between the kinetic states. In addition, we consider that the rate constants may be instantaneous functions of an experimentally manipulatable parameter (eg. voltage). We have found that patch-clamp data lack (n-x)(n-1) independent parameters necessary to determine all of the rate constants of a given model. This means that (n-x)(n-1) rate constants must be assigned values on the basis of other data or (more commonly) assigned arbitrary values. For stationary data (obtained at a single voltage), patch-clamp data can then be used to calculate x(n-1) rate constants. Values for these rate constants may be obtained from two-point correlation functions or from dwell time histograms. For nonstationary data (obtained during jumps among v different voltages), patch-clamp data may be used to calculate (x+vn-n)(n-1) rate constants. These rate constants may be obtained from three-point correlation functions or dwell time analysis. The choice of the (n-x)(n-1) assignments determines the form of the model and the values of the calculated rate constants. Assignments that contradict the data form invalid models that may be discarded. Assignments that do not contradict the data form valid models that cannot be distinguished on the basis of patch-clamp data. In general, there will be many sets of such assignments and valid models. Supported by NIH HL26528.

T-Pos3 **FRACTAL MODEL OF ION CHANNEL KINETICS**

L. Liebovitch, J. Fischbarg, and J. Koniarek, Dept. Ophthalmology, Columbia U., NY 10032

Ion channels have been widely modeled as consisting of a small number of discrete conformational states such as closed⇄closed⇄open, and the transitions between the states treated as a Markov process. We derive an alternative model based on a fractal scaling of the kinetic rate constants $k = At^{1-D}$, where A is a constant, t time, and D the fractal dimension. The frequency histogram of open or closed times predicted for such a fractal channel is $f(t) = At^{1-D}\exp\{-[A/(2-D)]t^{2-D}\}$. By measuring the effective kinetic rate constants at different time scales, we show how to determine if single channel records are best represented by models with discrete Markov states or continuum fractal kinetics. Analysis of patch clamp recordings from the corneal endothelium shows that its channels have fractal rather than Markov kinetics. This suggests that the multiple closed states postulated by Markov models to fit the histograms of closed times may not exist but are an artifact of trying to fit the sum of exponentials to histograms that are not the sum of exponentials. Supported by NIH grants EY6234 and EY1080.

T-Pos4 BROWNIAN DYNAMICS SIMULATION OF ION FLUX IN CHANNELS WITH MULTI-ION OCCUPANCY by E. Jakobsson and S.W. Chiu. Department of Physiology and Biophysics and Program in Bioengineering, University of Illinois, Urbana, Il. 61801.

Brownian dynamics programs have been written and are apparently working to simulate two situations of multiple occupancy in ion channels. One case is where the channel is so narrow that ions and water can not get past each other, so that ions move in the channel essentially as a unit, maintaining a fixed distance between themselves. This is almost certainly a good approximation to the situation in gramicidin channels. A second case is where the channel is slightly wider, so that ions and water can move past each other but ions of the same sign charge can not. It seems probable that many cation channels, or at least their most restrictive selective regions, are of this type. Our programs are validated to the extent that they give zero flux and appropriate equilibrium distributions of ions at the Nernst potential, and give appropriate net flux in the limiting conditions of independent ion movement (in which case the flux is analytically calculable). We are exploring through simulation the saturation and I-V properties of channels of these types as a function of the potential profiles and strength of ion-ion interactions. Comparison will be made to published data on gramicidin and other cation channels. Supported by Grant PHS 1 RO1 GM32356.

T-Pos5 ELECTRODIFFUSION THEORY OF ONE-ION CHANNELS by S.W. Chiu and E. Jakobsson, Department of Physiology and Biophysics and Program in Bioengineering, University of Illinois, Urbana, Il 61801.

The electrodiffusion theory of the one-ion channel presented by Levitt (1986) has been extended in several ways. The "semi-continuous concentration" boundary condition has been coupled with diffusion to convergence to extend the theory to include diffusion limitations outside the channel. The resulting equations are inconsistent with an earlier Levitt (1982) result describing the same situation. We believe the new result is the correct one, for reasons to be presented in this paper. The Levitt (1986) theory is also extended and combined with theory of passage times (Weiss, 1967) to calculate mean passage and occupancy times, for ions that pass through and block the membrane, respectively. One striking result is that mean passage times are the same for ions moving against and with voltage gradients. The basic and extended theories have been used to calculate potential functions and mobilities corresponding to published data on Na permeation of normal and substituted (Barrett-Russell et al, 1986) gramicidin, and to validate Brownian dynamics (Cooper et al, 1985) programs describing the same phenomena. It is found that the major effects of substitution of polar groups at the #1 position in gramicidin are to deepen a potential well near the channel mouth and reduce the mobility of the ion-water complex. Barrett-Russell, E.W., Weiss, L.B., Navetta, F.I., Koeppe, R.E., and O.S. Anderson, 1986. Biophys. J. 49:673-686; Cooper, K., Jakobsson, E., and P. Wolynes 1985. Prog. Biophys. molec. Biol. 46:51-96; Levitt, D.G. 1982. Biophys. J. 37:575-87; Levitt, D.G. 1986 Ann. Rev. Biophys. and Biophys. Chem. 15;29-57; Weiss, G.H. 1967 Adv. Chem. Phys. 13:1-18 Support by Grant PHS RO1 GM32356 from the NIH.

T-Pos6 THE INFLUENCE OF SURFACE CHARGE DISTRIBUTIONS ON THE ELECTRIC POTENTIAL IN A CHANNEL VESTIBULE. Peter C. Jordan, Dept. of Chemistry, Brandeis University, Waltham, MA 02254

Fixed surface charges may significantly affect the permeability of transmembrane ion channels. The magnitude of the effect depends both on the ionic strength of the electrolyte and on the geometry of the system (1,2). A vestibule isolates the channel entrance from surface charges at membrane-water interface; as a result the electric field, a fixed distance from this interface, is smaller in the vestibule than in the bulk electrolyte. Conversely, the field due to a charge in the vestibule is enhanced because the surrounding lipid confines the field to the aqueous electrolyte. I will consider ionic solutions dilute enough to be described by the linearized form of the Poisson-Boltzmann equation. Exact results for the electric potential, due to either a vestibule charge or a surface charge distribution, will be presented for two limiting cases-long narrow vestibules and short wide vestibules. Approximate results, useful for more general geometries, will also be described. In addition, the influence of counterion binding at the membrane surface will be considered.

1) Levitt, D.G. 1985. Biophys. J., 48:19-31.
2) Dani, J.A. 1986. Biophys. J., 49:607-618.

T-Pos7 A THEORETICAL STUDY OF DOUBLE ION OCCUPANCY IN A GRAMICIDINLIKE CHANNEL. Shen-Shu Sung and Peter C. Jordan, Dept. of Chemistry, Brandeis University, Waltham, MA 02254

Extending our previous work on valence selectivity in gramicidin (1), we are studying the possibility of double occupancy in order to understand the effect a second ion, in the opposite half of the channel, may have on selectivity and conductance. A number of potential energy profiles for Na^+-Na^+ double occupancy will be presented. The presence of intervening water molecules significantly reduce the electrostatic repulsion. Low energy configurations, emphasizing the influence of hydrogen bonding among water molecules and between water and polar groups of the channel, will be illustrated. The Na^+-Cl^- double occupancy study shows that the presence of Na^+ at one end of a channel substantially lowers the large entrance barrier for a Cl^- ion at the other end of the channel. This is consistent with the experimental observation of a possible anionic contribution to channel conductance at high salt concentrations (2). Some results of molecular dynamics simulations at 300°K will be presented to show the kinetic behavior for ions and water molecules in the channel mouth and in the channel interior.

1) Sung, S. and Jordan, P.C. 1986, Biophys. J. 49:376a.
2) Eisenman, G.; Sandblom, J. and Neher, E. 1978, Biophys. J. 22:307.

T-Pos8 UNIFORMLY ORIENTED GRAMICIDIN CHANNELS EMBEDDED IN THICK MONODOMAIN LECITHIN MULTILAYERS*--Glenn A. Olah and Huey W. Huang, Physics Department, Rice University, Houston, TX 77251

Phosphatidylcholine multilayers containing 20% water by total sample weight and gramicidin/lipid molar ratios up to 1/40 were aligned by low temperature annealing (< 60 C) and mechanical stressing. We were able to obtain large (> 80μ thick x 40mm^2 area) monodomain defect-free multilayers containing about 10^{17} uniformly oriented gramicidin channels. The alignment of lipid multilayers was monitored by conoscopy and polarized microscopy. The smectic defects which appeared during the alignment process were identified and dissolved. The incorporation of gramicidin in the multilayers in the form of transmembrane channels was proven by its circular dichroism (CD). A well defined CD spectrum of uniformly oriented gramicidin channels was obtained. The oriented samples will allow spectroscopic studies of the ion channel in its conducting state, and diffractive studies of the channel-channel organization in the membrane. Recently there were flourescence and electron microscopic studies on the channel - channel organization in membrane. It was suggested that gramicidin channels form rows of linear arrays of hexamers in membrane. We believe that small angle neutron scatterings of oriented multilayer samples provide the best way for determining the channel - channel correlations. The results of this and other experiments will be presented.

*This research was supported in part by the Office of Naval Research Contract N00014-86-K-0087, the National Institute of Health Grant No. HL 32593, and The Robert A. Welch Foundation.

T-Pos9 LARGE CONDUCTANCE CHANNEL IN RAT PINEAL CELLS. John Ives Halperin and Stephen Yeandle. Naval Medical Research Institute, Bethesda, Maryland 20814-5055; David C. Klein, Section on Neuroendocrinology, Laboratory of Developmental Neurobiology, National Institute of Child Health and Human Development, National Institutes of Health, Bethesda, Maryland 20892.

On-cell patch clamp studies of rat pineal cells demonstrate an outwardly conducting channel of approximately 150 pS. The voltage sensitiviy, magnitude and direction of conductance, and partial information on the ion specificity of these channels suggest that this is a calcium activated potassium channel, similar to those described for other cells. Preliminary data suggest that the presence of norepinephrine in the recording pipette increases the probability of channel openings at a given holding potential and may lower the holding voltage at which channel openings are first seen. The hyperpolarization of pineal cells by norepinephrine, as seen using standard intracellular micropipette electrodes (Freschi and Parfitt, Brain Research, 368 (1986) 366-370; Parfitt et al, Molecular Pharmacology 11 (1975) 241-255), may be caused by the opening of these channels.

T-Pos10 COLICIN Ia: BIOPHYSICAL STUDIES OF A KILLER ION CHANNEL *Stephanie F. Mel, Partho Ghosh, Robert M. Stroud, Departments of *Pathology and Biochemistry and Biophysics, University of California, San Francisco 94143.

Colicin Ia, a bactericidal protein, exists both as a water soluble as well as a transmembrane molecule. The mode of killing action involves the dissipation of the electrochemical gradient of a sensitive bacterial strain by the formation of an ion channel in the plasma membrane. We are interested in understanding the mechanism by which proteins insert into membranes as well as the structural basis for ion channel formation and gating. To answer the first question, we have investigated the pH dependence of colicin insertion into artificial membranes using a fluorescence leakage assay (ANTS/DPX) in unilamellar liposomes. We find that colicin does not readily insert into neutral PC vesicles, suggesting that insertion requires a negative surface charge on the lipid. We also find that colicin inserts preferentially into negatively charged liposomes at pH 4.5 rather than at pH 7, indicating that either the negative surface charge must not be too great or that the protein must be protonated to some degree. To determine if the pH dependence of insertion is due to a structural change in the molecule, we examined CD spectra. Results on soluble colicin show similar, strong α-helical signals at both pH values.

To further analyze insertion and channel phenomena, we are currently using a planar lipid bilayer with a Gigaohm seal to obtain single channel recordings. We are characterizing colicin in terms of its channel size, ion selectivity, and the effect of both lipid composition and pH on protein insertion.

T-Pos11 STRUCTURE OF A CHANNEL-FORMING COLICIN Ia

Seunghyon Choe, Jordan Konisky*, & Robert Stroud (Department of Biochemistry & Biophysics, Univ. California, San Francisco, *Department of Microbiology, University of Illinois, Urbana-Champaign)

The crystal structure of colicin Ia has been solved at 5 A resolution. Colicin Ia is one of E1-type bacteriocidal proteins that is produced by E. coli to kill other bacterial strains by forming an ion-permeable channel in the cytoplasmic membrane of the target cell. The protein folding of a channel-forming domain of the molecule seems to provide the thermodynamic stability of the molecule both in water and in a membrane lipid environment.

Crystal fragments of cilicin Ia were also observed by electron microscopy, which showed that the molecule is at least 70 A long and probably Y- or hockey stick-shaped. X-ray diffraction studies determined the space group to be C2221, a=66.3, b=176.6, c=289.6, and z=8. Data were collected on films using intense synchrotron X-ray source. The electron density maps were calculated with SIR phases from a PtCl4 derivative at 5 A that were further improved by B.C. Wang's solvent flattening methods. A possible domain structure is proposed. (The authors acknowledge S. Hershenson, N.Helmers, P. Ghosh, W. Montfort for the help throughout the work.)

T-Pos12 MEMBRANE POTENTIAL- AND CONCENTRATION-DEPENDENCE OF COLICIN E1 CHANNEL FORMATION IN ARTIFICIAL MEMBRANE VESICLES. Arnold A. Peterson and William A. Cramer, Dept. of Biological Sciences, Purdue University, West Lafayette, IN, 47907.

The in vitro channel-forming ability of colicin E1 is dependent on pH and membrane potential. While channel-forming colicins exhibit a pronounced dependence on trans-membrane potential in planar membranes, the voltage dependence of these colicins in artificial membrane vesicles has not always been observed. Potential-independent ionophoretic activity of colicins in vesicles may not represent normal channel activity. We have obtained conditions for vesicle studies under which the thermolytic M_r 18,000 COOH-terminal peptide of colicin E1 exhibits a strong voltage dependence. Channel activity was measured using a chloride electrode to follow the release of entrapped Cl^- from sealed vesicles. Large unilamellar vesicles (avg. diam. 200-300 nm) were used, as SUV's did not entrap a large enough amount of Cl^- to measure release. The presence of a valinomycin-induced potassium diffusion potential, arising from a K^+ gradient $\geq$ 20, resulted in a 10-fold increase in the rate of Cl^- efflux. In the presence of these diffusion potentials, less than 10 ng peptide/mg lipid released all entrapped chloride from the vesicles, suggesting that most of the peptide forms channels. The initial rate of Cl^- release versus peptide concentration was linear (3×10^4 Cl^-/peptide·sec at pH 4.0) at protein:lipid ratios $\leq$ 1:140,000. (We wish to thank Norm Olsen for the electron microscope determination of vesicle size; supported by NIH grant GM-18457.)

T-Pos13 INOSITOL 1,4,5 TRIPHOSPHATE OPENS DIPHTHERIA TOXIN CHANNELS. Bruce L. Kagan, Departments of Psychiatry and Physiology, UCLA School of Medicine and West Los Angeles Veterans Administration Medical Center, Los Angeles, CA 90024

Inositol 1,4,5 triphosphate (IP_3) acts as an intracellular chemical "second messenger" in many cells. Binding of a ligand to a cell surface receptor leads to increased production of IP_3 which in turn leads somehow to the final intracellular effects. Ca^{++} release into the cytosol often accompanies the production of IP_3 but the nature of the relationship between Ca^{++} and IP_3 is controversial. We report that 0.5-5.0 micromolar IP_3 on the trans or "cytosolic" side of the membrane cause dramatic (5-50 fold) increases in the opening rate of diphtheria toxin (DT) channels inserted in lipid bilayers. DT channels are voltage and pH gated ion permeable channels which are thought to play a role in transport of DT's enzymatic fragment A across membranes into cells. Channel opening by IP_3 is probably mediated through the "P site" of DT since DT ligands such as ApUp and ATP can block the effect of IP_3 and DT mutants lacking the "P site" such as CRM 45 are not stimulated by IP_3. Since DT channels are permeable to Ca^{++} they may provide a model for the action of IP_3 in which cytosolic IP_3 opens calcium permeable channels located in the plasma or intracellular membranes. We also suggest that IP_3 may play a role in facilitating the entry of DT into susceptible cells.

Supported by a Pfizer Postdoctoral Scholarship, Veterans Administration Career Developement Award and BRSG - RR5756 from NIH.

T-Pos14 PATCH CLAMP STUDY OF IONIC CHANNELS IN RAT PANCREATIC B-CELLS IDENTIFIED WITH THE REVERSE HEMOLYTIC PLAQUE ASSAY. M. Hiriart and D.R. Matteson, University of Pennsylvania, Philadelphia, PA. We have been using the reverse hemolytic plaque assay (RHPA) to study the secretory properties of isolated, adult rat B-cells, and the patch-clamp technique to study ionic channels in B-cells identified with the RHPA. Isolated single B-cells respond to the primary secretagogues and neurotransmitters that affect insulin secretion from intact islets. Insulin secretion (measured by plaque size) is larger in the presence of 20 mM glucose than in 5 mM glucose, and can be stimulated further by 1 mM 3-isobutyl-1-methyl-xanthine (IBMX). In the latter condition, 89% of the single cells formed plaques, and thus could be identified as B-cells. In 5 mM glucose, carbamylcholine (1 uM) increases the proportion of islet cells which form plaques, and increases plaque size. In 20 mM glucose, epinephrine (100 nM) decreases the proportion of islet cells which form plaques and decreases plaque size. For patch-clamp experiments, the RHPA was performed on small pieces of coverslips which could be kept in tissue culture for several days. Inward currents in identified B-cells were characterized with the whole-cell variation of the patch clamp technique. Almost all cells had a fast, transient inward current component which was identified as voltage-dependent sodium current by several criteria: the current had a reversal potential near the sodium equilibrium potential, was blocked by TTX and inactivated rapidly and almost completely. In the steady state, the Na channels are almost completely inactivated at -40 mV. In addition to Na current, another inward current component was present in some cells, which did not inactivate within 10 ms and deactivated in both a fast and a slow phase. This current is most likely due to the activity of FD and SD calcium channels.

T-Pos15 COMPARISON OF CATION CHANNELS IN ISOLATED AND IN SITU PEPTIDERGIC NEUROSECRETORY TERMINALS P. Ruben* and I. Cooke, Békésy Lab. of Neurobiology, Univ. of Hawaii, Honolulu, HI 96822.

Peptidergic neurosecretory terminals of the crab (Cardisoma carnifex) sinus gland were studied in terminal-attached and inside-out patch clamp configurations. F channels (Lemos, et al., Nature 319, 410, 1986) from acutely isolated and in situ terminals were compared. We confirmed that f channels show short, bursty openings, a conductance of 69 pS in symmetrical KCl, nearly equal conductance to Na and K, and no permeability to Cs, Ca, Ba, Cl or SO_4. In addition, the channels showed little activity in terminal-attached patches or when excised with 310 mM KCl on both sides of the inside-out patch, but were activated by an increase in $[Na]_i$. Mean open time and P_o increased up to 20X and 10X, respectively, when patches excised from isolated terminals were in $[Na]_i \geq 40$ mM. They increased up to 8X and 2X, respectively, when patches from in situ terminals were excised into physiological saline (490 mM NaCl). Reduced f channel activation in the latter case is attributable to the high saline Ca. Reduction in channel activity was also observed when Ca or Ba was added, in the presence of at least 40 mM Na, to the inside of patches excised from isolated terminals. In summary, we found no differences in the behavior of f channels between acutely isolated and in situ terminals. These observations confirm the validity of studying isolated neurosecretory terminals, demonstrate that single channel data can be obtained from intact neurosecretory terminals, and suggest experiments which test the activation of identifiable channels in nerve terminals by the more physiological route of axonal stimulation.

Supported by NSF Grant BNS84-04459 and NIH Grant NS15453 to I.C.

T-Pos16 NON-HYDROLYZABLE ANALOG OF GTP MIMICS MODULATION OF K AND Ca CURRENTS BY FMRF-AMIDE IN APLYSIA NEURONS. V. Brezina. Department of Biology, UCLA, Los Angeles, CA 90024.

In certain neurons in the abdominal ganglion of Aplysia californica, the endogenous neuropeptide FMRFamide enhances a K current resembling the serotonin-sensitive 'S' current (Brezina et al. 1987, J. Physiol. 382), and simultaneously suppresses the Ca current, and consequently the Ca-dependent K current (Brezina et al. and Erxleben et al. 1985, Biophys. J. 47, 435a). Further experiments (using two-electrode voltage clamp of cells L2-L6 and R2) reveal that all of these effects of FMRFamide are mimicked by iontophoretic or pressure injection into the cell of guanosine 5'-O-(3-thiotriphosphate) (GTP-γ-S). Thus, GTP-γ-S activates a steady current that has all the properties of the FMRFamide-induced 'S'-like current: it reverses at E_K, shows no voltage dependence apart from constant-field rectification, it is Ca-independent, only weakly blocked by TEA and 4-AP, but suppressed in Ba-containing solution and by elevation of intracellular cAMP. In addition, GTP-γ-S suppresses the Ca and Ca-dependent K currents elicited by depolarizing voltage steps; the pharmacologically isolated Ca current is suppressed by 50-70%. These effects of GTP-γ-S, unlike the parallel effects of FMRFamide, are slow to develop (10-30 min) and irreversible, and are observed even without prior exposure of the cell to FMRFamide, although, when the peptide is applied before the actions of GTP-γ-S are fully developed, its effects also become irreversible. Once the actions of GTP-γ-S are fully developed, FMRFamide has no further effect. These results suggest that suppression of Ca current and enhancement of 'S'-like current by FMRFamide in these cells may normally be mediated by a GTP-binding protein. Supported by NSF BNS 83-16417, USPHS RO1 NS08364 (both to Dr. R. Eckert) and USPHS NRSA GM07185.

T-Pos17 STRETCH-ACTIVATED CATION CHANNEL IN YEAST. M.C. Gustin, X.L. Zhou, B. Martinac, M.R. Culbertson, C. Kung (Intr. by Y. Saimi) Laboratory of Molecular Biology, University of Wisconsin, Madison, WI 53706

After enzymatic removal of the cell wall, patch clamp recording techniques can be used to study the ion channels of the yeast, Saccharomyces cerevisiae. Tight-seal, whole-cell recordings using yeast spheroplasts have revealed the presence of at least two ion channels in the plasma membrane - a previously described voltage-gated K^+-specific channel (Gustin, et al, 1986, Science 233:1195) and a stretch-activated channel. The latter channel has been studied in on-cell patches and in whole-cell mode and has the following properties. Applying pressure through the recording pipette, channel open probability was dependent on outward pressure (cell-inflating); inward pressure had no effect. Stretch-activation in whole-cell mode in symmetrical solutions displayed threshold behavior; at least 1-2 cm Hg pressure was generally required to observe channel openings. Lowering bath osmolarity while recording in whole-cell mode also increased channel open probability. The voltage-dependent K^+ channel in outside-out patches displayed no pressure sensitivity. Stretch-activated channels displayed at least two conducting states with conductances of 40 and 75 pS, respectively. Using a CsCl salt gradient to examine cation vs anion selectivity, the P_{Cs}/P_{Cl} (from reversal potential measurements) for both conducting states was greater than 40. The stretch-activated channels were cation-nonselective, since Na^+, K^+, Cs^+, tetraethylammonium$^+$, Mg^{2+}, Ba^{2+} and Ca^{2+} were all permeant. These channels may play a role in osmoregulation or budding, processes in which membrane expansion has been noted. (Supported by NIH GM22714, GM36386).

T-Pos18 A STRETCH-ACTIVATED ANION CHANNEL IN CULTURED TOBACCO CELLS. L. Falke, K.L. Edwards, B.G. Pickard, S. Misler, Jewish Hospital and Washington Univ., St. Louis, MO, 63110.

Many plant cells, like animal cells, transduce membrane deformation by external stimuli to localized changes in membrane permeability; stretch activated channels (S.A.) may be involved in both phyla. We present evidence for a S.A. anion selective channel in plasma membranes of protoplasts from stem derived tobacco cells in suspension culture. Long duration channels, whose probability of being open increased with pipette suction, were seen in both cell-attached and outside-out configurations (see figure below). In the outside-out patch, single channel conductance (at 0mV) was 100pS and the zero current potential was -37mV, with 200mM KCl+10mM $CaCl_2$ in the pipette and a 5mM KCl+10mM $CaCl_2$ bath. P_{Cl}/P_K was computed to be 9.5/1 using the Goldman-Hodgkin-Katz equation. This channel does not show significant voltage dependence, unlike S.A. cation channels in animal tissue. The probability of N channels being open with constant suction was binomially distributed, suggesting independent channel gating. Similar S.A. channels in plants may signal physical stimuli such as gravity, friction and internal tissue stress, and may mediate osmoregulation.

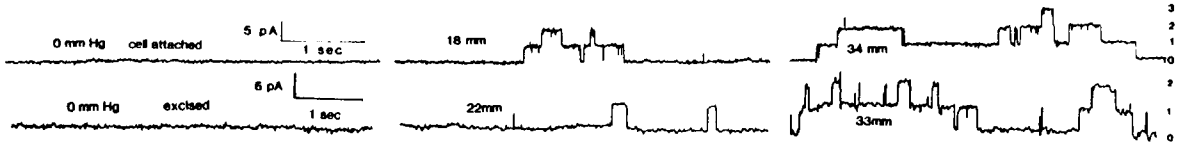

T-Pos19 STRETCH-ACTIVATED CHANNELS IN FRESHLY DISSOCIATED SMOOTH MUSCLE CELLS.
Michael T. Kirber, Joshua J. Singer, and John V. Walsh Jr. Dept. of Physiology, University of Massachusetts Medical School, Worcester, MA 01605.

Single-channel currents were recorded from stretch-activated channels in freshly dissociated smooth muscle cells from the stomach of the toad Bufo marinus. The probability that these channels are in a conducting state increases as greater suction is applied to the patch pipette. Under physiological conditions with the cell at normal resting potential (cell-attached patches, amphibian physiological saline solution in the bath and patch pipette) these channels carry inward, depolarizing currents in response to applied suction. The slope conductance under these conditions is approximately 55 pS. To eliminate the possibility of activation by Ca^{++} entering the cell due to membrane disruption caused by suction, experiments were carried out using a Ca^{++}-free saline (2mM EGTA) in the bath and pipette with similar results. In addition, inward currents in response to applied suction were also observed when the pipette contained 72mM $BaCl_2$, 30mM TEA-Cl, and 10mM HEPES and when the pipette contained 59mM $CaCl_2$, 50 mM TEA-Cl, and 10mM HEPES. These currents were, however, smaller and the slope conductance was only about one third of that observed when physiological saline was in the pipette. As an experiment progressed we frequently observed increased sensitivity to suction; this may be due to a change in the patch geometry as additional membrane is drawn into the patch pipette (Sachs, F. 1986, Update in Cardiovascular Neurobiology, FASEB, in press). We find these channels in a substantial fraction of the patches; thus, channels of this type could well be responsible for initiating stretch-activated contraction in smooth muscle. Supported by NSF DCB-8511674 and NIH DK 31620.

T-Pos20 STRETCH-ACTIVATED CHANNELS IN SEVERAL TISSUES. X.C. Yang and F. Sachs
(intr. D. Faber), Dept. Biophysics, SUNY, Buffalo, NY

Stretch-activated (SA) ion channels exist in Xenopus oocytes (Sakmann et al, Nature 318:538, 1985). We find that they have similar properties to those previously described for SA channels in chick muscle. SA channels have also been recorded from Amphiuma red blood cells and Xenopus myocytes in culture. However, detailed experiments have only been pursued on the oocytes and chick myocytes. SA channels in both preparations generally show one open and three closed states although a second, short lived, open state is sometimes seen. The time constants for Xenopus at 26 °C (T_{open} = 1ms, closed times: T_{slow} = 1-10ms, T_{medium} = 0.2ms, T_f = 0.05ms.) are similar to the values for chick at 37°C. As with the chick, only the longest closed time component is sensitive to membrane tension and follows a sigmoid relationship with tension saturating at about 2cmHg. This slow component is also voltage sensitive, decreasing lifetime with depolarization at ca.50mV/e. The tension sensitivity of SA channels from oocytes is much higher than that of channels from normal chick myocytes but resembles the sensitivity of cytochalasin treated myocytes. This result fits with the absence of actin stress fibers in the oocytes. The sensitivity to stretch increases with temperature as expected if the channel structure becomes more compliant with increasing temperature. This suggests an enthalpic rather than entropic origin to the elasticity. The oocyte channel conducts K, Na, Cs, and NH^+ approximately equally and Li somewhat less. The I/V relationship is inwardly rectifying. The conductance is about 90pS in the cell attached mode with 160mM K^+ in the pipette. The channel density in oocytes is ca. 4/patch compared to ca. 2/patch for chick.

Supported by NIADDK DK37792-09A1 and USARO 22560-LS.

T-Pos21 GLUTAMATE RESPONSE OF ADULT NEURONS ISOLATED FROM THE MEDIAL NUCLEUS TRACTUS SOLITARIUS (M-NTS): BLOCK OF A CHLORIDE CONDUCTANCE.
J.A. Drewe and D.L. Kunze*, Univ. of Texas Medical Branch, Galveston, TX, 77550. * Baylor College of Medicine, Houston, TX, 77030.

The M-NTS, situated at the obex of the fourth ventricle, is a major cardiovascular center. The baroreceptor afferents synapse in the M-NTS, primarily on 10-15 μM diameter bipolar neurons. Neurons of this morphology, enzymatically dissociated from adult guinea pig M-NTS, were studied acutely under voltage clamp conditions at 21°C. Glutamate has been proposed as an excitatory neurotransmitter in the M-NTS. Whole cell patch clamp recording with 3-8 MΩ electrodes was used to investigate the current response to brief external application of 0.1 mM glutamate. The solutions consisted of normal internal and external cationic concentrations, chloride as the sole anion (E_{Cl}=-1 mV). We have reported previously that a subset of these neurons, with GΩ input resistances at hyperpolarized potentials, respond to glutamate with an activation of a nonspecific cation conductance. Among this morphologically similar group of neurons another subset of neurons (33%), recognizable by input resistances <200 MΩ, respond to glutamate with a reversible resistance increase to >500 MΩ. The relationship of peak change in current in response to glutamate vs holding potential (n=25) for these neurons revealed 1) an outward current at potentials hyperpolarized to the reversal potential with an apparent net decrease in conductance 2) a current reversal near zero mV which shifted with internal or external Cl^- replacement with sulfate derivatives and 3) no apparent voltage dependence in symmetrical Cl^- solutions (-80 to 60 mV). This glutamate sensitive conductance was blocked by 1 mM Zn^{++} and was not observed in Cl^- free medium. We propose that some adult M-NTS neurons possess a primarily chloride permeable conductance which can be modulated by μmolar levels of glutamate. Supported by DHHS HL36840.

T-Pos22 THE EFFECT OF TEMPERATURE ON GABA-GATED CHLORIDE CURRENTS IN FROG SENSORY NEURONS. J.M.H.ffrench-Mullen, N.Tokutomi & N.Akaike, Department of Physiology, Faculty of Medicine, Kyushu University, Fukuoka 812, Japan.

GABA-induced I_{Cl} in frog dorsal root ganglion cells (DRG) show activation and inactivation phases each consisting of two exponentials (τ_f, fast; τ_s, slow), (Akaike et al., J. Physiol., in press). We have examined the effects of temperature (range 10-35°C; room temp. 25°C) on the kinetics of GABA-induced I_{Cl}. DRG cells were isolated, perfused internally and externally with Na, K, Ca free and 120 mM Cl solutions to isolate the Cl current. Cells were 'whole-cell' clamped and held at -20 mV to reduce the Cl driving force. GABA was applied by the 'concentration clamp' technique. Cells were kept at room temp. between exposures to GABA (1-2x 10^{-5} M) at different temperatures. Peak I_{Cl} was reduced by either decreasing or increasing temp. with recovery greater than 80% of control. Cooling led to a reversible increase in τ_f and τ_s of both activation and inactivation. Increasing temp. from room temp. to 35°C decreased τ_f and τ_s of both activation and inactivation. Good recovery was not obtained below 10°C and above 35°C.

Dose-response curves (10^{-6} to 10^{-4} M) at 10°C showed a shift to the left as compared to room temp., suggesting an increase in GABA receptor affinity. At 10°C, peak I_{Cl} from 10^{-5} M GABA increased with time (10-15 mins) to a steady-state but, there was still an increase in τ_f and τ_s for both activation and inactivation.

The increase on cooling and decrease on heating of τ_f and τ_s for both activation and inactivation suggest changes in Cl channel gating.

T-Pos23 CATION/ANION SELECTIVITY OF CL CHANNELS IN RAT HIPPOCAMPAL NEURONS. F. Franciolini and W. Nonner, Dept. of Physiology and Biophysics, Univ. of Miami, Miami, FL 33101.

Unitary currents from a voltage-dependent anion channel (conductance 30 pS in 150 NaCl saline) were studied in excised inside-out patches from cultured hippocampal neurons of embryonic rat. Previous experiments, measuring reversal potentials in the presence of a NaCl gradient, have revealed a significant permeability to Na cation (P_{Na}/P_{Cl} = 0.2). We have done further experiments in order to determine the conditions necessary for cation transport in this channel. Li, K, and Cs are also permeant (P_X/P_{Cl} = 0.38, 0.25, and 0.35). When exposed to gradients of TRIS Cl, the channel does not discriminate among cation and anion. Substitution of internal Cl by sulfate abolishes unitary current in the inward direction; with sulfate as the anion on both sides and Na or TRIS as the cation, no current is observed in either direction. The absence of current is not due to block by sulfate, as adding 100 mM of Na_2SO_4 to a 150 mM NaCl internal saline does not affect unitary conductance. It seems that cations require the presence of a permeant anion in order to pass through the channel. A converse experiment shows that the conductance depends on the species of cation present: substituting internal Na by Cs ion increases the unitary conductance 1.4-fold over that in 300 mM, symmetrical NaCl. The results may be understood in terms of a mechanism in which an anionic site in the pore adsorbs an alkali cation to form a dipole that allows anions to pass. The cation can be released and pass through only while a suitable anion is associated to it. The mechanism implies that reversal potentials are affected by cation permeability only in the presence of a cation gradient. Since the channel does not distinguish among Na and K ion, the physiological reversal potential would be determined solely by the permeant anions. Supported by NIH grant GM30377.

T-Pos24 EXTERNAL ANIONS REGULATE STILBENE-SENSITIVE PROTON TRANSPORT IN PLACENTAL BRUSH BORDER VESICLES. G. Cabrini, N.P. Illsley, and A.S. Verkman. UCSF, San Francisco, CA 94143.

The mechanism for HCO_3-independent proton permeability in microvillus membrane vesicles (MVV) isolated from human placenta was examined using the entrapped pH indicator 6-carboxyfluorescein (6CF). Proton fluxes (J_H) across MVV were determined from the time course of 6CF fluorescence in response to induced pH, anion and Na gradients using the MVV buffer capacity, and the 6CF pH calibration. In MVV voltage-clamped with K^+ valinomycin and in the absence of transportable anions, J_H was 12 ± 2 neq/s·mg protein (pH_{in} 7.4, pH_{out} 6.0, 23°C), corresponding to a proton permeability coefficient of 0.02 cm/s, and an activation energy of 9.1 ± 0.3 kcal/mol. For a 0.5 unit pH gradient J_H increased from 1.5 to 4.6 neq/s·mg as internal MVV pH was increased (5.5-7.5). J_H was inhibited 20% by dihydro-4,4'-diisothiocyano-2,2'-stilbenedisulfonic acid (H_2DIDS) with K_I = 8 μM. External Cl, Br, and I (but not SO_4 and PO_4) increased J_H 1.3-2.5-fold for both inwardly and outwardly directed pH gradients with K_D = 1.0 ± 0.4 mM (Br) and >100 mM (Cl). This increase was blocked by 100 μM H_2DIDS but not by amiloride or furosemide. Internal Cl did not alter J_H induced by pH gradients. Proton fluxes were not induced by anion gradients in the absence of a pH gradient nor were Cl fluxes induced by pH gradients. Experiments in which J_H was driven by membrane potentials (induced by valinomycin and K gradients) indicated that proton transport in the absence of Na^+ was voltage-sensitive. In the absence of Cl, inwardly directed Na gradients enhanced proton efflux driven by a 1.4 pH unit outwardly directed H gradient; transport was neutral, blocked by 100 μM amiloride and had activation energy 12 kcal/mole (<28°C) and 33 kcal/mole (>28°C). These experiments demonstrate neutral Na/H exchange, and stilbene-sensitive proton conductance in MVV that is regulated allosterically by anions at an external binding site.

T-Pos25 CHLORIDE CHANNELS IN HUMAN MACROPHAGE T. Kanno, H. Sasaki and T. Takishima(Intr. by T. Shibata) First Department of Internal Medicine, Tohoku University, Sendai,Japan.

Important macrophage functions include inraphagolysosomal killing of microorganisms, antigen presentation to T-lymphocytes as well as recycling of some types of receptors. In these processes, acidic phagosome or receptosome is necessary and participation of an anionic channel is assumed. Because endosomal membrane is thought to be derived from plasma membrane, we studied ionic channels in plasma rather than endosomal membrane of human macrophage cell line, U937, using the inside-out configuration of the patch clamp method. We identified three Cl^- channels with different original conductances of 395, 24 and 14pS around OmV with symmetrical 150mM Cl^- solutions. The 24pS and 14pS channels were observed as fully open states rather than degraded components of a larger one. However, all three channels had multiple subconductance levels, at least 6 levels for the 395pS and 24pS channels. It took tens of minutes for these chnnels to be observed whereas the K^+ channel was observed immediately after excision of the patch, suggesting some factor inhibitory to the Cl^- channels. Current-voltage relationships of the 24pS and 14pS channels showed outward-going rectification whereas that of the 395pS channel was linear. The burst kinetic of 395pS channel was clearly voltage dependent; most active around OmV and less active with polarization in either direction. That of the 24pS channel was mildly voltage dependent, (Ca)i independent and pH_i dependent and less active at low pH_i. That of the 14pS channel was voltage independent. Endosomal acidification is accompanied with hyperpolarization of the membrane. We, therefore, suggest that the 24pS and 14pS channels, which are active at and blow resting membrane potential, may be involved in cancelling the electrogenic effect of the process during acidification of phagosome and receptosome.

T-Pos26 SINGLE CHLORIDE AND POTASSIUM CHANNELS IN DISSOCIATED AMPHIBIAN GASTRIC SMOOTH MUSCLE CELLS. Brendan S. Wong, Department of Physiology, Baylor College of Dentistry, Dallas, TX 75246

The patch-clamp technique was used to study single channel currents in dissociated Rana pipien gastric smooth muscle cells obtained by repeated enzymatic digestion with 0.1% trypsin and 0.1% collagenase in calcium-free Ringer solution. The most prominent potassium-selective channel is the previously reported large-conductance calcium- and voltage-activated channel, with a unit conductance of 113±16 pS (n=10) in physiological K ionic gradients. A second potassium-selective channel was observed with a single-channel conductance of 60±11 pS (n=5). The opening probability of this channel was dependent on voltage and independent of the cytoplasmic calcium concentrations. The properties of this channel are similar to the slow voltage-sensitive potassium channels found in isolated rabbit jejunum longitudinal smooth muscle cells and thus may play a role in the generation of slow-wave potentials. Two chloride-selective channels were also observed in these cells. A large unit conductance channel (524±41 pS (n=3)) was occasionally observed in excised patches bathed in symmetrical 116 mM NaCl solutions. These channels open and close spontaneously at +10 mV but their probability of opening decreases with either membrane hyperpolarization or depolarization. This channel was observed in less than 5% of all the patches studied. More frequently, a second chloride-selective channel with a single channel conductance of 66±9 pS (n=5) was observed which flickered rapidly between the open and closed states. Varying the cytoplasmic calcium concentrations had little effect on the activity of either chloride-selective channels. Tetraethylammonium reversibly blocked both potassium-selective channels, while having no effect on the chloride-selective channels. (Supported by BCD Research Fund.)

T-Pos27 ATP-ACTIVATED CURRENTS IN SINGLE VAS DEFERENS SMOOTH MUSCLE CELLS. David D. Friel, Department of Neurobiology, Harvard Medical School, Boston, MA 02115

Stimulation of the nerves supplying the rat vas deferens elicits a biphasic contraction, and it has been suggested that ATP is the transmitter that is responsible for the initial transient component of the mechanical response. I have studied the electrophysiological effects of ATP on single vas deferens smooth muscle cells using the whole-cell voltage clamp technique. Cells were isolated from vasa deferentia of six week-old male rats using an enzymatic dissociation procedure and were kept in culture for 1-5 days. Smooth muscle cells were identified by their characteristic morphology and by their contractile responses to exogenous ATP. Electrical recordings were made at 37°C in an external solution containing (in mM) 150 NaCl, 4 KCl, 2 $MgCl_2$, 10 glucose, and 10 Hepes, pH 7.4 (with NaOH); pipets contained 120 K glutamate, 5 $MgCl_2$, 10 EGTA, 10 Hepes, and (sometimes) 5 ATP and 1 GTP, pH 7.4 (with KOH). External ATP (200 µM) elicited inward currents at negative potentials (eg. I_{peak}=-86±7 pA at -130 mV, N=5) which were rapid in onset and which slowly desensitized ($t_{\frac{1}{2}}$=2.1±.6 s, N=5); resensitization ocurred over several minutes. When Na was replaced with N-methyl-D-glucamine, ATP elicited a much smaller current, while substituting for external K had relatively little effect. These results demonstrate that ATP activates a current in vas deferens smooth muscle that is carried mainly, but not entirely, by Na.

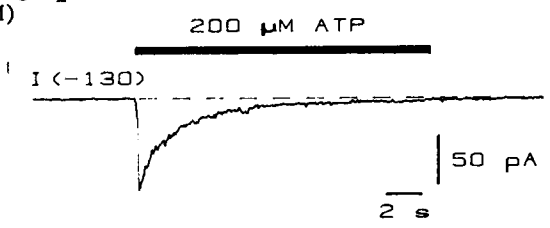

T-Pos28 STRETCH-ACTIVATED NET PLASMALEMMAL ION FLUXES AND DEPOLARIZATION IN RAT ATRIA. Donald D. Macchia[1] and Ernest Page,[2] Indiana University School of Medicine,[1] Gary IN 46408; and The University of Chicago,[2] Chicago IL 60637.

Since stretch stimulates secretion of atrial natriuretic peptides, we have sought evidence for stretch-activated plasmalemmal ion transport processes that might be implicated in stimulating exocytotic extrusion of the peptide. For this purpose we devised an apparatus permitting systematic distension of unstimulated atria at 38° C in vitro for 5 - 20 min by hydrostatic pressures (P) of 0 - 20 cm of modified Krebs-Henseleit solution oxygenated with 95% O_2/5% CO_2, under conditions allowing measurement of membrane potential as well as of cell volume and cell concentrations and contents of Na, K, and Cl. Mean cellular concentration ([ ]$_i$), in mmoles/kg cell water, at P = 0, for 6 atria incubated for 5 min at external K concentration of 5.9 mM were: $[Na]_i$ 42 ± 2, $[K]_i$ 82 ± 3, $[Cl]_i$ 36 ± 7. Stretch of 6 atria at P = 7 cm caused cell Na content to fall by 22 mmoles/g dry weight, while cell K and Cl contents and concentrations were unchanged. Concurrently, resting potentials (measured in the presence of saxitoxin to suppress action potentials) fell in less than 1 min from 63 ± 2 mvolt at P = 0 (n = 20 measurements in 5 atria) to 52 ± 2 mvolt at P = 7 cm (n = 25 measurements in 2 atria). Longer (10 min) or more forceful (P = 15 cm) stretches significantly increased net loss of cell Na. Cell Na loss was reversed in 5 min by changing from P = 7 cm to P = 0 cm. Ouabain prevented or obscured stretch-activated cell Na loss. ^{45}Ca uptake of atria stretched to P = 15 cm for 10 min significantly exceeded that of unstretched atria. Supported by the Indiana Heart Association[1] and the USPHS NHLBI[2].

T-Pos29 PERIOD DOUBLING AND IRREGULAR DYNAMICS OF PROPAGATION IN CARDIAC PURKINJE FIBERS. D. Chialvo; P.A. Chiale; J. Jalife. Syracuse, NY, USA and Rosario, Argentina.

Period doubling, quasiperiodic behavior and chaos have been demonstrated in oscillatory systems. However, no attempt has been made to show irregular dynamics in excitable non-pacemaker tissues. Unbranched sheep Purkinje fibers placed in a three chamber bath were driven by surface stimuli applied to one end of the fiber. Conduction velocity (CV) was measured between two microelectrodes, one proximal (P) and the other distal (D) to the stimulating electrodes. When all three segments were superfused with normal Tyrode, impulses initiated at 1/sec propagated in 1:1 manner, with CV >3 m/sec. Stimulation at increasing rates led to progressive increase in P-D conduction time until the pattern evolved directly into 2:1. When conduction impairment was induced in the central segment (1-2 mm) by compression or by superfusion with 1.25 to 1.5 mM heptanol, 1:1 CV at a rate of 1/sec became 2 to 6 times slower than in control. When CV was 3 to 1.5 m/sec, stimulation at increasing rates also led to progressive increase in P-D conduction time, until intermittent block occurred. However, the 2:1 pattern was preceded by 2:2 periodicities (doubling). Finally, sequences of 1:1 →2:2 →P:D-1 or 1:1 →P:D-1 preceded the 2:1 pattern when CV was < 1.5 m/sec. The sequence obtained was similar to the Farey's "universal" progression of self-sustained oscillators. Indeed, the commonest period found between 1:1 and 2:1 was 3:2, between 3:2 and 1:1 was 4:3, between 2:1 and 3:2 was 5:3, etc. In addition, quasiperiodicities were observed between the patterns described above. The space parameters, depicted by plotting rate and CV (at a rate of 1/sec), showed a structure similar to that of one half of an oscillatory system's map. Conclusions: irregular dynamics and chaos behavior can occur in heterogeneous, non-pacemaker excitable tissues; this may have implications in clinical arrhythmias.

T-Pos30 PROPAGATION OF ELECTRICAL ACTIVITY IN SIMULATED ATRIAL STRANDS: THE ROLE OF DISK RESISTANCE. J.W. Clark, C.R. Murphey, W.R. Giles*, and R.L. Rasmusson, Dept. of Elec. & Comp. Engr, Rice Univ., Houston, TX & *Dept. Med. Physiol., Univ. Calgary

A mathematical model for simulating the propagation of electrical activity in an idealized cylindrical strand of atrial tissue is developed. The strand consists of many unit cells coupled end to end via resistive intercalated discs. Important to the simulation of propagation in this strand, is the adoption of adequate models of the electrical characteristics of the cell and its surround, as well as its coupling with other cells. We have utilized an atrial cell model that consists of two major parts: (a) a cell membrane model comprised of membrane capacitance, gated ionic channel currents, as well as electrogenic pump and exchanger currents, and (b) a lumped fluid compartment model that describes changes in three ionic species (Na, K, and Ca). This model is capable of simulating the electrical behavior of the bullfrog atrial cell under normal, as well as a variety of abnormal conditions. The cell coupling model utilized is the well-known resistive T-network model of Heppner and Plonsey, with two axial resistances representing the inter-myoplasmic channels (connexons) and a radial leakage resistance to the extracellular space. The extracellular medium for the cells comprising the strand is considered to be a uniform, homogeneous, conducting medium of finite dimensions that may, depending on its size, offer a substantial resistance to longitudinal current flow. Propagation of electrical activity observed with the use of 'typical' model parameters is strongly influenced by disc resistance (Rd). At higher values of Rd, propagation exhibits a discontinuous nature, proceeding at a relatively fast velocity along the individual cell but exhibiting small delays across the resistive intercalated disc. Propagation through a region of slowed conduction is also simulated.

T-Pos31 EFFECTS OF EXTERNAL AND INTERNAL K^+ ON THE ACTIVATION AND DEACTIVATION OF THE INWARD RECTIFYING BACKGROUND K CURRENT (I_{K1}) IN ISOLATED CANINE PURKINJE MYOCYTES. +P. Pennefather, N. Mulrine, *D. DiFrancesco, and I.S. Cohen. Physiology & Biophysics, SUNY Stony Brook, +Faculty of Pharmacy, University of Toronto and *Physiology, University of Milan.

We studied the voltage dependence of steady-state activation and the kinetics of I_{K1} in acutely dissociated Purkinje myocytes using a whole-cell patch-clamp technique. Patch electrodes contained (mM) 120 KCl,1 $MgCl_2$,5 EGTA,5 Na_2ATP,5 HEPES-25 KOH,pH 7.2. The position of the activation curve is nearly constant relative to the reversal potential of I_{K1} (E_{rev}) when external K^+ ($[K]_o$) is altered (12,42,82 mM, choline-substituted). At 8-10°C I_{K1} activates exponentially with a voltage dependent tau which decreases e-fold per 20 mV hyperpolarization below E_{rev}. At the potential which produces half maximal activation tau is between 10 and 30 msec, also shifting with E_{rev}. We monitored deactivation of I_{K1} with a three pulse protocol. The majority of deactivation positive to E_{rev} proceeded rapidly, with a time constant (<15msec) that decreases with depolarization. A small component (<30%) was 1 to 2 orders of magnitude slower.

Patch pipettes containing 25mM K^+ (choline substituted) were employed to reduce internal K^+. The activation curve was shifted to more positive potentials, but by much less than the shift in E_{rev}. Nevertheless, the position of the activation curve remained constant relative to E_{rev} when $[K]_o$ was changed. Activation was still exponential with a voltage dependent tau which decreases e-fold per 20 mV hyperpolarization below E_{rev}. However tau at half maximal activation was an order of magnitude longer. In addition, the fast component of deactivation was almost eliminated. Positive to E_{rev}, the tau of deactivation could be as long as several seconds, increasing e-fold per 20 mV of depolarization. Thus, both internal and external K^+ modulate this inward rectifying K^+ current.

T-Pos32 COMPARISON OF K^+ CURRENTS IN SINGLE CELLS FROM RABBIT ATRIUM AND VENTRICLE. Y. Imaizumi and W. Giles. Univ. of Calgary, T2N 4N1.

The sizes and time-courses of three different K^+ currents in single cells from rabbit atrium (A) and ventricle (V) have been studied using a one-microelectrode voltage clamp technique to compare the mechanism(s) of repolarization of the action potential (AP). In both types of myocytes three different outward currents can be recorded consistently: (i) I_A, a transient outward current, (ii) I_{K_1}, an inwardly rectifying K^+ current, and (iii) I_K, a time- and voltage-dependent K^+ current. The sizes and kinetics of these currents differ significantly in A and V. I_A is much larger in A than in V. In contrast, I_{K_1} is much larger in V than A, and in V it exhibits a negative slope conductance. I_K is rather small (e.g. < 50 pA in response to 3 sec depolarizations from -40 to +40 mV) in both A and V. In most cells from atrium a very small Ca^{2+}-activated K^+ current is also present; however, this type of K^+ current was observed only very infrequently in cells from ventricle.

The functional role of I_A and I_{K_1}, was assessed by eliciting frequency-dependent changes in them and/or by applying pharmacological blockers. In atrium, 4-aminopyridine (4-AP, 0.3 mM) decreased I_A and increased the height and duration of the plateau of the AP. This 4-AP effect was much smaller in ventricle cells. In atrium, the τ for recovery of I_A (-80 mV) is approx. 7 sec at 23 C; this can account for much of the frequency-dependence of AP duration at low rates of stimulation. In ventricle cells, $BaCl_2$ (50 μM) selectively blocks I_{K_1} and lengthens the final phase of repolarization. This effect was much smaller in atrium. Supported by NIH Awards HL-3362 to W. Giles; and Canadian MRC, CHF, and AHFMR Awards to W. Giles.

T-Pos33 EFFECTS OF ELEVATED K^+ AND HYPOXIA ON CANINE SUBENDOCARDIAL ACTION POTENTIAL PROPAGATION. R.C. Tan, B.M. Ramza, and R.W. Joyner, Dept. of Physiology and Biophysics, The University of Iowa, Iowa City, IA, 52242 (Intro. by B. Schottelius)

In vitro studies of normal subendocardial action potential propagation demonstrate a pattern in which Ventricular Muscle (VM) activation by the overlying Purkinje (P) cell layer occurs at discrete junctional sites. At these P-VM junctional sites, there are Transitional (T) cells located between the P and VM layers that electrically interconnect these two layers. In our studies, we measured the combined effects of two common components of myocardial ischemia: elevated K^+ (8mM) and hypoxia, on canine in vitro endocardial preparations, with respect to: a) P layer conduction velocity, b) VM layer conduction velocity, and c) P-VM site conduction delay. The percentage changes were: a) -8 %, b) +2 %, and c) +85 % at Basic Cycle Length (BCL) 1000 mSec and a) -9 %, b) -6 %, and c) +107 % at BCL 400 mSec, indicating a relatively selective effect on the P-VM junctional sites with an enhanced effect at lower BCL. Microelectrode studies showed that the action potential amplitude and maximum dV/dt of T cells were selectively affected compared to those of P and VM cells. We propose a) that the anatomical arrangement of the T cells with the much larger number of VM cells imposes an electrical load on the T cells, and b) it is this relatively large current demand of the VM cells coupled with the generalized decrease in excitability by the 8 mM K^+ and hypoxia combination that accounts for the selective response of the T cells and the increased P-VM site conduction delay.

T-Pos34 EFFECTS OF LIDOCAINE ON RABBIT VENTRICULAR CONDUCTION VELOCITY AND ON ACTION POTENTIALS OF ISOLATED CELLS. B.M. Ramza, J. Matsuda, T.T. Do, R.C. Tan and R.W. Joyner. Dept. of Physiology and Biophysics, The University of Iowa, Iowa City, IA, 52242.

We used in vitro rabbit Ventricular (V) Papillary muscles to measure the effects of Lidocaine on V conduction velocity in normal (4 mM) and elevated (8 mM) $[K^+]$ and at a Basic Cycle Length (BCL) of 1000 or 400 milliseconds:

$[K^+]$ (mM)	BCL (mSec)	[Lidocaine] (uM)	Velocity (% change from control)
4	1000	0,10,20,50,100	0, -2, -2, -7, -13
8	1000	0,10,20,50,100	+3, -5, -7,-19, -44
4	400	0,10,20,50,100	0, -5,-11,-18, -32
8	400	0,10,20,50,100	-7,-21,-29,-54, -96

The results show a dose-dependent effect of Lidocaine that is accentuated by decreased BCL and by increased $[K^+]$. We studied isolated rabbit ventricle cells to determine whether the mechanism of the velocity decrease was an increase in the current required to activate a single cell or a decrease in the ability of a cell in a syncytial array to generate current to activate successive cells. For the intervention described above with the greatest decrease in velocity (8K, BCL 400, 100 uM Lidocaine) we found that the mean threshold current for stimulation was unchanged from control (1.64 nA vs. 1.65 nA) even though the mean maximum dV/dT of the action potential was greatly reduced (359 vs. 154 V/Sec), indicating that the decreased ability to generate inward current after activation was a primary mechanism for the decreased velocity.

T-Pos35 BACKGROUND K^+ CURRENT IN ISOLATED CANINE CARDIAC PURKINJE MYOCYTES. A. Shah, I.S. Cohen and N.B. Datyner. Dept. of Physiology and Biophysics, SUNY at Stony Brook.

The background K^+ current, I_{K1}, was studied in isolated canine cardiac Purkinje myocytes using the whole cell patch clamp technique. Patch pipettes contained (in mM): 140 KCl, 10 NaCl, 2 $MgCl_2$, 10 dextrose, 1 EGTA and 5 HEPES. Experiments were performed at 35.5 $\pm$ 1°C. Since Ba^{2+} and Cs^+ block I_{K1}, these cations were used to separate the I-V relation of I_{K1} from that of the whole cell. The I-V relation of I_{K1} was measured as the difference between the I-V relations of the cell in normal Tyrode (control) solution and in the presence of either Ba^{2+} (1mM) or Cs^+ (10mM). Results indicate that I_{K1} is an inwardly rectifying current whose conductance increases with $[K^+]_o$ and whose I-V relations in different $[K^+]_o$'s exhibit crossover. The permeability ratio P_K/P_{Na} for I_{K1} is greater than 150 for $[K^+]_o$'s ranging from 1 to 12mM, suggesting that this current is carried almost exclusively by K^+ ions. Furthermore, the I-V relation of I_{K1} contains a region of negative slope (even when that of the whole cell does not). Consequently, I_{K1} is virtually absent at plateau potentials.

We also examined the relationship between the resting potential of the myocyte, (V_m), and $[K^+]_o$ and find that it exhibits the characteristic anomalous behaviour first reported in Purkinje strands, where at low values of $[K^+]_o$ ($\leq$2 to 4mM) V_m depolarizes. In conclusion, our results indicate that I_{K1}, in Purkinje myocytes, is an inwardly rectifying K^+ current, whose conductance increases with $[K^+]_o$ and whose I-V relation contains a region of negative slope. Further, the similarity of the V_m versus $[K^+]_o$ relation of the Purkinje myocyte to the Purkinje strand, suggests that such a relationship is intrinsic to the cell membrane and is independent of strand geometry.

T-Pos36 CELL-ATTACHED RECORDINGS OF LARGE CONDUCTANCE K CHANNELS IN VENTRICULAR MYOCYTES. M.C. Sanguinetti, Searle R&D, Skokie, IL 60077.

In addition to the commonly observed inward rectifier (IK_1) K channels (γ=33 pS), two large conductance K channels were sometimes observed during cell-attached patch recordings of single guinea pig ventricular myocytes. GΩ seals were made with electrodes containing 145 KCl, 1 $MgCl_2$, 1 $CaCl_2$ & 5 Hepes on cells exposed to normal Tyrode's soln (21-23°C). The great majority of patches contained only IK_1 channels, however in 4 patches (7% of total), an inwardly rectifying, large conductance channel (γ-150 pS) was observed. Openings of this channel occurred in bursts and were characterized by multiple, long-lasting subconductance states. The probability of channel opening (P) was voltage (V)- dependent. P was 0.8 at potentials positive to -60mV, but about 0.2 at the most negative V tested (<-150mV). The probability density histogram (pdh) for open and closed times during a burst were best fit by biexponential equations: t_{O_1}=1.9ms, t_{O_2}=13.4ms, t_{C_1}=0.5ms, t_{C_2}=7.3ms @ -80mV. This 150 pS channel has many similarities to the Na_i-activated K channel (Kameyama, et al, Nature, 309:354). In 20% of the patches another large conductance K channel (γ=79 pS) was observed. Openings of this channel also occurred in bursts, but without long-lived substates, and P was not V-dependent. The number of this type of channel per patch was usually 1, but upon excision sometimes several (up to 6) identical channels could be recorded in the inside-out mode from the same patch. Best fits of pdh's for both open and closed times were biexponential in cell-attached patch mode: t_{O_1}=2.9ms, t_{O_2}=11.1ms, t_{C_1}=0.7ms, t_{C_2}=9.1ms at -60mV. A third closed state, corresponding to the long interburst intervals occurred too infrequently to be quantified in either type of channel. The 79 pS channel is the ATP_i-regulated K channel described previously by others in excised patches.

T-Pos37 K CHANNELS DURING THE SPONTANEOUS BEAT IN HEART CELLS. M. Mazzanti, L. J. DeFelice, S. Raph, Dept. of Anatomy & Cell Biology, Emory University, Atlanta, GA 30322.

Five apparently different channels conduct K during the repetitive, spontaneous firing of 7-day chick ventricle cells. We studied these channels using cell-attached and whole-cell electrodes simultaneously. The investigation emphasized physiological conditions by filling the cell-attached pipette with the bath solution (in mM: 133 Na, 1.3 K, 1.5 Ca, 0.5 Mg, 10 Hepes, 5 dextrose; pH 7.35). This condition was possible for four of the K channels conducting during the plateau: three of these are delayed-rectifier-type channels with conductances of 60, 30, and 15 pS. The fourth plateau channel conducts an early outward current shortly after the upstroke of the action potential. We have not yet obtained a reliable conductance for the early outward K channel. The fifth K channel occurs during the diastolic phase of the action potential. It is too small to record using the bath solution in the patch pipette. Filling the cell-attached electrode with different K concentrations, starting from 120 mM K and systematically replacing K with Na until reaching a K concentration of 10 mM, the conductance of the diastolic K channel (IK1) changed from 47 pS in 120 K, to 13 pS in 10 K; by extrapolation, the conductance of the IK1 channel is 2 to 3 pS in 1.3 mM K. Unlike the IK1 channel, which is present in almost every patch, the probability of recording single-channel events for the four plateau K-conducting channels is very low.

Even though three separate conductances occur for delay-rectifier type channels, we occasionally observed interconversions between one and another of the three conductances, which leads us to speculate that the three conductances are different states of the same channel. (Supported by NIH HL27385)

T-Pos38 PURPORTED K CHANNEL OPENER, BRL 34915, BLOCKS INWARDLY RECTIFYING K CURRENT IN ISOLATED GUINEA PIG VENTRICULAR MYOCYTES. M.L. Conder and J.R. McCullough, (Intr. by H.H. Shlevin), Research Department, Pharmaceuticals Division, CIBA-GEIGY Corp., Summit, NJ 07901.

The vasorelaxant BRL 34915 (BRL, 6-cyano-3,4-dihydro-2,2-dimethyl-trans-4-[2-oxo-1-pyrrolidyl]-2H-benzo[b]pyran-3-ol) has been reported to increase K permeability ($\overline{PK}$), thereby resulting in a hyperpolarization of the resting membrane potential (RP) of smooth muscle cells (Br J Pharmac 88:103-111, 1986). Using whole cell patch clamping techniques, we examined the effects of BRL on $\overline{RP}$ and whole cell K currents in freshly isolated guinea pig ventricular myocytes (GPVM). Exposure of GPVM to 2-5 μM BRL in 1 to 10 mM K Tyrodes solution reversibly hyperpolarized RP 8 mV in 1 mM K and 1 mV in 10 mM K. Voltage clamp studies utilizing either 5 second step potentials or ramp voltage protocols were used to study the effects of BRL on the inwardly rectifying background K current (IK1). In 1, 2 or 4 mM K Tyrodes solution, BRL caused an outward shift in the current voltage relationship (IVR) of IK1 for potentials more negative than the RP of the cells and an inward shift of the outward current potentials between the RP and -20 mV. Slope conductance of the linear portion of the IVR (<-90 mV) was reduced 30-50% by BRL. Much smaller changes in IVR were observed in 10 mM K, consistent with the smaller degree of hyperpolarization observed. Treatment of the cells with 0.05-0.2 mM Ba caused similar changes in the IVR. Addition of BRL in the presence of Ba, linearized the IVR and depolarized RP. Addition of BRL in the presence of 10^{-6} M acetylstrophanthidin did not block the effects of BRL on the IVR, but reduced the hyperpolarization of RP. These results suggest that the vasodilation of BRL may result from mechanisms other than an increase in PK, perhaps by increasing electrogenic Na/K pumping.

T-Pos39 INWARD SINGLE CHANNEL CURRENT INDUCED BY BATRACHOTOXININ-A BENZOATE IN CANINE ATRIAL MYOCYTES. James K. Bubien, G. B. Brown and W. T. Woods, Jr., Dept. of Physiology and Biophysics and Neurosciences Program, Univ. of Alabama at Birmingham, Birmingham, Alabama 35294.

Inward single channel currents can be observed in canine atrial sarcolemma by elevating extracellular K^+ (K^+_o) to 200 mMol./l. to drive K^+ across the membrane. However, inward Na^+ current was not observed when Na^+_o was elevated to 200 mMol./l. Channels were recorded in inside-out patches with (mMol./l.) 150 KCl, 10 NaCl, 4 x 10^{-3} Ca^{++}, 5 HEPES, pH 7.0; 25°C. Pipettes contained 150 NaCl, 10 KCl, 4 x 10^{-3} Ca^{++}, 5 HEPES, pH 7.0; 25°C. Batrachotoxinin-A Benzoate (BTX-B, 3 x 10^{-6} Mol./l.) promotes the open state of Na^+ channels. Therefore, BTX-B was added to some pipettes. Inward currents were observed only after BTX-B was added. Unitary single channel events had a linear current/voltage relation with a slope conductance of 16 pS. The reversal potential of +22 mv. was closest to that for Na^+ (+71 mv.) among the potential charge carriers. At membrane potentials of 0 and -30 mv. respectively, open time constants were 3.1 and 7.1 msec., closed time constants were 18.2 and 3.3 msec. Addition of tetrodotoxin to the bath (10^{-7} Mol./l.) was accompanied immediately by disappearance of all inward unitary events at all relevant pipette potentials. Substitution of gluconate for Cl^- had no effect on inward current. These observations suggest that BTX-B promotes opening of channels that selectively allow Na^+ to carry current in the inward direction at physiological transmembrane potentials, these channels retain voltage sensitive transition kinetics and time constant durations which are consistent with I_{Na^+}.

T-Pos40 K AND Na SENSITIVITY OF I_{K1} IN ISOLATED CAT VENTRICULAR MYOCYTES.
Robert Harvey and Robert TenEick (Intro. by Raymond Novak)
Department of Pharmacology, Northwestern University, Chicago, IL 60611

The inwardly rectifying K current (I_{K1}) was identified in isolated cat ventricular myocytes using a suction electrode voltage clamp technique. I_{K1} was viewed to consist of a strictly voltage (V) dependent instantaneous component and a V and time dependent component, exhibiting both activation and inactivation phases. This resembled inwardly rectifying K currents in skeletal muscle (SM) and tunicate egg cells (TE). The sensitivity of each component to external K (K_o) and Na (Na_o) was examined to determine whether I_{K1} was similar to these other currents. As expected for a pure K current, changing $[K]_o$ caused a shift in the reversal potential (V_K) of both components, with a slope of ~-60mV per 10 fold change in $\log[K]_o$. Slope conductance measured at potentials negative to V_K indicated a K_o sensitivity of I_{K1} proportional to $\sim[K]_o^{1/2}$. Calculation of the chord conductance (g_K) at various $[K]_o$ indicated a V dependence related to V_K (i.e., $V-V_K$). The activating portion of the inward current could be fit by a single exponential, showing a V and $[K]_o$ dependence similar to that of g_K. Inactivation occurred at more negative potentials, resulting in a negative slope region in the steady state (SS) I-V relationship between -140 and -180mV. Unlike the current in SM and TE, this property was reduced but not abolished by removal of Na_o. There was a dependence of g_K on $[Na]_o$ opposite to that expected if Na were an ion blocking I_{K1}. Negative to V_K the Na sensitivities of i_{inst} and i_{peak} were constant. However, the sensitivity of i_{SS} to $[Na]_o$ was reduced at more negative potentials making inactivation appear to have a Na dependence.

T-Pos41 INFLUENCE OF $[Na^+]_o$ ON THE RESPONSE OF ISOLATED GUINEA PIG HEARTS TO REPERFUSION. M.P. Moffat (Intr. by C.P.S. Taylor) Dept. of Pharmacology & Toxicology, University of Western Ontario, London, Canada, N6A 5C1.

The effects of lowering $[Na^+]_o$ on the functional and electrophysiological responses of isolated guinea pig hearts to reperfusion were examined. Hearts were perfused for 10 min with a Tyrode's solution modified to mimic conditions associated with ischemia followed by 30 min of reperfusion with oxygenated Tyrode's solution. To study the influence of $[Na^+]_o$, some hearts were reperfused in the presence of 68.5 mM NaCl and an equiosmolar concentration of either LiCl or sucrose. Ischemic conditions resulted in a rapid loss of contractile force and the development of contracture. Reperfusion in the presence of 137 mM NaCl caused a 79% recovery of contractile force and a gradual decline in diastolic tension. Ventricular tachycardia, bigeminy, trigeminy and fusion beats accompanied reperfusion. Reperfusion of ischemic hearts with Tyrode's solution modified by partial substitution of NaCl by LiCl depressed recovery of contractility to 46% of the pre-ischemic value ($p < 0.05$). Diastolic tension remained greater than in control hearts ($p < 0.05$). Arrhythmias were similar to those observed in control hearts, however, 33% developed ventricular fibrillation. Substitution with LiCl resulted in a sustained decrease in the sinus rate following 10 min of reperfusion and an increase in atrioventricular conduction time at 5 and 10 min ($p < 0.05$). Partial substitution of NaCl by sucrose resulted in recovery of contractile function to 97% of the pre-ischemic value ($p < 0.05$). Diastolic tension declined, but was greater than in control hearts following 20 and 30 min ($p < 0.05$). Arrhythmias were similar to those observed in control hearts. The differing results of LiCl and sucrose substitution suggest that the effects of lowering $[Na^+]_o$ cannot be explained solely on the basis of effects on Na^+Ca^{2+} exchange.

T-Pos42 BLOCK OF CARDIAC SODIUM CHANNELS BY TOCAINIDE: EVIDENCE FOR TWO COMPONENTS OF CHANNEL BLOCK AND LACK OF STEREOSPECIFICITY. C. W. Clarkson and T. Wang. Department of Pharmacology, Tulane Univ. School of Medicine, New Orleans, LA 70112

Tocainide is an antiarrhythmic drug that is administered as a racemic mixture of D(+) and L(-) enantiomers for the treatment of ventricular arrhythmias. We used the whole-cell voltage clamp technique with enzymatically isolated guinea pig ventricular myocytes (15°C, $[Na]_o$ = 25 mM) to define the mechanism of sodium channel block by tocainide and to determine whether such block was stereospecific. Block by 200 μM (46 μg/ml) tocainide could be divided into tonic and use-dependent components. Tonic block by both enantiomers was not significantly different: 22 ± 5% for (-) tocainide vs. 30 ± 10% for (+)tocainide (mean ± S.D.) ($n=7, P>0.05$). Similarly, use-dependent block produced by both enantiomers during a 5 second pulse to +20 mV from -140 mV was not significantly different: 49 ± 11% for (-)tocainide vs. 43 ± 9% for (+)tocainide ($n=7, P>0.5$). Time constants for recovery from block (1-2 seconds) at -120, -140 and -160 mV were also not significantly different ($P>0.05$, $n=5-7$). The mechanism underlying block development was defined using a two pulse protocol to conditioning voltages between -90 and +20 mV. Over the voltage range of -70 to +20 mV, two phases of block were defined: a rapid phase (τ = 1-30 msec) and a slow phase (τ = 4-8 sec). However, at voltages below threshold for channel opening only a slow component of block development could be defined. Both enantiomers had similar time constants and amplitudes of block development. These data suggest that the rapid phase of block development may be due to binding to open channels, while the slow component of block is due to drug binding to channels in the inactivated state. We conclude that tocainide block of cardiac sodium channels is not stereospecific.

T-Pos43 * BLOCKADE OF CARDIAC SODIUM CHANNELS BY LOW CONCENTRATIONS OF BA 42730A. J.R. McCullough, G. Trube & M.L. Conder. Research Dept., Pharmaceuticals Div., CIBA-GEIGY Corp., Summit, NJ 07901 & Cell Physiology Dept., Max-Planck-Institute for Biophysical Chemistry, Goettingen, FRG

Whole-cell patch-clamp recording techniques were used to study the effects of BA 42730A (N-[3-methoxy-2-(2'-phenylthiazolyl-4'-methoxy)benzyl]-octahyroazocin HCl) and lidocaine on the fast-inward sodium current in freshly isolated guinea-pig atrial and ventricular myocytes, and in rat ventricular myocytes and bovine chromaffin cells maintained in short term culture (1-5 days). Under conditions designed to minimize contamination by potassium and calcium currents, the inward sodium current of cardiac cells, bathed in low external sodium (20-40 mM), was inhibited approx 50% by low concentrations of BA 42730A (10^{-9} - 10^{-8} M). Little or no use-dependent block was observed. The sodium current in bovine chromaffin cells was inhibited to the same extent by ~10^{-7} M BA 42730A. The sensitivity of the isolated cardiac myocytes to lidocaine (20 μM) was normal. The steady-state inactivation of the sodium current was shifted to negative potentials by lidocaine, while little shift occurred in the presence of BA 42730A. These results suggest that, in the isolated myocytes, BA 42730A is about 1000X more potent than lidocaine and that the mechanism of block of sodium channels by BA 42730A may differ from that of other known sodium channel blockers such as lidocaine or tetrodotoxin.

T-Pos44 **Voltage- and temperature-dependent recovery of quinidine-blocked cardiac sodium channels.** Dirk J. Snyders and Luc M. Hondeghem (Intr. B.G. Katzung). Stahlman Cardiovascular Research Program, Department of Medicine, Vanderbilt University, Nashville, TN 37323.

The recovery from Na-channel block induced by quinidine (20 uM) was studied in small cardiac myocytes isolated from adult guinea pig using the whole cell voltage clamp technique (Na_o=20mM). Block was induced by 200 pulses from -120 to +30 mV at 10 Hz. In control, after these pulse trains I_{Na} reactivated to 95% in 125 msec at -160 mV and 295 msec at -120 mV. In the presence of quinidine the drug-free channels reactivated similarly fast, while the drug-associated channels unblocked either very quickly (<10 msec) or required over 30 sec to recover. Thus recovery assessed at 1 sec after induction of a fixed amount of block can be used as an estimate of the fast unblocking. The latter increased as a function of hyperpolarization. At 22°C this I_{Na} availability was shifted by about 20 mV in the hyperpolarizing direction as compared to control, and saturated at about -140 mV. At 17°C it was smaller, its voltage dependence was shifted to more negative potentials, and upon hyperpolarization to -160 mV the amplitude of this process was still increasing. These results are compatible with quinidine shifting the reactivation of blocked channels to more negative potentials in a temperature-dependent fashion. Following strong hyperpolarizations, upon opening the channels, quinidine can quickly dissociate from the channel.

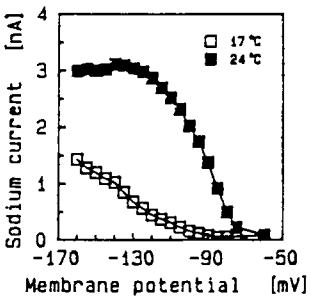

T-Pos45 RELATIONSHIP BETWEEN MODULATED RECEPTOR AND GUARDED RECEPTOR FORMALISMS REGARDING RATES OF DRUG UNBLOCKING FROM SODIUM CHANNELS. Kenneth R. Courtney, Palo Alto Medical Foundation, 860 Bryant Street, Palo Alto, CA 94301

The time constant (T) that governs the rate of local anesthetic unblocking from sodium channels has been described using the guarded receptor formalism, where Bc and Bn are channels blocked by charged and neutral forms of tertiary drug, respectively (below left). T can be expressed as a function of 3 parameters - the rates of protonation (kpH^+), deprotonation (lp) and unblocking for neutral drug (ln), according to $T = (ln+lp+kpH^+)/(ln*lp)$. This expression has been especially useful for explaining the pH-dependence of T with protonation "trapping" drug in the channel. The modulated receptor hypothesis can be formalized in terms of gated states of the channel (Resting, Open, Inactive and R*, O*, I* for drug-blocked channels). The rate limiting transitions that occur at resting potential levels are depicted below. They can be expressed by an analogous equation for the time constant, noting that the parallel pathway ($li+\alpha_h^*$) replaces ln. Thus T is being fit by only 2 parameters for the case on the right - li and the voltage shift ΔV that determines α_h^* and β_h^*. Note the opposing (unblocking and trapping) actions of α_h^*. This new equation explains the voltage-dependence of T, subject to the assumptions used to fit T to measurements. Supported by NIH HL24156.

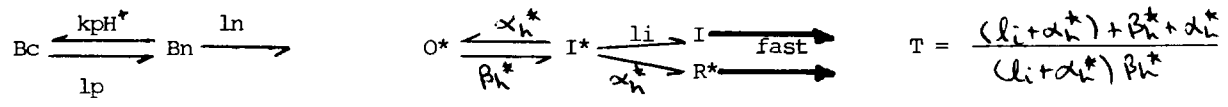

T-Pos46 INTRACELLULAR DIFFUSION OF NA FROM PATCH ELECTRODES IN CARDIAC MYOCYTES: IMPLICATIONS FOR NA ACTIVITY AT INTERNAL NA PUMP SITES

David Mogul, Donald Singer, & Robert TenEick (Intr. by Arthur Veis)
Depts. of Electrical Engr., Medicine, & Pharmacol., Northwestern Univ., Chicago, IL

Using the whole cell patch clamp technique, a significant problem in determining the dependence of the current generated by the ATP dependent Na,K transport (Na pump) on the activity of Na at the internal Na binding site ($(Na)_i$) arises because of difficulties in relating $(Na)_i$ to the (Na) in the patch pipette ($(Na)_p$). We formulated a 3-dimensional quantitative model which permits $(Na)_i$ to be estimated from $(Na)_p$. The model shows that diffusion from the pipette to the membrane ligand binding site depends on several parameters, including: 1) pipette tip diameter, 2) Na pump current density , 3) competitive binding of cations to membrane phospholipids, and 4) cellular geometry. A change in any of these parameters can alter the Na gradient between the pipette/cell interface and the sarcolemma, and therefore alter the apparent dependence of Na pump function on $(Na)_i$. For example, depending upon cellular geometry and pump current density, decreasing pipette diameter can increase the pipette-to-sarcolemmal Na gradient. In addition, when $(Na)_p$ is increased, the time course required for the (Na) at the Na pump site to achieve steady state increases as a function of the new $(Na)_p$ and on pipette tip diameter. Under conditions in which Na:H and Na:Ca exchange are inhibited this model will facilitate in defining the relationship between $(Na)_i$ and Na pump function of single cardiac myocytes subjected to whole cell voltage clamp.

T-Pos47 SINGLE CHANNEL INWARD CURRENTS IN SPONTANEOUSLY BEATING CARDIAC PACEMAKER CELLS. W. T. Woods, Jr., James K. Bubien, Richard M. Martin and Candace G. Snider, Dept. of Physiology and Biophysics, Univ. of Alabama at Birmingham, Birmingham, Alabama 35294

Inward current is responsible for the spontaneous depolarization of cardiac pacemaker cells, but the ion channel that opens to pass this current has not been described. Sinus node pacemaker cells were identified by impaling microelectrodes into isolated, perfused, adult canine right atria. We developed methods to disperse and culture these cells. Ca^{++}-tolerant, isolated cells began to beat spontaneously 45±20 beats/min) after 72 (±24) hours in culture. Suction pipettes were attached to cell membranes via gigaohm seals (cell-attached) to record single channel activity during spontaneous (phase 4) depolarization. Extracellular suction pipettes (low seal resistance) were used to record action currents during spontaneous depolarization. Inward single channel currents carried by Na^+ (the only charge carrier in the pipette) were recorded. Their current/voltage relationship was linear with a slope conductance of 60 pS. Transition kinetics were voltage-sensitive. Open time constants decreased from 2.4 to 0.8 msec when the membrane patch was hyperpolarized by 50 mv from the resting potential. Closed time constants increased from 2.7 to 21.3 msec for the same hyperpolarization. Single channel openings occurred in bursts separated by 200 msec closures suggesting 2 kinds of closed states. Single channel activity correlated with phase 4 depolarization. These observations are consistent with the hypothesis that automaticity in sinus node pacemaker cells may be attributed to single channels that conduct inward current carried partly by Na^+.

T-Pos48 Na-Ca EXCHANGE CURRENT IN ISOLATED ADULT VENTRICULAR MYOCYTES.

M. Horackova and G. Isenberg*. Dept. of Physiology and Biophysics, Medical School, Dalhousie University, Halifax, N.S., Canada, and *II. Physiolgisches Institut, Universitat des Saarlandes, Homburg/Saar, W. Germany.

Single ventricular myocytes isolated from feline and bovine hearts were used to investigate the changes in action potentials and in the ionic currents resulting from alterations of the Na gradient. Since we attempted to investigate, specifically, the ionic current possibly generated by Na-Ca exchange, the effects of the fast transient changes in $[Na]_o$ were studied in the presence of 20 mM CsCl to inhibit K currents. To facilitate the blocking effect of Cs, in some experiments the solution was K-free and the patch electrode was filled with 150 mM Cs-glutamate. The application of 20 mM $[Na]_o$ (LiCl replacing NaCl) resulted in hyperpolarization and the action potential duration was progressively reduced. Under voltage-clamp conditions, the Na-poor solutions (20 mM or 45 mM) generated an outward current at all investigated membrane potentials. The initial part (100-200 msec) of this outward current was partially blocked by 5 mM $NiCl_2$, indicating that it may result from a decrease of slow inward current (i_{si}). The remaining steady-state outward current normally generated by the reduced $[Na]_o$ was completely absent in solutions containing 20 mM $MnCl_2$ (which presumably inhibit Na-Ca exchange). Our observations are consistent with the hypothesis that the Na-Ca exchange in cardiac myocytes is electrogenic and it generates an outward current when the Na gradient is decreased. Supported by MRC Canada (MT 4128) and Deutsche Forschungsgemeinschaft.

T-Pos49 DIHYDROPYRIDINE GATING OF CALCIUM CHANNELS. A.E. Lacerda and A.M. Brown. Dept. of Physiology & Molec. Biophys., Baylor College of Medicine, Houston, TX 77030.

Some dihydropyridines (DHP's) are calcium channel modulators and the DHP agonist Bay K 8644 produces prolonged channel openings (Hess et al,1984). It has been proposed that calcium channels switch physiologically among a normal mode (1), a mode with long openings (2) and a mode without openings (0); DHP's are thought to stabilize Modes 2 and 0 possibly by acting on an endogenous regulator. Other ideas are that DHP's act by prolonging the open time (Sanguinetti et al,1986) or react only with open channels (Bechem and Schramm,1986). We have investigated these by studying whole cell (5 mM Ca_o) and cell-attached single channel Ca currents (isotonic Ba in pipette,-isotonic K in the bath) in primary cultures of neonatal rat and adult guinea pig cardiac myocytes. A variety of DHP stereoisomers was tested. We found that the agonists -Bay K 8644 and +202-791 and the antagonist ± Nitrendipine (NTD) prolonged channel open times but to very different extents. The agonists produced frequency distributions that were fitted with a fast and a slow tau. The slow taus differed by about a factor of 2 and the tau for NTD differed from the agonist taus. The number of openings per trace belonging to the fast tau class and the fast tau were concentration dependent as were number of openings per burst, burst duration and tail current taus. The waiting times were shortened. Prolonged openings were seen very infrequently in control. These results are not consistent with any of the above hypotheses of DHP action. It seems most likely that DHP's bind with high and low affinities to a single receptor site and produce complex changes in calcium channel gating among all three channel states, closed, open and inactivated. Supported by HL36930 and HL07348.

T-Pos50 ISOPROTERENOL REDUCES CYTOSOLIC CALCIUM CONCENTRATION MEASURED WITH FURA 2 IN RESTING SINGLE ISOLATED RAT VENTRICULAR MYOCYTES. D.J. Williford, V.K. Sharma, M.K. Walton and S-S. Sheu, Depts. of Pharmacology and Medicine, University of Rochester, Rochester, NY 14642.

The effect of isoproterenol (ISO) on cytosolic calcium concentration $[Ca]_i$ has been studied by quantitative fluorescent digital microscopy in single isolated rat ventricular myocytes loaded with fura 2. A previous report from this laboratory showed that ISO (1 μM) produced a decrease of $[Ca]_i$ in quin 2 loaded suspensions of dissociated rat ventricular myocytes under conditions in which cells have normal polarized resting membrane potential (Sheu et al., Biophys J 49:350a, 1986). Due to the heterogeneity of cells in suspension, we have repeated this study in single cells. Dissociated ventricular cells were loaded with fura 2 by exposure to fura 2-AM ester and then placed on an inverted microscope equipped for epifluorescence. Single cells were viewed with a 100X objective and illuminated at 340 nm and 380 nm wavelength light. Fluorescence emission at 500 nm was recorded with a silicon intensifier target camera and video images digitized using a microcomputer-based processor. The ratio of the 340/380 images was determined on a pixel by pixel basis and the $[Ca]_i$ determined at any single point by reference to an in vitro calibration with solutions of known calcium concentration. In 49 cells, the average cell $[Ca]_i$ was 140±6 nM (mean±sem). Exposure of cells to ISO (5 μM) for 3 min caused a reduction in average $[Ca]_i$ of 8 nm ($p<.01$, n=15), whereas untreated cells monitored for 15 min did not show any decrease in $[Ca]_i$. These data confirm that ISO decreases $[Ca]_i$ in resting polarized cells. This effect is presumably due to stimulation of either intracellular buffering mechanisms or Ca^{2+}-efflux, and is currently under investigation. In addition, these results show the utility of digital imaging for detecting small changes in $[Ca]_i$ in single cells loaded with fura 2.

T-Pos51 CALCIUM-TRANSIENTS IN VOLTAGE-CLAMPED GUINEA-PIG VENTRICULAR MYOCYTES. Laura Barcenas-Ruiz and W. Gil Wier. Dept. of Physiology, Univ. of Maryland at Baltimore, Baltimore MD 21210.

Cells were loaded with fura-2 by exposure to fura-2 AM (5uM, 15 min.), perfused with physiological saline at 22°C and studied in an inverted microscope equipped with an ultra-violet epifluorescence illuminator and a photomultiplier tube. With illumination at 380 nm, decreases in fluorescence, as shown in the lower traces below, indicate increases in $[Ca^{2+}]_i$. Because of uncertainty in the calibration curve to use, fluorescence transients (fluor. trans.) are shown rather than $[Ca^{2+}]_i$-transients. The holding potential was -40 mV and each test pulse was preceded by 8 conditioning pulses (0 mV, 300 msec), in order to achieve a steady state before the test pulse. Shown below are the superimposed fluor.trans. elicited by the last conditioning pulse and the test pulse. Pulse voltage (left): Fluor. trans were observable at the first test pulse (-30 mV, not shown) and became maximal at 20 mV with little further change up to 40 mV. The time-to-peak (measured from depolarization to 90% of peak) decreased with increasing test pulse amplitude (from 250 msec at -20 mV to 40 msec at 20 mV). Pulse duration (right): Brief pulses reduced the amplitude of fluor. trans. by cutting short its rising phase. The fluor. trans. declined slowly throughout the duration of the depolarisation (up to 800 msec) and then declined more rapidly upon repolarization. These results demonstrate the feasibility of recording $]Ca^{2+}]_i$-transients in single voltage-clamped guinea-pig cardiac cells.

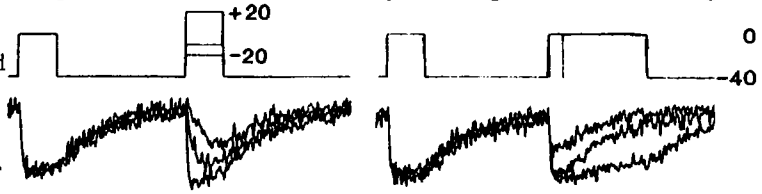

T-Pos52 TWO COMPONENTS OF CONTRACTION IN GUINEA PIG PAPILLARY MUSCLE AND THEIR RELATIONSHIP WITH TWO CALCIUM CURRENTS. E. HONORE°° and C.E. CHALLICE°. °Department of Physics, The University of Calgary, Calgary, Alberta, Canada T2N 1N4, and °Laboratoire de Pharmacologie, Faculté de Médecine, 1 Place de Verdun, 59045 Lille Cédex, France.

Guinea pig papillary muscle fibers in low Na^+ (25 mM) and high K^+ (17 mM) solution, in the presence of either 0.3 μM isoproterenol or 2 μM histamine, demonstrate biphasic contractions. The introduction of 1 mM caffeine decreases the first component (P1) and increases the second (P2), while increasing the frequency of stimulation from 0.2 to 1 Hz has the reverse effect. P2 is significantly more sensitive to isoproterenol, Bay K 8644, nifedipine, Cd^{++} and acetylcholine than P1. When Ca^{++} ions are replaced by Sr^{++} ions (which do not replace Ca^{++} in the fast inward current) only P2 is recorded. Similarly treated guinea pig atrial, and rat papillary fibers produce only monophasic contractions, which behave as P1 above. With frog ventricular trabeculae (which have a very sparse sarcoplasmic reticulum - SR) contractions behaving as P2 above occur (Honoré et al., Can. J. Physiol. Pharmacol., in press).

It is suggested that the two components of contraction arise by two distinct mechanisms. P1 is generated when Ca^{++} is released by the SR which is stimulated by the Ca^{++} crossing the sarcolemma in the fast inward current, and P2 arises due to direct diffusion of the slow transmembrane Ca^{++} current through the sarcoplasm, to the myofibrils. However, these are both phasic, and in normal function there is also a tonic component which is here eliminated by the method used (Horackover and Vassort, J. Gen. Physiol. 73, 403).

Supported by a grant from the Natural Sciences and Engineering Research Council of Canada.

T-Pos53 TEMPORAL VARIATIONS IN ELICITED LOCAL RESPONSES IN DEPRESSED VENTRICULAR MUSCLE. George J. Rozanski. Departments of Internal Medicine/Physiology and Biophysics, University of Nebraska Medical Center, Omaha, NE 68105

In isolated ventricular muscle depressed with elevated $[K^+]$, a distinct nonregenerative local response (LR) participates in the voltage displacement induced by subthreshold depolarizing currents. This LR is mediated by either the inward Na^+ or Ca^{2+} channel when resting membrane potential is near -70 or -50 mV, respectively. We examined temporal changes in LR characteristics to define their role in determining the frequency-dependence of impaired propagation in depressed cardiac tissues. Papillary muscles and ventricular trabeculae were isolated from canine and feline hearts and mounted in a sucrose gap. Transmembrane potentials were recorded from the test segment (< 1 mm) while suprathreshold basic and subthreshold depolarizing test current pulses (100 msec duration) were applied through Ag-AgCl electrodes placed across the gap. The time courses of Na^+ and Ca^{2+} channel-mediated LRs were markedly different, however the rate of development and peak amplitude of both were attenuated when the interval between successive test current pulses was reduced. The decrease in LR amplitude by preceding pulses was associated with lower excitability. Thus, transient suppression of basic regenerative action potentials could be achieved by applying a properly timed subthreshold current pulse during diastole. When trains of subthreshold pulses were applied, the suppression of basic regenerative responses lasted for several beats. These data suggest that excitability of depressed ventricular muscle is determined in part, by the LR. Furthermore, temporal changes in the LR may help explain the frequency-dependence of impaired conduction that is often a characteristic of depressed cardiac tissues.

T-Pos54 ROLE OF I_f IN PACEMAKER ACTIVITY OF THE SINOATRIAL NODE. R. D. Nathan, Department of Physiology, Texas Tech University Health Sciences Center, Lubbock, TX 79430.

Single pacemaker cells were isolated from rabbit sinoatrial node and cultured for 1-3 days (R. D. Nathan, Am. J. Physiol. 250: H325-H329, 1986). The whole-cell voltage clamp technique was employed with patch pipettes filled with 155 mM KCl (resistances, 5-10 MΩ). The results described below have been corrected for a +5-mV pipette junction potential. Temperature was 32° C. When measured at the end of 10-sec voltage steps, an inward current (i_f) became activated at -65 ± 3 mV (mean ± SEM, n = 6); however, i_f was not measurable during the first 300 msec of the voltage step. In fact during the first 100 msec, i_f remained insignificant until the potential reached -85 mV. When extracellular $[K^+]$ was increased from 1.8 to 5.7 mM, i_f rose to -4 pA during the first 100 msec of a voltage step to -75 mV; however, at -65 mV, it still was not measurable within this time frame. In the presence of 1.8 mM K^+, a "quasi" steady-state activation curve for i_f, derived from current tails following 10-sec voltage steps, exhibited a threshold of -65 mV, half activation at -83 mV, and saturation at -115 mV. Application of the voltage clamp at -65 mV, during the initial phase of diastolic depolarization, resulted in an inward current that increased to -4 pA in less than 100 msec, much larger than the amplitude of i_f measured at that time and potential. Conventional microelectrode recordings from rabbit sinoatrial node have shown that during diastole, the membrane potential either does not exceed -65 mV, or it does so for less than 100 msec. Thus, the present results suggest that i_f is not responsible for pacemaker activity. On the other hand, background (time-independent) inward current, which was substantial (-10 ± 1 pA, n = 6) at -65 mV, in conjunction with the decay of outward i_K following repolarization of the action potential, could account for the initial phase of diastolic depolarization. Supported by NIH grant HL 20708.

T-Pos55 pH REGULATION IN ISOLATED VENTRICULAR RAT MYOCYTES. M. A. Wallert and O. Fröhlich. Department of Physiology, Emory University School of Medicine, Atlanta GA 30322.

The pH-sensitive fluorescent dye BCECF was used to study the pH regulation in isolated quiescent ventricular myocytes at 25°C. In accordance with electrophysiological observations by others we have demonstrated the existence of a Na-H exchanger in these cells. Addition of 1 mM amiloride to a cell preparation at steady-state pH lead to a gradual intracellular acidification. Recovery from a 20 mM NH_4Cl prepulse occurred with a $t_{1/2}$ of 2.4 ± 0.1 min. This recovery could be reduced to 15% of its normal rate by adding 1 mM amiloride or by removing extracellular Na from the bathing medium. Amiloride also blocked the alkalinization which occurred when Na-depleted cells were reintroduced to normal Na buffer. The Na-H exchanger appears to be the primary mechanism by which cells prevent and recover from intracellular acidification. We have also shown the existence of a $Cl\text{-}HCO_3$ exchanger in these cells. Substitution of gluconate for extracellular Cl caused a marked increase of the intracellular pH, which occurred with a $t_{1/2}$ of 2.0 ± 0.2 min. This alkalinization could be inhibited by 1 mM SITS. SITS also accentuated the alkalinization seen when cells were incubated in buffer containing 10mM trimethylamine. This suggests a role for of $Cl\text{-}HCO_3$ exchange in the recovery from and the prevention of alkaline loads. An additional, though minor role for the $Cl\text{-}HCO_3$ exchanger in the recovery from acid challenges is suggested by the observation that the rate of recovery from an intracellular acidification in Na-free buffer could be further inhibited by the addition of SITS. However, the significance of this observation is uncertain due to the high concentration of SITS (>1mM) needed to see this effect.

T-Pos56 EFFECTS OF ALPHA ADRENERGIC STIMULATION ON ISOLATED CANINE PURKINJE MYOCYTES. A. Shah and I.S. Cohen. Dept. of Physiology and Biophysics, SUNY at Stony Brook.

Alpha adrenergic agonists, at low concentrations ($\leq 10^{-6}$M), slow the spontaneous beating rate in canine cardiac Purkinje fibers. We have investigated the mechanism underlying this effect in acutely dissociated canine cardiac Purkinje myocytes, using the whole cell patch clamp technique. Patch pipettes contained (in mM): 140 KCl, 10 NaCl, 2 $MgCl_2$, 10 dextrose, 1 EGTA, 5 HEPES and 0.1 GTP. Experiments were performed at 35.5 ± 1°C. Exposure of the cells to the alpha adrenergic agonist phenylephrine (10^{-7}M), results in a hyperpolarization of the cell membrane potential and a shift in the outward direction of the I-V relation at all potentials negative to -60mV in 8mM K Tyrode solution. Phenylephrine has two effects on the ionic currents: (1) the background K^+ current is decreased, and, (2) an outward current, (which preliminary results suggest is the Na^+/K^+ exchange pump current), is increased.

Both these effects are blocked by the α_1-adrenergic blocker prazosin (10^{-6}M) and remain unaffected by the β -adrenergic blocker propranalol ($2x10^{-7}$M). To elucidate the coupling mechanism between phenylephrine binding and its effects on the ionic currents, we used pertussis toxin, which has been shown to specifically ADP-ribosylate the GTP-binding proteins N_i and N_o. We find that pretreatment of the cells (18-22 hrs.) with pertussis toxin (5µg/ml) abolished both the effects of phenylephrine, suggesting that a GTP-binding protein couples phenylephrine binding to its effects on the ionic currents. In conclusion, our results suggest that exposure to low concentrations of phenylephrine decreases background K^+ permeability and increases the Na^+/K^+ pump current in Purkinje cells, and, both these effects are coupled to phenylephrine binding by a GTP-binding protein.

T-Pos57 EFFECT OF PROTEIN KINASE C ACTIVATION ON THE INOTROPIC RESPONSE INDUCED BY α-ADRENOCEPTOR STIMULATION IN RAT MYOCARDIUM. By A. Uglesity, V.K. Sharma, and S-S. Sheu. Department of Pharmacology, University of Rochester, Rochester, NY 14642.

Recent studies suggest that the effects of α-adrenoceptor stimulation are mediated through phosphoinositide (PI) hydrolysis. We investigated the effect of the α-agonist phenylephrine on twitch tension in rat papillary muscles electrically driven at 1 Hz. Phenylephrine (50 µM) induced a biphasic inotropic response; a 50% reduction in tension occurred 1 min. after exposure to drug, followed by an 83% increase 15 min. later (Fig. a). The specific α_1-adrenoceptor blocker prazosin (1 µM) totally blocked or reversed this response. To identify the mechanism(s) underlying the two phases of the response to phenylephrine, we investigated the possible role of activated protein kinase C (PKC). The direct PKC activator phorbol myristate (PMA) (160 nM) reduced twitch tension by 55% (Fig. b). In enzymatically isolated ventricular myocytes, PMA (100 nM) caused a 15% reduction of free cytosolic calcium measured with quin 2 (Fig. c). Pretreatment of papillary muscles with PMA (160 nM) abolished the negative inotropic response induced by phenylephrine (Fig. d). These results suggest the negative phase of the α_1-adrenoceptor induced response in rat papillary muscles may be due to a cytosolic calcium reduction mediated through the activation of PKC via PI hydrolysis.

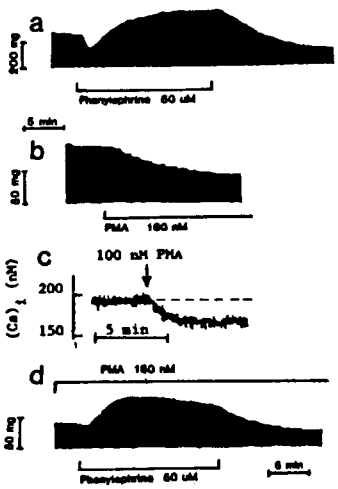

T-Pos58 GTP PREVENTS RECEPTOR-INDEPENDENT BASAL ACTIVATION OF I_{ACh} BY NON-HYDROLYZABLE GTP ANALOGS. G.E. Breitwieser and G. Szabo, UTMB, Galveston, TX.

We have demonstrated muscarinic receptor-mediated, persistent activation of a potassium conductance (I_{ACh}) by 5'-guanylylimidodiphosphate (GppNHp) in isolated bullfrog atrial cells, under conditions which minimize dialysis of cell constituents into the patch pipet (Nature, 317, 538-40 (1985)). When low resistance pipets are used, the same electrode solutions elicit a variable, receptor-independent spontaneous activation of I_{ACh}, which could result from a significant loss of cellular GTP. To test this hypothesis, we examined the effects of including GTP in the perfusion pipet. The rate of activation of I_{ACh} was found to be a simple saturating function of the GppNHp/GTP ratio (maximal rate ≅ 31%/min; half maximal GppNHp/GTP concentration ratio ≅ 3), independent of the absolute value of the nucleotide concentrations in the range of 0.1mM - 2.0mM of GppNHp. Another nonhydrolyzable GTP analog, guanylylmethylenediphosphonate, also elicits a spontaneous activation of I_{ACh}, at rates which are significantly lower than the rates observed for GppNHp at the same analog/GTP ratios. Our results reveal a significant basal rate of G protein turnover in vivo, and indicate that the relative affinity of the G protein for GTP analogs is similar to that observed for purified preparations in vitro. Moreover, the lack of measurable basal activation of I_{ACh} in the absence of nonhydrolyzable GTP analogs suggests that the rate of GTP hydrolysis in vivo is rapid enough to render the effects of basal turnover negligible. Supported by a grant in aid from the AHA and DHHS HL37127.

T-Pos59 POSTNATAL CHANGES IN THE ELECTRICAL RESPONSES OF RAT HEART. EFFECTS OF DEXAMETHASONE.

Zia J. Penefsky and Frances V. McCann, Depts. of Physiology and Biophysics, Mount Sinai Sch. of Med. The City Uni. of New York, N.Y. and Dartmouth Medical School, Hanover, N.H.

The effects of DEXAMETHASONE (DEX) on postnatal changes in the properties of rat heart sarcolemma were studied. Rats were injected with DEX on the second day after birth. An initial slow depolarization disappeared in both DEX-treated and untreated hearts by day 14 after birth. A latent slow depolarization persisted only in the DEX-treated hearts. The plateau persisted in the DEX-treated hearts and was abbreviated and preceded by a "spike" in controls. A plateau was only observed in the pace-maker tissue of the adult controls. A delayed plateau was seen in the Purkinje fibers (P.F.) which exhibited a latent pace-maker activity.

A single injection of DEX (0.01 mg/5 g body weight) was sufficient to prevent normal alterations in the contour of the action potentials in the neonates. DEX treatment of mature and aged rats (1 mg/kg, for 3 days) reversed the contour of the action potentials from a "spike" to a plateau. Possible involvement of DEX in the control of calcium handling elements of the heart is discussed.

T-Pos60 IONIC MECHANISMS OF POST-REPOLARIZATION REFRACTORINESS AND RATE-DEPENDENT BLOCK IN VENTRICULAR MUSCLE. Mario Delmar, Donald C. Michaels and Jose Jalife. SUNY/Health Science Center at Syracuse. Syracuse NY 13210.

Rate-dependent conduction disorders in depressed cardiac tissues are usually associated with foot potentials and subthreshold responses in tissues distal to a zone of block. We studied rate-dependent changes in excitability of single, enzymatically dissociated, guinea pig ventricular myocytes. Action potentials were initiated through intracellular current injection. Frequency-dependent activation delay and cyclic block patterns (Mobitz I, Mobitz II) were demonstrable in well polarized cells, along with post-repolarization refractoriness and subthreshold local events. The ionic bases of these changes were studied in computer simulations using a modified version of the Beeler & Reuter model. The i_{K1} current had a current/voltage relation with a negative slope region, and the inward currents (i_{Na}, i_{si}) were deleted. In the presence of i_K and i_{K1} only, test current pulses of low but constant amplitude and 150 msec in duration were applied from the resting potential (-83 mV), at various intervals after a 300 msec conditioning pulse to +10 mV. At long intervals, the shape of responses to depolarizing pulses was identical to that of subthreshold events in multicellular preparations and single myocytes. As the test interval was abbreviated, the amplitude of the responses diminished and their shape gradually changed to that of an RC change. Voltage clamp simulations demonstrated that these changes were related to slow deactivation of i_K. No time-dependent changes were observed for hyperpolarizing responses. Our results suggest that slow i_K deactivation and inward-going rectification of i_{K1} are major determinants of diastolic changes in excitability and rate-dependent conduction block.

T-Pos61 FREE RADICALS INDUCE CHANGES IN MYOCYTE ACTION POTENTIALS WHICH ARE INDEPENDENT OF GENERATING SYSTEM, $[Ca^{2+}]_o$ OR STIMULATION RATE.

Peggy L. Barrington and Charles F. Meier, Jr. (Intr. by W.B. Weglicki).
Pharmacology Department, Northwestern University, Chicago, Il. 60611 and Pharmacology Department, University of Oklahoma Health Sciences Center, Oklahoma City, OK. 73190.

Oxygen free radicals cause a reproducible sequence of changes in myocardial cell action potentials that can be prevented by simultaneous exposure to scavenger enzymes. The mechanism of the free radical-induced alterations is unknown. Action potentials were recorded in isolated canine myocytes using standard microelectrode techniques. Following a control period, cells were exposed to 1 of 3 free radicals generating systems (3 mM dihydroxyfumaric acid (DHF), 2 mM xanthine:0.01 Units xanthine oxidase (X:XO) or H_2O_2 (0.01 to 0.000001%). DHF, X:XO and 0.001% H_2O_2 each produced a similar sequence of electrophysiological changes including increased plateau voltage and action potential duration, followed by early and/or late after-depolarizations, and finally by reduced plateau voltage, shortened action potential duration and loss of resting membrane potential. Cells depolarized (<-40 mV) and became unresponsive in <20 min. Varying $[H_2O_2]$ altered the time course and magnitude of these changes. Reduction of $[Ca^{2+}]_o$ from 5 to 1.25 mM decreased plateau voltage and action potential duration in control cells but did not alter the sequence of 0.001% H_2O_2 induced changes. Likewise, neither periodic quiesence nor stimulation rates from 0.5 to 2 Hz altered free radical-induced changes. We conclude that H_2O_2 superfusion produces action potential changes similar to DHF or X:XO, which are independent of $[Ca^{2+}]_o$ and stimulation rate.

T-Pos62 **HETEROGENEITY OF RABBIT VENTRICULAR ACTION POTENTIALS AND DIFFERENTIAL EFFECTS OF RYANODINE.** **Michael J. Shattock, Kim C. Warner, James G. Tidball and Donald M. Bers. Division of Biomedical Sciences University of California, Riverside, CA 92521. U.S.A.**

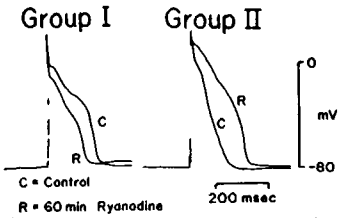

We have observed that small trabeculae isolated from rabbit right ventricle can be grouped into two populations on the basis of action potential (AP) configuration and electrophysiological response to ryanodine. Group I muscles were characterized by a long AP and fast early repolarization. Group II muscles showed a shorter AP and a higher plateau. Ryanodine (0.1μM) shortened the AP in Group I from 210±22(6) msec (± sem(n)) to 176±19 msec while lengthening the AP in Group II from 178±8 msec to 236±22 msec. No significant differences in the mechanical response to ryanodine were observed between the two groups. We have attempted to correlate these electrophysiological differences with the ultrastructural differences (with and without T-tubules) as described by Johnson and Sommer (J.Cell.Biol.33,103-129,1967). Electron-microscopic examination, however, revealed that T-tubules were clearly present in both groups and therefore the two populations cannot be distinguished on this basis. It was considered possible that the difference in the populations is related to the existence of two transient outward currents (one dependent on SR Ca release and the other that is 4-aminopyridine (4-AP) sensitive). The relative importance of these two currents to repolarization may be different in the two groups. This was investigated by adding ryanodine in the presence of 4-AP. The difference between the two groups was not abolished by 4-AP as 3 out of 7 muscles showed a decrease in AP duration and 4 out of 7 showed an increase. In conclusion, two populations of trabeculae exist within the rabbit right ventricle but the cellular basis of the electrophysiological differences has yet to be elucidated.

T-Pos63 WAVELENGTH REGULATION IN A CONE PIGMENT, CHICKEN IODOPSIN J.G. Chen*, T. Nakamura*, T.G. Ebrey*, K. Odashima+, K. Koono+, F. Derguini+, K. Nakanishi+, and B. Honig‡. *University of Illinois, Department of Physiology and Biophysics, Urbana, Il 61801, +Columbia University, Department of Chemistry, New York, N.Y., ‡Columbia University, Department of Biochemistry, New York, N.Y.

Visual pigments, consist of 11-cis retinal covalently bound as a protonated Schiff base to the ϵ-amino group of lysine in the opsin. The protonated Schiff base of 11-cis retinal absorbs at 440 nm while the chicken cone pigment, iodopsin, has its absorption maximum at 560 nm. The magnitude of the protein induced shift in the absorption maxima (the "opsin" shift) is about 4900 cm^{-1} (rhodopsin is about 2700 cm^{-1}). To understand the mechanism of wavelength regulation in this cone pigment, a series of synthetic dihydro-11-cis retinals were used to regenerate the cone pigments opsin. Our preliminary data ($\pm$10 nm) below will be discussed in the context of a simple model for wavelength regulation.

ENTRY	-CHO	-SBH	IODOPSIN	OPSIN SHIFT
	max nm	max nm	max nm	cm^{-1}
11-cis	380	440	560	4870
5,6-diH	370	432	497	2970
7,8-diH	342	392	410	800
9,10-diH	284	322	332	940

T-Pos64 ON THE RELATION BETWEEN THE SPECTRAL ABSORBANCE FUNCTIONS OF VISUAL PIGMENTS. E. F. Mac Nichol, Jr., G. J. Jones, M. C. Cornwall, and R. J. W. Mansfield, Boston University School of Medicine, Boston, MA 02118

Little is known about how the attachment of different opsins to retinal causes changes in its spectral absorbance function. However, two empirical relations have been shown to fit the data well. Averaged microspectrophotometric spectral absorbance data from 18 different rod and cone types having the same chromophore and wavelengths of maximum absorbance (λmax) ranging from 426nm to 567nm were smoothed by a Fourier-transform method, and the wavelength (λ.5) of the longwave half-maximum determined by linear regression of the nearly straight portion of the absorbance curve from 30% to 70% of the peak density. The constancy of the difference between λ.5 and λmax for all the pigments was tested against the two models: that proposed by Barlow which predicts constancy of the difference of the 4th roots of the wavelengths, and Mansfield's model, which predicts that the frequency of the half-maximum (F.5) is a constant fraction of the frequency of maximal absorbance (Fmax): The Mansfield model, which assumes that a single spectral absorbance function describes all pigments having the same chromophore when relative absorbance is plotted against relative frequency, fits our data very slightly better than Barlow's. It has the advantage of being able to predict in a simpler way the absorbance of any pigment at any wavelength given only the peak absorbance and its wavelength. Also, we have found that among the isomers of retinal the all-trans form fits the Mansfield template closely, whereas the others do not, the 11-cis form fitting least well. We hope that these findings may be useful in developing a theoretical explanation of spectral absorption by visual pigments.
Supported by NIH grants: EY06537, EY01157

T-Pos65 USE OF A CANONICAL SPECTRAL CURVE TO ANALYZE VISUAL PIGMENT BINDING. Leo E. Lipetz, Dept. of Zoology and Institute for Research in Vision, The Ohio State University, Columbus, OH 43212 and Thomas W. Cronin, Dept. of Biological Sciences, University of Maryland Baltimore County, Catonsville, MD 21228.

Visual pigment (VP) bleaching difference spectra for rhodopsin and metarhodopsin/rhodopsin mixtures for 8 species of crustaceans were collected by T.W.C. (2 species in collaboration with T.H. Goldsmith) and were analyzed by L.E.L.

All 16 VP spectra collapsed to one curve when plotted by the canonical description of Mansfield. The same curve also fitted vertebrate retinal-based VPs. The inference is that all these VPs have a similar energy-dissipating bond between opsin and chromophore, presumably the Schiff linkage.

For 5 crab species the VP spectra differed from the canonical curve at short wavelengths in a way consistent with the presence of photostable products of photobleaching. For both VPs in each of 4 species the ratio of peak wavelength of the VP to that of the difference spectrum is about 1.20, while for the 5th species it is 1.14. The inference is that the conversion from VP to bleaching product involves similar changes in the configuration of the non-energy-dissipating coupling between chromophore and opsin for all 5 species. This might be simply a change in the orientation of the free portion of the chromophore.

For 2 species the difference (photoproduct) curves for both the rhodopsin and the metarhodopsin/rhodopsin mixture fitted the canonical description. In these species the energy-dissipating chromophore-to-opsin bond of the VP is apparently not changed in the bleaching product.

T-Pos66 RHODOPSIN CHROMOPHORE PROBED BY POLARIZED FTIR-DIFFERENCE SPECTROSCOPY

D. A. Gray, J. Gillespie, W. J. DeGrip†, and K. J. Rothschild
Department of Physics and Program in Cellular Biophysics, Boston University, Boston, MA 02215
†Department of Biochemistry, University of Nijmegen, Nijmegen, The Netherlands

FTIR-difference spectroscopy can detect alterations of single groups in the chromophore, protein, and lipid components of photoreceptor membrane. Polarized FTIR-difference spectroscopy can determine the *orientation* of the chromophore and protein groups relative to the membrane plane. Thus, we can get detailed structural information on the retinylidene chromophore by using this technique to measure localized hydrogen out-of-plane (HOOP), C-C stretch, and C=C stretch modes at different stages in the rhodopsin bleaching sequence. Similar work has recently been reported for bacteriorhodopsin (Earnest *et al., Biochemistry* (1986)).

Parallel and perpendicular difference spectra were obtained of the rhodopsin/bathorhodopsin transition at 80K for hydrated, oriented, bovine rhodopsin films. From the dichroism, we calculated transition moment angles relative to the membrane normal. Based on the HOOP mode angles, we discuss the degree of twisting about C-C bonds in the C10 to C14 region of the polyene chain.

(Supported by a grant from the NIH-NEI to KJR.)

T-Pos67 RESONANCE RAMAN SPECTROSCOPIC STUDY OF THE PROTONATED SCHIFF BASE IN BOVINE RHODOPSIN AND BATHORHODOPSIN. H. Deng and R. H. Callender, Physics Department, City College of New York, New York 10031 and H. Rodman and B. Honig, Dept. of Biochemistry, Columbia University, New York, 10032.

We have obtained the resonance Raman spectra of bovine rhodopsin and bathorhodopsin for a series of isotopically labelled pigments at 77K using previously reported techniques (Narva and Callender, Photochem. Photobiol. 32, 273, 1980). The retinals used in this study are labelled at the protonated Schiff base moiety and include $-HC=NH^+-$, $-HC=ND^+-$, $-H^{13}C=NH^+-$, $-DC=NH^+-$, and some doubly labelled retinals. Apart from the doubly labelled retinals, we find the protonated Schiff base frequency is the same for both rhodopsin and bathorhodopsin in all the substitutions measured here and for others previously reported. In order to assess which factors play a role in determining the position of the protonated Schiff base frequency, we have developed a force field which very accurately fits the observed ethylenic (C=C) and protonated Schiff base stretching frequencies of rhodopsin and its labelled derivatives. We find that the Schiff base mode is quite localized to the Schiff base moiety. MINDO3 calculations are used to estimate how various factors influence the magnitude of the force field parameters. We find that hydrogen bonding between the protonated Schiff base moiety and its immediate protein environment as well as the electrostatic field at the Schiff base resulting from close by point charges can have a significant influence on the force field parameters and, hence, on the Schiff base frequency.

These results are important in understanding the light to chemical energy conversion in the rhodopsin to bathorhodopsin photoreaction because it is widely believed that electrostatic factors are key in the transduction process (Honig et al., PNAS 76, 2503, 1979). Our results suggest that either hydrogen bonding effects essentially cancel electrostatic effects on the Schiff base frequency in the rhodopsin to bathorhodopsin transformation or that the electrostatic field at the Schiff base is not well modeled by a point change which is hydrogen bonded to the Schiff base.

T-Pos68 NEAR-INFRARED LIGHT-SCATTERING SIGNALS RECORDED FROM THE ISOLATED RETINA: EFFECT OF BACKGROUND LIGHT, AND RELATIONSHIP TO VISUAL RESPONSES. D. R. Pepperberg*, M. Kahlert, A. Krause, and K. P. Hofmann. Institut für Biophysik und Strahlenbiologie, Albert-Ludwigs Universität, Freiburg i.Br., FRG; and *Dept. of Ophthalmology, University of Illinois, Chicago, Illinois 60612.

Among the known light-scattering (LS) responses of retinal rod outer segments (ROS) is the "AT" signal, properties of which suggest, as its basis, activation of the ROS phosphodiesterase [Kamps, et al., FEBS Lett. 188:15-20 (1985)]. To examine the relationship between LS signals and the visual process, we simultaneously measured LS and electroretinographic (ERG) responses from the bovine retina. Near-IR LS signals and transretinal ERG's were recorded from the isolated retina, in response to green, 20 μs test flashes. A separate source provided continuous, green background light.

LS responses contained an early component, the amplitude of which was graded with flash intensity. The waveform of this component generally resembled that of the AT signal from ROS. At the limit of detection of the "AT-like" response of the retina, the ERG rod response was near saturation. Accompanying the AT-like response was a slow component of opposite polarity. Background light depressed the amplitude of (desensitized) the AT-like response. For a given background intensity, relative desensitization of the ERG rod response exceeded that of the LS signal. The extinction of weak background light led to recovery of both the ERG and LS responses. Transient desensitizations of both responses also were observed after presentation of an intense flash. The data suggest a link between photoreceptor light adaptation and operation of the reaction yielding the AT-like signal. Supported by the Deutsche Forschungsgemeinschaft (SFB-60), and by NIH grant EY-05494. D.R.P. is a Robert E. McCormick Scholar of Research to Prevent Blindness, Inc.

T-Pos69 EFFECT OF LIGHT CYCLE AND VITAMIN A DEPRIVATION ON G PROTEIN BINDING. Rosalie K. Crouch, Medical University of South Carolina, Charleston, SC 29425

In order to determine if there is a relationship between the G protein binding and levels of rhodopsin in the rat retina, and to study the effect of dark rearing on this protein, Long Evans rats were maintained on vitamin A deprived diets for 12-20 weeks in a 12 hour light cycle or in total darkness with matched controls. Rhodopsin levels were quantitated by the electroretinogram response in vivo and by absorption spectroscopy of extracted pigments. G protein GTP binding was determined by use of the nonhydrolyzable ^{35}S GTPγS analogue of GTP. Rod outer segments show increased binding of the analogue on exposure to light. The following results were obtained:
1. Rats dark reared from birth had comparable amounts of rhodopsin (~1-2 nmole/eye for a 120-150g animal) regardless of diet. Therefore in the absence of light, the retina conserves vitamin A.
2. The GTPγS binding of the cyclic light reared animal is dependent on the amount of rhodopsin present. Deprived animals administered vitamin A have the rhodopsin levels restored to control levels and the GTPγS binding is likewise restored.
3. The GTPγS binding in dark reared animals is not light activated, regardless of diet.

In conclusion, the G protein binding of GTP is not affected by vitamin A deprivation, other than as a factor of the rhodopsin level. However, dark rearing appears to change the light activated G protein GTP binding, possibly either due to a decrease in G protein or an alteration in one of the components involved in this activation. This research is supported by NIH grant EY-01612.

T-Pos70 GUANYLATE CYCLASE ACTIVITY IN SQUID PHOTORECEPTOR MEMBRANES. P.R. Robinson, R.H. Cote* and J.E. Lisman; Biol. Dept. Brandeis U., Waltham MA 02254 and *Lab of Molec Biol. U. of Wisc. Madison, WI 53706.

A rapid, light induced increase in cGMP levels in dark adapted squid retina as well as the observation that cGMP injection mimics the light responses of Limulus ventral photoreceptors suggest that light activates enzymes involved in cGMP metabolism in invertebrate photoreceptors (1). To better understand the visual transduction pathway, we measured guanylate cyclase (G.C.) activity in isolated squid (Loligo paeli) photoreceptor membranes.

In the absence of detergent, G.C. activity (measured with a radiotracer assay) is low (~0.13 pmoles cGMP synthesized/mg protein-min.), regardless of the method employed to isolate photoreceptor membranes. Measurements of cGMP phosphodiesterase activity rule out its potential interference in the G.C. assay. Addition of Triton x-100 causes a 100 fold increase in G.C. activity. After subcellular fractionation this G.C. activity is exclusively associated with the particulate, not soluble fraction. Detergent-activated G.C. requires divalent cations, Mn^{2+} giving 10 fold greater maximal activity than Mg^{2+}. Under our experimental conditions bright illumination has no significant effect on detergent-activated G.C. The modulation of G.C. by other enzyme activators and light is currently being studied.

1. E.C. Johnson,P.R.Robinson and J.E. Lisman,Nature in press.

(Supported by NIH grants EY1496 and EY05798)

T-Pos71 GTPase ACTIVITY AND INACTIVATION OF G PROTEIN IN ROD DISK MEMBRANES. Ari Sitaramayya and Carmen Casadevall. Dept. of Biomedical Sciences, Pennsylvania College of Optometry, Philadelphia, PA 19141 and Dept. of Biochemistry and Biophysics, University of Pennsylvania, Philadelphia, PA 19104.

Activation of G protein (G) by bleached rhodopsin (G.GDP → G.GTP) and of cGMP phosphodiesterase by G GTP are believed to be reactions leading to the photoresponse in vertebrate rods. Presumably, recovery from activation requires inactivation of G.GTP. The hydrolysis of bound GTP (G.GTP → G.GDP + Pi) has been hypothesized to inactivate G.GTP. However, published reports on the rate of this reaction (1-2 min^{-1}) indicate that it is too slow to be the inactivation mechanism. We have investigated the kinetics of this reaction in bovine rod disk membranes (RDM) and found that dark adapted RDM have two GTPase activities with K_m's for GTP of about 3 and 60 uM. On the basis of the measured G protein content of our RDM, the respective V_{max}'s of these activities were 0.6 and 5.7 GTPs hydrolysed/min/G protein at 22°C. Activation by bright light flashes did not significantly change the K_m's of these activities, but their V_{max}'s increased to 2.7 and 13.5 respectively. Assuming that all G proteins were activated by bright flashes, the light-activated GTPases have turnover numbers of 2.1 (low K_m) and 7.8 (high K_m) per min. The turnover number for the high K_m GTPase activity comes within a factor of 2 of the number required to qualify this GTPase activity as the rate-limiting step in the recovery in intact rods at 22°C. (Supported by NSF grant BNS 84 19341)

T-Pos72 REGULATION OF THE PHOSPHORYLATION AND SUBCELLULAR DISTRIBUTION OF COMPONENTS I AND II IN FROG ROD OUTER SEGENTS. H. E. Hamm, Department of Physiology and Biophysics, University of Illinois at Chicago College of Medicine, Chicago IL 60612

Frog rod outer segments (ROS) contain a set of phosphopeptides called Components I and II (p-CI&II) whose phosphorylation is stimulated by cyclic nucleotides. The regulation of this phosphorylation and its relationship to the G-protein/cGMP phosphodiesterase complex (G-PDE) was studied. The kinase involved in this phosphorylation was determined by immunoblotting, photoaffinity labelling and autophosphorylation studies. These methods reveal no evidence of a cGMP dependent protein kinase in frog ROS, while there is ample evidence for the Type II cAMP-dependent protein kinase (cAPK). Additional evidence that cAPK phosphorylates CI&II in vitro is the concentration dependence of cAMP and cGMP-stimulation of their phosphorylation, and the effect of the inhibitor protein specific for cAPK (PKI). The K_m for 8-br-cAMP-stimulation of CI&II phosphorylation is 0.37uM, while it is 65uM for 8-br-cGMP stimulation, and PKI (10 ug/ml) inhibits CI&II phosphorylation.

The membrane bound form of CI&II is subject to regulation by cAPK and light, while phosphorylation of the soluble form doesn't respond to these agents [Soc. Neurosci. Abstr. 11 (1):474 (1985)]. The possible relationship of both soluble and membrane-bound p-CI&II to the G-PDE complex was of interest, because of a recent report on effects of cGMP on G-protein affinity for GTP and GDP. We tested this by measuring CI&II phosphorylation in ROS treated with non-hydrolyzable guanine nucleotide analogs in the dark or after light bleaching 1% rho. We found that when G-protein binding to the membrane increases, the amount of membrane p-CII increases, whereas when G is irreversibly activated in the presence of GTP-δ-S and light, and becomes soluble, membrane p-cII decreases. Also, addition of purified G-protein to ROS membranes increases the amount of p-CII bound. Addition of a partially purified preparation of PDE also increases the amount of bound p-cII. The possible role of P-CI&II in regulating some aspect of the G-PDE complex is currently being tested.

T-Pos73 CHOLESTEROL INFLUENCE ON THE ACTIVATION OF PHOSPHODIESTERASE IN ROD OUTER SEGMENT DISK MEMBRANES

John Marrone and Arlene Albert. Department of Biochemistry, SUNY/Buffalo School of Medicine, Buffalo, N.Y. 14214

The role of cholesterol in the activation of bovine rod outer segment phosphodiesterase has been investigated using cholesterol depleted and non-depleted disk membranes. We find that there is no difference in light activation of the phosphodiesterase when the disk membrane is depleted from approximately 12 mole-percent cholesterol (native level) to less than 6 mole-percent. This is consistent with spectral studies which indicate no difference in the percent Meta I found in depleted and non-depleted samples after a flash. In preliminary experiments, rhodopsin-phosphatidylcholine recombined membranes were compared to rhodopsin-phosphatidylcholine-cholesterol recombined membranes. When cholesterol was present at 10 mole-percent and 30 mole-percent an increase in the light induced activation of the phosphodiesterase over that found in non-cholesterol containing membranes was observed.

T-Pos74 DEFINITION OF THE CYCLIC GMP METABOLIC EVENTS SUBSERVING PHOTOEXCITED AND ATTENUATED STATES IN TOAD PHOTORECEPTORS. S.M. Dawis, R.M. Graeff, T.F. Walseth, E.A. Butz, and N.D. Goldberg, Dept. of Pharmacology, University of Minnesota, Minneapolis MN 55455

Changes in the cGMP metabolic system of intact toad photoreceptors induced by continuous photic stimulation of varying duration (20 to 360 s) and intensity were monitored by measuring: the cGMP hydrolytic flux, by the rate of ^{18}O incorporation into the α-phosphoryls of guanine nucleotides; the total cellular concentrations of guanine nucleotides; and the total concentration of metabolically effective (i.e. free) GDP, estimated from the fraction of total α-GDP labeled with ^{18}O and interpreted to reflect the state of equilibrium between the GDP and GTP forms of G-protein. Over a range of approximately 5 log units of intensity there is an increase of up to 10-fold in cGMP metabolic flux. Characteristics of the cGMP metabolic response over the first 3 log units of intensity are readily distinguishable from those at higher intensities where they are progressively attenuated by an intensity- and time-dependent process. In the low intensity range the accelerated cGMP flux is a logarithmic function of intensity and is sustained for at least 200 s with little or no change in total levels of guanine nucleotides including cGMP but corresponding increases of up to 10-fold occur in metabolic GDP concentration. The attenuated cGMP flux in the higher intensity range is closely associated with proportional decreases in cGMP concentration and decreases in the concentration of metabolic GDP. A new model for light regulation of photoreceptor cGMP metabolism consistent with these observations was developed which contradicts the concept that activated G-protein is a link in a linear cascade that directly increases phosphodiesterase velocity for the purpose of lowering cGMP concentration. In the proposed model of regulation activated G-protein coordinates a network of interrelated regulatory events that result in a rapid acceleration of the cGMP metabolic unit which is suggested to subserve phototransduction and can be attenuated to meet the requirements of photoadaptation. This model and supporting evidence will be presented. (NIH grants EY 04877, GM 28818, and AM 07203).

T-Pos75 RELEASE OF γ SUBUNIT DURING LIGHT ACTIVATION OF cGMP PHOSPHODIESTERASE: GTP-TRANSDUCIN TRIGGERS INCORPORATION OF FLUORESCENT-TAGGED γ .

Theodore G. Wensel and Lubert Stryer, Dept. of Cell Biology , Stanford University School of Medicine, Stanford CA 94305

Photoactivation of a retinal rod cell depends on the rapid activation of a cGMP phosphodiesterase (PDE) which is inactive in the dark. The GTP-form of the α subunit of transducin (Tα-GTP) removes an inhibitory constraint imposed by the γ subunit of PDE. We recently reported that γ subunit binds to $PDE_{\alpha\beta}$ with a dissociation constant < 10^{-11}M, and that γ purified by gel electrophoresis or other methods, when added to rod outer segment membranes at nanomolar concentrations, reverses the activation of PDE by Tα-GTPγS [Wensel & Stryer (1986) Proteins 1: 90]. Does the added γ replace γ removed from $PDE_{\alpha\beta}$ by Tα-GTP? To answer this question, we prepared a fluorescent derivative of γ by reaction with iodoacetamido fluorescein and purification on reverse phase HPLC. The labelled γ was a potent inhibitor of PDE. When added to illuminated rod outer segment membranes, fluorescein-γ was incorporated into a peripheral membrane protein that could be eluted at low, but not physiological, salt concentrations. This incorporation was greatly enhanced by addition of GTP. The incorporated fluorescent γ coeluted with PDE from an HPLC gel filtration column, demonstrating that it had replaced γ removed by Tα-GTP. When Tα-GTP activates PDE, γ remains on the membrane, despite the low intrinsic affinity of γ for disk membranes. Since γ is released from PDE, it must bind to the membrane as a complex with another molecule, most likely with Tα-GTP. The fully active PDE we have prepared, specifically labelled in the γ subunit, can be used in energy transfer experiments with acceptor-labelled Tα to test for the presence of such a complex.

T-Pos76 GDP INFLUENCES cGMP PHOSPHODIESTERASE (PDE) ACTIVITY IN BOVINE PHOTORECEPTORS: KINETICS AND MODEL FOR ACTIVATION/DEACTIVATION.

Jeffrey A. Schmidt and Juan Yguerabide. Department of Biology, UCSD, La Jolla, CA 92093

We have obtained experimental results which suggest a regulatory role for GDP in visual excitation. The kinetics of PDE activity stimulated by a weak pulse of light (<$1x10^{-4}$ fractional bleach) was measured in suspensions of Bovine ROS by continuous monitoring of the stochiometric proton release produced by cGMP hydrolysis. Measurements were done at several [GTP] and [GDP]. The most significant results are 1) PDE activity vrs time is bimodal and can be characterized in terms of a GDP, GTP sensitive rise time, fall time and peak velocity (Vpeak), 2) GDP at concentration <100 μm has a significant stimulatory effect on peak velocity in the presence of GTP, 3) Vpeak vrs [GTP] plots display multiple maxima and GDP has striking effects on the amplitude and [GTP] at which these maxima appear. The PDE velocity vrs time profiles can be fitted quantitatively by the schematized 2 path kinetic model (showing only rate limiting steps, T=transducin, R=rhodopsin, k=turnover number). The fits yield values for the GDP and GTP sensitive lifetimes (τ_R and τ_T) for several [GTP] and [GDP]. The PDE Vpeak vrs [GTP] can be fitted by an allosteric model in which the T molecule has 4 ligand binding sites which bind GDP and GTP competitively to regulate the PDE activity. This analysis is consistent with the view that transducin is a tetramer. (Supported by NIH Grant EY04475 to J.S.)

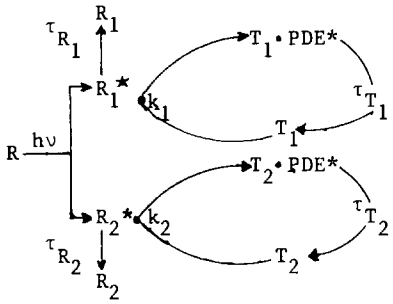

T-Pos77 **PHOTOCURRENTS IN DETACHED ROD OUTER SEGMENTS.** W.Sather and P.Detwiler,Univ.Washington, Seattle, WA. We reported previously (Neurosci.Abst.1986) that rod outer segments without attached inner segments are able to support a light-sensitive inward current during whole-cell recording with pipets filled with solutions containing cGMP, GTP and ATP. Here we report on the ability of other solutions to support the generation of dark-current and describe the effect of changes in [cGMP] on light-sensitive current. Giga-seals on detached outer segments (DOS) from Gecko and frog were obtained with pipets filled with:(mM) 92 KAsp, 7 NaCl, 2.2 $MgCl_2$, 0.22 EGTA, 2.8 HEPES, pH 7.4 and supplemented with varing amounts of cGMP,GTP, or ATP. Breakthrough from cell-attached to whole-cell recording was signalled by an abrupt increase in capacitance followed by either no change in current or growth of an inward current (V_{hold} -20 or -40mV) that was suppressed by light. The former result, obtained with 0 nucleotide solutions, indicates light-sensitive channels in DOS are normally closed. A standing inward dark current developed when the solution contained mM ATP or GTP or uM cGMP. Pipets containing solutions supplemented with 5mM ATP or GTP recorded a 40 to 60 pA dark current that was abolished by light. This result, which was essentially unaltered by the substitution of 10uM $CaCl_2$ for EGTA in the ATP supplemented filling solution, suggests that the outer segment contains guanyl cyclase. Breakthrough to whole-cell recording with pipets filled with solutions containing cGMP, either alone or in combination with ATP and GTP, was followed by rapid development of an inward light-sensitive current. The longevity of whole-cell recordings increased with increasing [cGMP]. Low [cGMP] recordings were typically terminated by bursts of inward current events which were attributed to the activation of large (300 to 400 pS) single channels. Recordings with solutions containing 5mM ATP, 100uM GTP and 20 to 2000uM cGMP were associated with light-sensitive noise that consisted of three components: a prominent low-frequency noise and a high-frequency noise that could be fitted by the sum of two Lorentzians. The low-f. noise (0.01 to 10Hz) was large amplitude (p-p 50 to 75 pA) and reflected the coordinated modulation of a large number of light-sensitive channels. The smaller amplitude high-f. noise (10 to 10 kHz) was attributed to the activity of single light-sensitive channels. The two Lorentzian components are either due to two different channels or different frequency behavior of the same channel. Low- and high-f. dark noise variance increased biphasically with [cGMP]; the noise peaked around 500uM and declined with further increase in cGMP. Light reduced noise recorded in the presence of 500uM cGMP or less and increased the noise in the presence of 2000uM cGMP.

T-Pos78 AN AMILORIDE DERIVATIVE BLOCKS THE LIGHT- AND CYCLIC GMP-REGULATED CONDUCTANCE IN FROG ROD PHOTORECEPTORS. G.D. Nicol[1], P.P.M. Schnetkamp[2], Y. Saimi[1], E.J. Cragoe, Jr.[3], and M.D. Bownds[1]. [1]Laboratory of Molecular Biology, University of Wisconsin, Madison, WI, 53706; [2]Dept. of Medical Biochemistry, University of Calgary, Calgary, Canada, T2N 4N1; and [3]Merck Sharp & Dohme Research Laboratories, West Point, PA, 19486

The light-regulated current recorded from vertebrate rod photoreceptors is not sensitive to tetrodotoxin or amiloride, potent blockers of voltage-dependent and epithelial Na channels, respectively. We report that an amiloride derivative, 3',4'-dichlorobenzamil (DCPA), designed previously as an inhibitor of Na/Ca exchange, completely suppresses the light-regulated current at a concentration of 50 μM. Also, DCPA blocks both a cyclic GMP-activated current in excised patches of rod plasma membrane and a cyclic GMP-induced Ca^{++} flux from rod disk membranes. This is consistent with the notion that the Ca^{++} flux mechanism in the disk membrane and the light-regulated conductance in the plasma membrane are identical. Lower concentrations of DCPA partially suppress the photoresponse; 1 μM DCPA reduces the response by about 25%, 10 μM DCPA reduces the response by about 50%. In excised patches, 1 μM DCPA reduces the cyclic GMP-activated current by about 44% while 10 μM completely suppresses this current. In suspensions of ROS with "leaky" plasma membranes DCPA blocks a cyclic GMP-induced Ca^{++} release in a dose-dependent manner (apparent $K_i \sim 10$ μM). In suspensions of intact rods, increasing concentrations of DCPA progressively inhibit the Na/Ca exchange mechanism (apparent $K_i \sim 50$ μM). Recordings from intact rods show that the blocking action of DCPA is different in 10 nM Ca^{++} compared to 1 mM Ca^{++}, suggesting either that the conductance state of the light-regulated channel may be modified in high and low Ca^{++} or that there may be two ionic channels in the ROS membrane. (Supported by NIH grant EY-00463).

T-Pos79 MECHANISM OF cGMP STIMULATED Ca^{2+} UPTAKE BY ROS DISKS.
John S. George, Life Sciences Division, Los Alamos National Laboratory, Los Alamos, NM 87545.

Addition of cGMP to preparations of isolated, leaky rod outer segments stimulates Ca^{2+} uptake by disks under appropriate experimental conditions. In previous studies, the process appeared specific for cGMP since individual additions of GMP, cAMP, or 8Br-cGMP did not produce stimulation of uptake comparable to cGMP. Enhanced Ca^{2+} uptake is ATP dependent, and is associated with increased hydrolysis of ATP, however, ATP alone does not support the process. Creatine phosphate (CrP), included routinely in previous experiments as an ATP regenerating system, is required for cGMP-stimulated Ca^{2+} uptake. When hydrolyzed ATP is regenerated from CrP, the result is net alkalinization of experimental media, instead of the acidification observed when ATP is hydrolyzed in the absence of CrP. pH changes alone do not account for the effect of cGMP, since an addition of GMP to an ROS preparation can produce alkalinization comparable to that produced by cGMP without comparable Ca^{2+} uptake. However, stimulation of ATP hydrolysis by either cGMP or GMP appears due to rephosphorylation of GMP by ROS enzymes. If GMP was added shortly following an addition of cGMP or 8Br-cGMP Ca^{2+} uptake rates were significantly enhanced. These observations suggest that alkalinization of the medium in the presence of an open cGMP dependent conductance in disk membranes may account for the observed effect of cGMP. Such a mechanism might regulate cytoplasmic Ca^{2+} as a function of cGMP hydrolytic rates, in addition to the regulation provided by the cGMP dependent cation conductance of the plasma membrane.

T-Pos80 Ca^{2+} INHIBITION OF THE ATP DEPENDENT QUENCH OF ROD PHOSHPHODIESTERASE.
A. Edwin Barkdoll III, E.N. Pugh Jr. and A. Sitaramayya
Depts of Psychology and Biochemistry/Biophysics, University of Pennsylvania, Phila. PA 19104

Using the pH assay, we have studied Ca^{2+} inhibition (Kawamura and Bownds, 1981; Del Priore and Lewis,1983) of the ATP dependent quench of light activated PDE in crude toad rod disk membranes (RDM) with 2mM ATP, 1mM GTP, 5mM cGMP and BAPTA buffered Ca^{2+}. With no added Ca^{2+}, ATP decreases the Vmax of the linear flash response ($3x10^{-5}$ bleach) c. 10-15 fold and decreases the decay time constant (t_{off}) 5-fold relative to GTP alone controls. Ca^{2+} reverses the effects of ATP: Vmax increases nearly 10-fold over responses without Ca^{2+} and t_{off} increases 5-fold from 8-20 sec to 50-60 sec. Responses in very high Ca^{2+} (c.5 mM) are nearly indistinguishable from those without ATP. Ca^{2+} added 2 sec after flash activation inhibits the quench as effectively as when added prior to activation. The $K_{1/2}$'s for Ca^{2+} disinhibition of Vmax and t_{off} are between 10^{-4} and 10^{-3} M Ca^{2+}. Minimal disinhibition is observed below 10^{-6} M Ca^{2+}. We also observe that the ATP dependent quench of a reconstituted system of rhodopsin, G-protein, PDE and rhodopsin kinase(1), is inhibited by Ca^{2+}. As with RDM the t_{off} and Vmax increase nearly 5- and 10-fold as Ca^{2+} is added with $K_{1/2}$'s between 10^{-4} and 10^{-3} M Ca^{2+}. Supported by NIH Grant EY02660 and NSF Grant BNS 84 19341

1 Sitaramayya, A. (1986) Biochemistry 25, 5460-5468.

T-Pos81 CONE INNER SEGMENTS CONTAIN A CALCIUM ACTIVATED CHLORIDE CONDUCTANCE THAT CONTROLS REGENERATIVE ELECTRICAL ACTIVITY. A.V. Maricq*# and J.I. Korenbrot#, *Dept. of Biophysics, University of California, Berkeley, CA 94720, and #Dept. of Physiology, University of California, San Francisco, CA 94143.

Cone photoreceptors, but not rod photoreceptors, respond with a regenerative depolarizing photovoltage to a bright annulus of light. This response is mediated by horizontal cell feedback onto the cone synaptic endings. In single cone cells, lacking only an outer segment, and isolated from the lizard retina, we have recorded regenerative depolarizing membrane voltage changes (spikes) in response to outward current pulses. We identified two ionic currents that are primarily responsible for the spike production. Depolarization is accomplished by a voltage dependent inward calcium current(I_{Ca}), and repolarization results from a calcium dependent outward current carried mostly by the anion chloride($I_{Cl(Ca)}$). The inward current activates within msec. at potentials above -45 mv, shows little voltage dependent inactivation, and is blocked by external cobalt. Activation of the outward chloride current depends on prior calcium entry since its latency is inversely proportional to the magnitude of I_{Ca}. Moreover, the latency is also proportional to the level of intracellular calcium buffering. In the presence of 10 mM EGTA the latency may be as long as several seconds, whereas in 0.1 mM EGTA the latency is about 100 fold shorter. Barium may substitute for calcium as an inward current carrier, but is incapable of activating $I_{Cl(Ca)}$. Bright annular light limits horizontal cell feedback onto the cone synaptic ending (O'Bryan, J. Physiol., 235, 1973). Our findings suggest that this inhibition may allow I_{Ca} to become regenerative, and that this current and $I_{Cl(Ca)}$ then directly mediate the regenerative response of the cone inner segment.

T-Pos82 **POTASSIUM TURNOVER IN VERTEBRATE ROD PHOTORECEPTORS,** **Burks Oakley II, Departments of Electrical Engineering and Biophysics, University of Illinois at Urbana-Champaign.**

Ion-selective microelectrodes (ISMs) were used to measure the turnover of intracellular K^+ (K^+_i) in rods in the isolated retina of the toad, Bufo marinus. The light-evoked hyperpolarization of rods decreases their passive K^+ efflux, which in combination with active K^+ uptake, decreases extracellular K^+ concentration, K^+_o. In this process, Rb^+ substitutes for K^+, since rod photoresponses are essentially unchanged when Rb^+ replaces K^+, and the light-evoked decrease in Rb^+_o is nearly identical to the light-evoked decrease in K^+_o. The turnover of K^+_i was measured as Rb^+ and K^+ were exchanged, using ISMs that were ~5-times more sensitive to Rb^+ than to K^+. When K^+_o was replaced by Rb^+, the light-evoked decrease in K^+ efflux produced only a small change in ISM voltage, $\Delta V\{ISM\}$, due to the background of Rb^+_o. As Rb^+_i replaced K^+_i, the efflux shifted from K^+ to Rb^+ and the $\Delta V\{ISM\}$ grew in amplitude. After loading the rods with Rb^+, Rb^+_o was replaced by K^+_o. The light-evoked decrease in Rb^+ efflux lead transiently to a large $\Delta V\{ISM\}$, since the change in Rb^+_o was superimposed upon a background of K^+_o. As K^+_i replaced Rb^+_i, the amplitude of $\Delta V\{ISM\}$ declined. When measured using this technique, the turnover of K^+_i was essentially completed in ~15 min, which is somewhat longer than estimated previously. In solutions having only 90 μM calcium, transmembrane fluxes of K^+ (Rb^+) increased and turnover of K^+_i occurred more rapidly. During background illumination, transmembrane fluxes of K^+ (Rb^+) decreased, and turnover of K^+_i was slowed. Overall, these experiments have provided independent corroboration of earlier observations concerning rod K^+ fluxes. This ISM-based technique also may be useful in measuring K^+ turnover in other cell types, as well. **Supported by NIH grant EY04364.**

T-Pos83 Evidence for Electrogenic Na/Ca-Exchange in *Limulus* Ventral Photoreceptors.
Peter M. O'Day and Mark P. Keller. Institute of Neuroscience, University of Oregon, Eugene OR

Na/Ca-exchange is thought to operate in *Limulus* ventral photoreceptors to maintain a large transmembrane [Ca]-gradient. (e.g. Waloga *et al.*1975 Biol.Bull.149:449). We have suggested that Na/Ca-exchange can operate in the reverse (Na_i-dependent Ca-entry) as well as forward (Na_o-dependent Ca-efflux) directions in this preparation (Biophys J. 49:282a and ARVO 1986).

In the present study we have examined the possibility that Na/Ca-exchange is electrogenic. Cells were bathed in 0-Na, 0-Ca, 0-K saline (Li- & Mg- subst.) & voltage clamped to -80mV in the dark. We found (a): an inward current (2-15nA) induced by raising Na_o to 425mM, and (b): an outward current (1-5nA) induced by raising Ca_o to 10mM. These observations are consistent with electrogenic Na/Ca-exchange in forward and reverse directions.

Using Aequorin, we examined changes in Ca_i elicited by procedures designed to stimulate or inhibit Na/Ca-exchange. Na_o-removal (Li-subst) in 10mM Ca_o evoked aequorin luminescence (indicating a rise in Ca_i) that peaked and declined to a plateau. Restoration of normal Na_o caused a rapid decline in the aequorin signal, indicating a drop in Ca_i. But removal of Ca_o following Na_o-removal caused a much slower decline in the aequorin signal. This result is consistent with the interpretation that a fast Ca_i decline resulted from restoration of normal Na_o due to forward Na/Ca-exchange. Injection of Na in the absence of Na_o, a procedure that causes a Ca_o-dependent decline in light-response amplitude, also caused a transient rise in the aequorin signal. This result is consistent with the interpretation that a rise in Ca_i induced by raising Na_i resulted from reverse Na/Ca-exchange. Supported by NSF:BNS84204463

T-Pos84 LIGHT-DEPENDENT ION CHANNEL ACTIVITY IN CHLAMYDOMONAS.
J.M. Sullivan and K.W. Foster; Dept. of Physiology-Biophysics, Mount Sinai School Medicine New York, N.Y., 10029 and Dept. Physics, Syracuse Univ., Syracuse, N.Y. 13210.

Chlamydomonas reinhardii is a single-celled green algae that employs a bovine-like rhodopsin as its receptor for phototaxis. Like other ciliated photoreceptors this organism requires ions to mediate signal transduction processes. Possibly, Chlamydomonas shares with vertebrates a common ancestral phototransduction pathway. In order to understand phototactic signal processing we applied the cell-attatched patch (CAP) clamp methodology.

In the presence of continuous white light action potential-like currents were seen as well as inward and outward directed slow macrocurrents. With a CAP over the eyespot and rhodopsin patch slow macrocurrents were found that were inward in response to light ON but outward in response to light OFF. This modulation was only possible with blue-green but not red light suggesting that activation of the rhodopsin is necessary for their appearance. Discrete single channel phenomenon were also seen in the presence of blue-green light and which disappeared with light OFF. Reasonable estimates for whole cell potential and reversal potentials provide an estimate of about 50 pS for the conductance of these light-dependent channels. As only K^+ and Ca^{2+} cations are essential for phototaxis in Chlamydomonas, it is possible that the light-dependent channels are of such selectivity. Moreover, the similarity of the receptor potential in this algal family to the vertebrate rod or other higher ciliated photoreceptors suggests that Chlamydomonas could serve as a model rhodopsin-modulated photoreceptor cell.

Supported in part by NIH (Grant # EY 03760). JMS is a trainee on Medical Scientist Training grant GM-07280 from the NIH.

T-Pos85 OPSIN SHIFTS OF DIHYDRORETINALS AND THEIR ELECTRONICALLY EQUIVALENT POLYENE ALDEHYDES IN THE RHODOPSIN OF THE ALGA, CHLAMYDOMONAS REINHARDTII. Kenneth W. Foster and Jureepan Saranak, Syracuse University, Syracuse, N.Y. and V-Jayathirpharao, Nobuko Shimizu, Randy Johnson, Fedila Derguini, and Koji Nakanishi, Columbia University, New York, N.Y.

We take advantage of the high sensitivity, thousandfold dynamic range, and the convenient in vivo assay for rhodopsin function provided by phototaxis of the unicellular alga, Chlamydomonas. This work was carried out in vivo to determine whether the analogs work in a living system and therefore to evaluate results obtained by in vitro assays and spectroscopic means. Dihydroretinals and a broad range of polyene aldehydes having from zero to six carbon-carbon double bonds were incorporated into Chlamydomonas opsin. The differences between the action spectra maxima determined in vivo and their protonated equivalents in solution ("opsin shift") were compared to previous in vitro studies of bovine rhodopsins with incorporated dihydroretinals.

All analogs efficiently excited rhodopsin at their respective photon energies of absorption. Opsin shifts were obtained of approximately 1 eV if there were less than 3 carbon-carbon double bonds and about 0.3 eV if more. With in vitro bovine rhodopsin absorption measurements the transition between the high (1 eV) opsin shift and the low (0.3 eV) opsin shift is displaced from the three to the one carbon-carbon double bonds.

The opsin sites of bovine and Chlamydomonas are similar, but the specific position of the negative charge from opsin is significantly different. [Supported by NIH grants GM-34218 to KWF and GM-36564 to KN]